universität wien

DISSERTATION

Titel der Dissertation

Deciphering the role of the TRAIL pathway as potential tumor escape mechanism in ovarian cancer

angestrebter akademischer Grad

Doktor/in der Naturwissenschaften (Dr. rer.nat.)

Verfasserin / Verfasser:	Ahmed El-Gazzar
Matrikel-Nummer:	0200236
Dissertationsgebiet (lt. Studienblatt):	Genetik - Mikrobiologie
Betreuerin / Betreuer:	Univ.-Prof. Dr. Michael Krainer

Wien, im November 2009

Table of Contents

Summary **3**

Zusammenfassung **6**

1. Introduction **9**

1.1. Ovarian Cancer 9

1.2. TRAIL and its receptors 9

1.3. TRAIL signaling pathway 12

1.4. c-FLIP as inhibitor of TRAIL functional receptors-mediated apoptosis 13

1.5. TRAIL and immunosurveillance 16

1.6. References 19

2. Aim of my PhD thesis **27**

3. Results and Discussion **29**

3.1. Natural immunity enhances the activity of a DR5 agonistic antibody and carboplatin in the treatment of ovarian cancer (manuscript submitted) 29

Abstract *31*

Introduction *32*

Material and methods *34*

Results *40*

Discussion *55*

References *59*

3.2. The role of c-$FLIP_L$ in ovarian cancer: chaperoning tumor cells from immunosurveillance and increasing their invasive potential (manuscript submitted) 65

Abstract *67*

Introduction *68*

Material and Methods *70*

Results *76*

Discussion *88*

References *92*

Supplementary data *100*

3.3. Characterization of the TRAIL pathway in a syngeneic mouse model of ovarian cancer 103

Introduction *103*

Material and Methods *106*

Results *113*

Discussion *123*

Future Directions *127*

References *128*

4. Conclusions 134

5. Acknowledgments 137

6. Curriculum Vitae 139

Summary

Tumor necrosis factor (TNF)-related apoptosis-inducing ligand (TRAIL) triggers apoptosis in a variety of tumor cells, but not in normal cells. Therefore, TRAIL and in particular agonistic antibodies to the functional TRAIL receptors TRAIL-R1 (DR4) and TRAIL-R2 (DR5) are currently being explored in pre-clinics and clinical trials for the treatment of various malignancies.

TRAIL is highly prevalent in ovarian tumor microenvironment and is being associated with prolonged survival. In addition, more than two third of ovarian cancer (OC) patients have a disturbed TRAIL signaling pathway, a fact important not only for prognosis, but also for future therapeutic options. Defects in the TRAIL pathway include a downregulation of TRAIL functional receptors DR4 and DR5, and/or an overexpression of the long isoform of caspase-8 inhibitor protein cellular Fas-associated death domain-like interleukin-1β-converting enzyme (FLICE)-like inhibitory protein (c-$FLIP_L$).

The central aim of my PhD thesis was to gain further insight into the deregulation of the TRAIL signaling axis as potential tumor escape mechanism in OC. In the first part of my PhD thesis I elucidated whether human OC resistance to TRAIL may be overcome by an agonistic anti-human DR5 monoclonal antibody (AD5-10). I identified that co-administration of AD5-10 with carboplatin exhibits more than an additive effect *in vitro*, which may be explained by the finding that carboplatin upregulates DR5 expression on OC cells irrespective of the p53 status. The combination therapy of AD5-10 with carboplatin eliminated large established platin resistant ovarian tumors *in vivo*,

reducing tumor size to undetectable levels in more than 50% of mice (*P*=0.002). In addition, I found that TRAIL and natural killer (NK) cell expression are abundant in the tumor microenvironment, and that depletion of NK cells abolishes the antitumor activity of AD5-10. Taken together, these data show that a combination of agonistic anti-DR5 monoclonal antibody such as AD5-10 and carboplatin is a promising regimen for treatment of OC. These results also highlight the interplay between a therapy addressing the apoptosis cascade and the role of the immune system.

In the second part of my PhD thesis I focused on the physiological role of c-FLIP$_L$ in OC progression. To address this question, a loss of function approach was applied utilizing RNA interference (RNAi) in OC *in vitro* and *in vivo*. I was able to demonstrate that suppression of c-FLIP$_L$ enhanced sensitivity of human OC cells to TRAIL-mediated apoptosis and significantly decreased tumor development *in vivo*. Interestingly, I observed that downregulation of c-FLIP$_L$ decreased the rate of apoptosis and proliferation *in vivo*. The knockdown of c-FLIP$_L$ particularly inhibited the invasion of OC cells into the peritoneal cavity, which might be due to the high expression of TRAIL by NK cells in the tumor-stroma. Altogether, these results indicate that c-FLIP$_L$ regulates TRAIL-induced apoptosis in OC cells.

I complemented my work by utilizing an established syngeneic ovarian tumor model kindly provided by a collaboration partner, and obtained some very first insights into the interplay between the TRAIL pathway and OC in the immunocompetent situation. I observed that DR5 expression is reduced in all ten transformed mouse ovarian surface epithelial (MOSE) cell lines when compared to normal (non-tumorigenic) MOSE cells. About 70% of tumorigenic

MOSE cell lines were resistant to TRAIL-induced apoptosis. In a preliminary animal experiment, the downregulation of mouse DR5 accelerated the development of ascites and decreased mouse life span, which is in line with previous observations that TRAIL receptors play a key role in human OC.

In conclusion, the data generated in the course of my PhD thesis indicate that DR5 and c-FLIP$_L$, in the context of the TRAIL signaling pathway, play a fundamental role in OC pathogenesis and thus are potential targets for future OC therapy.

Zusammenfassung

TRAIL (Tumor necrosis factor (TNF)-related apoptosis-inducing ligand) induziert in einer Vielzahl von Tumorzellen Apoptose, nicht jedoch in gesunden Zellen. Deshalb werden TRAIL selbst, sowie agonistische Antikörper für die funktionellen TRAIL-Rezeptoren (TRAIL-R1 (DR4) und TRAIL-R2 (DR5)) gegenwärtig in präklinischen und klinischen Studien für die Behandlung von diversen Erkrankungen untersucht.

TRAIL ist im Mikroumfeld von Ovarialtumoren prävalent und wird mit verlängertem Überleben assoziiert. Mehr als zwei Drittel der Ovarialtumorpatientinnen haben einen gestörten TRAIL-Signalweg, ein wichtiges Faktum für Prognose und Therapiemöglichkeiten. Defekte im TRAIL-Signalweg beinhalten eine Reduzierung der funktionellen Rezeptoren DR4 und DR5 und/oder eine Überexpression der langen Isoform von c-FLIP (cellular Fas-associated death domain-like interleukin-1β-converting enzyme (FLICE)-like inhibitory protein, c-$FLIP_L$).

Das Hauptziel meiner Doktorarbeit war Einblicke in die Deregulierung des TRAIL-Signalweges als potentiellen Tumor-Escape-Mechanismus beim Ovarialkarzinom zu erhalten. Im ersten Teil meiner Arbeit habe ich untersucht, ob eine Resistenz gegen TRAIL beim Ovarialkarzinom durch einen agonistischen anti-humanen DR5 monoklonalen Antikörper (AD5-10) aufgehoben werden kann. Ich konnte zeigen, dass die gemeinsame Anwendung von AD5-10 mit Carboplatin einen mehr als additiven Effekt *in vitro* hat. Dies könnte dadurch erklärt werden, dass Carboplatin die DR5-Expression an Ovarialkarzinomzellen, unabhängig von deren p53-Status,

steigert. Eine Kombinationstherapie von AD5-10 mit Carboplatin eliminiert etablierte, platinresistente Ovarialtumore *in vivo* und reduziert deren Größe in mehr als 50 % der Mäuse (*P*=0.002) bis unter die Nachweisgrenze. Zusätzlich konnte ich zeigen, dass TRAIL und Natürliche Killerzellen (NK-Zellen) im Tumor-Mikroumfeld in sehr hohem Ausmaß vorhanden sind und der Abbau von NK-Zellen die antitumorale Aktivität von AD5-10 aufhebt. Zusammengefasst zeigen diese Daten, dass eine Kombination eines agonistischen monoklonalen anti-DR5 Antikörpers wie AD5-10 und Carboplatin eine vielversprechende Therapie für die Behandlung des Ovarialkarzinoms sein kann. Diese Ergebnisse zeigen auch die Interaktion zwischen einer Therapie, die die Apoptose-Kaskade in Gang setzt, und der Rolle des Immunsystems.

Im zweiten Teil meiner Arbeit habe ich mein Hauptaugenmerk auf die physiologische Rolle von c-FLIP$_L$ in der Ovarialkarzinomentstehung gelegt. Um auf diese Frage einzugehen, habe ich die Loss-of-Function-Methode, unter Verwendung von RNA Interferenz (RNAi) im Ovarialkarzinom *in vitro* und *in vivo,* angewendet. Es war mir möglich zu zeigen, dass durch die Unterdrückung von c-FLIP$_L$ die Sensitivität von menschlichen Ovarialkarzinomzellen für TRAIL-induzierte Apoptose erhöht und die Tumorentstehung *in vivo* gehemmt wird. Von besonderem Interesse war die Beobachtung, dass eine Reduzierung von c-FLIP$_L$ die Apoptoserate und die Proliferation *in vivo* senkt. Die Reduzierung von c-FLIP$_L$ verhinderte insbesondere die Invasion der Ovarialkarzinomzellen in die Peritonealhöhle, eine Beobachtung die auf die hohe Expression von TRAIL durch die NK-Zellen im Tumorstroma zurückzuführen sein könnte. Alles in allem zeigen

diese Resultate, dass c-FLIP$_L$ die TRAIL-induzierte Apoptose in Ovarialkarzinomzellen wesentlich beeinflusst.

Ich habe meine Arbeit durch die Verwendung eines etablierten, immunkompetenten Ovarialtumor-Modells ergänzt, welches freundlicherweise von einem Kooperationspartner zur Verfügung gestellt wurde. Durch die Anwendung dieses Modells erhielt ich allererste Einsichten in die Interaktion zwischen dem TRAIL-Signalweg und dem Ovarialkarzinom in einer immunkompetenten Situation. Ich konnte beobachten, dass DR5 in allen zehn tumorigenen MOSE (Mouse-Ovarial-Surface-Epithel)-Zelllinien weniger exprimiert wird als in normalen (nicht-tumorigenen) MOSE-Zellen. Rund 70 % der tumorigenen MOSE-Zelllinien waren resistent gegen TRAIL-induzierte Apoptose. In einem vorangegangenen Tierexperiment hat die Reduktion von Maus-DR5 die Entstehung von Aszites beschleunigt und die Lebensspanne der Mäuse verkürzt. Dies stimmt mit unseren früheren Beobachtungen, bezüglich der zentralen Rolle von TRAIL-Rezeptoren im menschlichen Ovarialkarzinom, überein.

Zusammenfassend zeigen die Ergebnisse meiner Dissertation, dass DR5 und c-FLIP$_L$ im Zusammenhang mit dem TRAIL-Signalweg eine fundamentale Rolle in der Pathogenese des Ovarialkarzinoms spielen und dass DR5 und c-FLIP$_L$ potentielle Ziele für die Therapie des Ovarialkarzinoms darstellen.

1. Introduction

1.1. Ovarian Cancer

Ovarian cancer (OC) is the most lethal gynecological malignancy and the fifth leading cause of cancer-related deaths among women (1, 2). OC originating from the ovarian surface epithelium (OSE) is the most common form and is displayed in a range of histological subtypes. The OSE consists of a single layer of squamous to cuboid cells covering the surface of the ovary and arises ontogenetically from the mesothelial lining of the embryonic coelom. It shares many common histological features with the rest of the peritoneum, albeit being phenotypically different and developmentally less mature than the peritoneum itself (3). Generally accepted risk factors for OC include genetic predispositions based on germline mutations in DNA repair genes (BRCA1, BRCA2, HNPCC), and hormonal and lifestyle factors such as early menarche, late menopause and number of pregnancies. Most of these risk factors influence the number and quality of the repeated trauma to the OSE during ovulation (incessant ovulation theory (4)) and in parallel paracrine hormonal exposure from ovarian stroma. Surface papilations, invaginations and inclusion cysts of OSE, which may develop in an ovulating ovary, are therefore thought to be putative premalignant lesions due to their increased incidence in high-risk populations.

1.2. TRAIL and its receptors

Tumor necrosis factor (TNF)-related apoptosis-inducing ligand (TRAIL), also designated as Apo2L, is a type II transmembrane protein of about 33-35 kDa

(5). TRAIL was identified by homology search of a highly conserved sequence motif characteristic for the TNF family members (6, 7). Like Fas ligand (FasL) and TNF-α, TRAIL can be cleaved from the membrane by metalloproteases, and the resulting soluble TRAIL has been shown to maintain biological activity. The extracellular domain of TRAIL forms a bell-shaped homotrimer, like other ligands of the TNF family (8, 9), by a cysteine residue at position 230 that coordinates with divalent zinc. Human TRAIL has been proven to bind to five different paralogous receptors; TRAIL-R1/DR4, TRAIL-R2/DR5, TRAIL-R3/DcR1, TRAIL-R4/DcR2 and osteoprotegrin (10). While DR4 and DR5 are intact functional TRAIL receptors, the others do not contain a functional death domain and may thus act as decoy receptors competing with DR4 and DR5 for TRAIL (Fig. 1.1) (11). Interestingly, the genes for the DR4, DR5, DcR1, and DcR2 receptors are tightly clustered on human chromosme 8p21-22 (12-14). Osteoprotegrin (OPG) is a soluble receptor stimulating osteoclastogenesis by competing with receptor activator of NF-KB (RANK) for RANK ligand. It has however been shown to bind TRAIL with only a very low affinity (15).

Interestingly, in mice it has been shown that there is only one death-inducing receptor homologous to human DR5 (mTRAIL-R2/mDR5), and two potential decoy receptors (mDcTRAIL-R1/mDcR1 and mDcTRAIL-R2/mDcR2) specific for mouse TRAIL (Fig. 1.1) (16). Mouse DR5 (mDR5) contains the death domain and signals apoptosis in response to both mouse and human TRAIL. mDcR1 is a GPI-anchored membrane protein that binds mouse, but not human TRAIL. mDcR2 can be expressed as two alternative splicing variants, a secreted form (mDcR2S) and a transmembrane form (mDcR2L),

which binds with both mouse and human TRAIL. OPG can also bind to mouse TRAIL, and may act as soluble decoy receptor for TRAIL.

In humans, DR4 and DR5 receptors are characterized by an extracellular cystein-rich domain and an intracellular death domain giving them the ability to trigger the assembly of the death-inducing signaling complex (DISC) upon ligand stimulation which initiates the apoptotic cascade. The cytoplasmic regions of both DR4 and DR5 contain a death domain homologous to Fas and TNF-R1. Recent studies have shown that DR5, and less clearly DR4, signal apoptosis in a similar way to Fas (17). Mutations in DR5 encoding gene have been described in several cancers like in head and neck cancer (18), non small cell lung (19), breast cancer (20), colorectal cancer (21), gastric cancer, and hepatocellualr carcinoma (22).

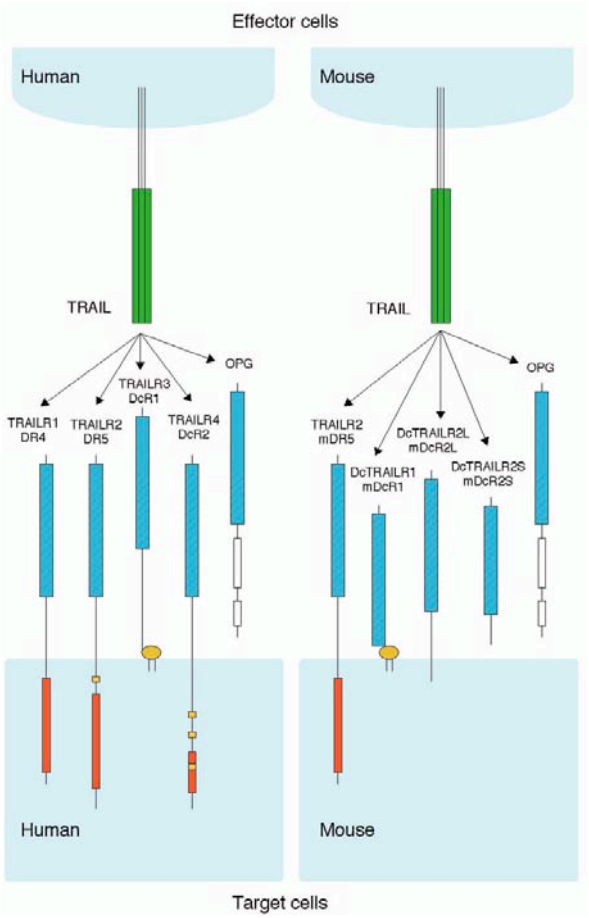

Figure 1.1. TRAIL receptors in human and mouse (adapted from (23)). TRAIL binds to two functional receptors, DR4 and DR5, in human, and one functional receptor in mouse, mDR5. Functional receptors encode intact death domain and can therefore transmit signals, which may result in induction of apoptosis. Also, TRAIL can bind with DcR1, DcR2 and OPG in both species (mDcR1 and mDcR2 in mouse), which lack functional death domain and therefore act as decoy receptors.

1.3. TRAIL signaling pathway

Trimerization of DR4 and DR5 by TRAIL on the surface of target cells leads to recruitment of adaptor molecule Fas-associated death domain protein (FADD), which in turn leads to recruitment and activation of caspase-8 (24). In certain cell types, type I (type I proteins are characterized by having their amino terminus side exposed on the exterior side of the membrane and the carboxy terminus exposed on the cytoplasmic side), activation of caspase-8 is sufficient for subsequent activation of the effector caspase-3 to execute cellular apoptosis (extrinsic pathway, Fig. 1.2) (25). In other cell types, type II (type II membrane proteins are characterized by having their amino terminus exposed on the cytoplasmic side of the cell and the carboxy terminus exposed on the exterior), amplification occurs through the mitochondrial pathway (intrinsic pathway, Fig. 1.2), which is initiated by cleavage of Bid by caspase-8 (25). The truncated Bid (tBid) translocates to the mitochondria and leads to Bax and Bak-mediated release of cytochrome-c (cyt-c) and Smac/DIABLO from mitochondria. The released cyt-c binds to Apaf-1 to activate caspase-9, which in turn activates caspase-3. The Smac/DIABLO promotes caspase-3 activation by preventing IAPs from attenuating caspases. Activation of extrinsic and intrinsic pathways by TRAIL depends on the cellular context. As a potential resistance mechanism, in contrast to DR4 and DR5, DcR1 is a GPI-anchored membrane protein and does not mediate apoptosis; DcR2 contains a truncated death domain, which also does not mediate apoptosis. Hence, DcR1 and DcR2 may act as decoy receptors, which compete with DR4 and DR5 for TRAIL binding. Cellular Fas-associated death domain-like interleukin-1β-converting enzyme (FLICE)-like inhibitory protein (c-FLIP) can

prevent the recruitment of caspase-8. Bcl-2 and Bcl-xL can suppress the Bax/Bak-mediated release of cyt-c and Smac/DIABLO from mitochondria. IAPs can attenuate the activities of caspase-9 and caspase-3, although Smac/DIABLO can counteract IAPs (Fig. 1.2) (23). The cytoplasmic regions of DR5 and DcR2 contain potential TRAF-binding motifs, which may be responsible for NF-kB and MAP kinase activation by these receptors (23).

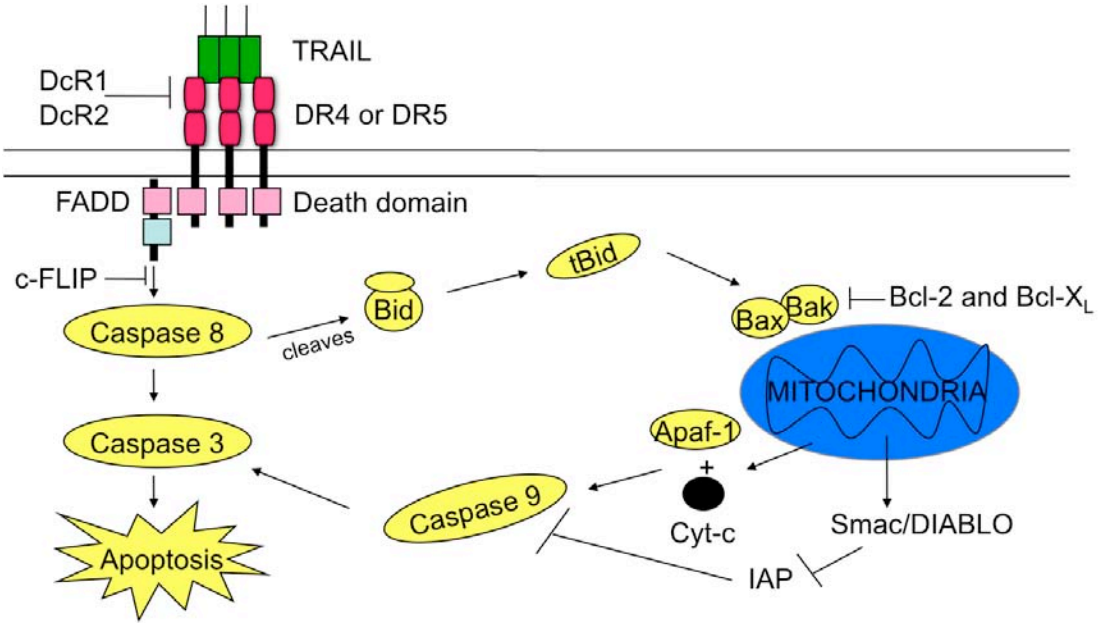

Figure 1.2. Schematic overview illustrating the TRAIL-induced apoptosis signaling pathway. Upon ligation of TRAIL ligand to its respective receptors DR4 and DR5, FADD protein is recruited, which in turn leads to recruitment and activation of caspase-8. Activation of caspase-8 leads to either activation of cell- extrinsic (mitochondria independent) or cell-intrinsic (mitochondria dependent) pathway. Both pathways lead to activation of active caspases such as caspase 3, which cause chromatin condensation and apoptosis.

1.4. c-FLIP as inhibitor of TRAIL functional receptors-mediated apoptosis

c-FLIP was initially identified in 1997 in various γ-herpesviruses and poxvirus MCV (26-28). Viral FLICE inhibitory proteins (v-FLIP) were named so as they displayed inhibitory effects on apoptosis through caspase-8 inhibition. In 1997 human cellular-FLIP (c-FLIP) was identified, also named FLAME-1, I-FLICE,

Casper, CASH, MRIT, CLARP, and usurpin, which is located on chromosome 2q33-34 (29-36). While there are 13 distinct splice variants of c-FLIP mRNA (37), three splice variants were detected at the protein level: c-FLIP$_L$, c-FLIPs and c-FLIP$_R$ (38).

Both c-FLIP$_L$ and c-FLIP$_s$ have been shown to interact with FADD and procaspase-8 and consequently, inhibit apoptosis induced by death receptors like FAS, DR4 and DR5 (Fig. 1.3 and Fig. 1.4) (29-31, 33-36). Although, c-FLIP proteins (c-FLIP$_S$ and c-FLIP$_L$) are recruited to the DISC, they do not preclude capsase-8 from recruitment to the DISC (39). c-FLIP$_L$ is cleaved into two subunits p43 and p12 subunits, p43 subunit remains at the DISC and p12 subunit releases (Fig. 1.4*A*) (39). In the presence of large amount c-FLIP$_L$, caspase-8 is incompletely cleaved upon recruitment to the DISC (Fig. 1.4.*C*) (39, 40). However, in presence of large amount of c-FLIPs, processing of capsase-8 is completely prevented at the DISC (Fig. 1.4.*D*) (40).

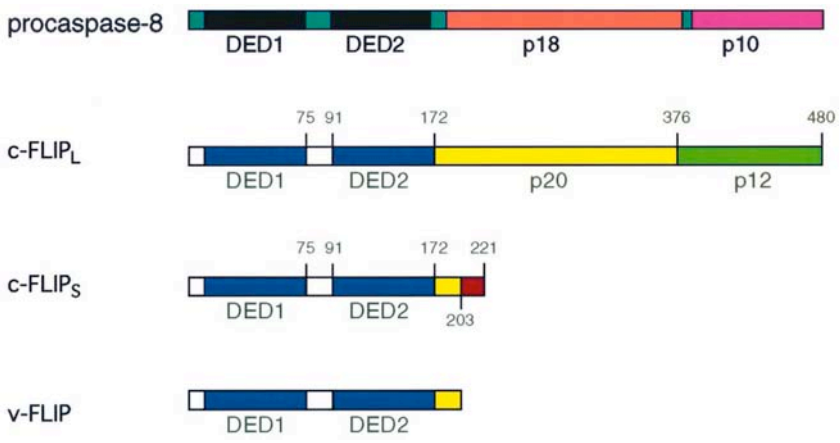

Figure 1.3. Diagram showing structural similarities between caspase-8 and c-FLIP proteins [adapted from (41)]. c-FLIP$_L$ encoded tandem death effector domains (DEDs) and caspase like domain; however, it lacks amino acid residues that are required for caspase activity. c-FLIPs and v-FLIP are similar consisting of two DEDs and a short c-terminal part.

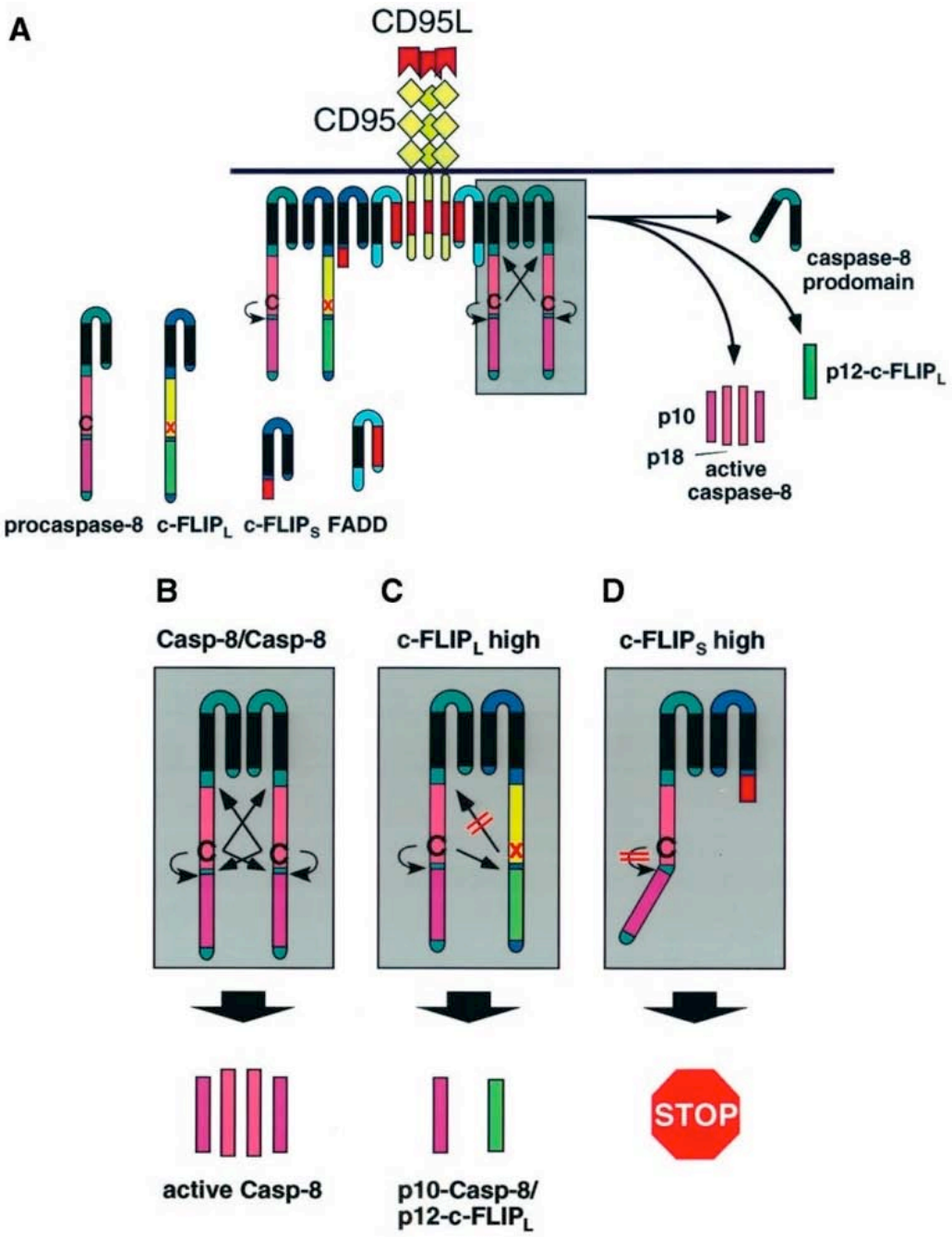

Figure 1.4. Model showing mechanism of action of c-FLIP at the DISC [adapted from (41)]. **A)** CD95L binds with CD95 and induces formation of the DISC. B-D) The ratio of procaspe-8 and c-FLIP proteins at the DISC controls cleavage and activation of caspase-8. **B)** In presence of small amount of c-FLIP, procaspase-8 is cleaved, producing active caspase-8 heterotetramer composed of the p18 and p10 subunits. **C)** In the presence of high amount of c-FLIP$_L$, procaspase-8 is cleaved upon recruitment to the DISC; however, its cleavage is incomplete. **D)** In the presence of a large amount of c-FLIP$_s$ recruitment of procaspase-8 at the DISC occurs; however, procaspase-8 remains unprocessed.

1.5. TRAIL and immunosurveillance

Natural killer (NK) cells and cytotoxic T lymphocytes both have the ability to destroy tumor cells by various mechanisms, one of them being the production of death ligands such as FasL or TRAIL. While TRAIL mRNA is constitutively expressed in a wide variety of normal tissues, the expression of functional TRAIL protein appears to be rather restricted to immune cells (42-48). In addition, TRAIL-deficient mice do not show large abnormalities, except for impaired tumor immunosurveillance and higher sensitivity to experimental autoimmune diseases, such as collagen-induced arthritis (CIA), streptozotocin-induced diabetes, and experimental autoimmune encephalomyelitis (EAE). These facts support the hypothesis of the physiological role of TRAIL in the immune system (23, 49-51).

TRAIL is involved in the cytotoxic activity of activated NK cells directed against tumor cells *in vitro* (52), and is at least in part responsible for their antimetastatic activities *in vivo* (53, 54). The physiological regulation of NK cell activity is largely dependent on expression of MHC class I molecules. In normal cells, NK cells receive inhibitory stimulation from MHC class I molecules on the surface of their respective target cells. Nevertheless, expression of stimulatory molecules, such as CD27 or CD28, was also found in NK cells. These receptors may activate NK cell function upon interaction with their specific ligands, CD70 or CD80/CD86 respectively, which are found to be expressed in a variety of tumors (55). TRAIL has been shown to play a critical role in interferon (IFN)-γ-dependent NK cell protection from tumor metastasis (56, 57). Malignant transformation of cells may result in expression of some ligand for NK cell-activating receptor (NKR) and/or downregulation of

MHC class I (MHC-I) molecules engaging NK cell inhibiting receptor (KIR), thereby activating NK cells. The activated NK cells produce IFN-γ, which in turn up-regulates TRAIL expression on NK cells and sensitizes transformed cells to TRAIL, resulting in tumor suppression (Fig. 1.5).

Furthermore, IFN-producing killer dendritic cells (IKDCs) mediate lysis of tumor cells, which are poorly recognized by NK cells, by secreting high levels of IFN-γ followed by TRAIL dependent apoptosis (58). A number of recent studies using neutralizing antibodies to TRAIL, or TRAIL-/- mice, showed that TRAIL could limit the development of experimental tumors (52, 54). In these mouse tumor models, liver NK cells were the important source of TRAIL, and were responsible for protection against liver metastasis of TRAIL-sensitive tumors (49, 52, 54, 59). The *in vivo* effect of IL-12 or α-galactosylceramide (α-GalCer) appeared to be due, at least, to an increase in the level of IFN-γ and TRAIL in these mice following the biological therapies (57, 60). A role for TRAIL in host immunosurveillance against primary tumor development has also been described (49, 52, 61). All these findings provide support for the physiological function of TRAIL as a tumor surveillance factor.

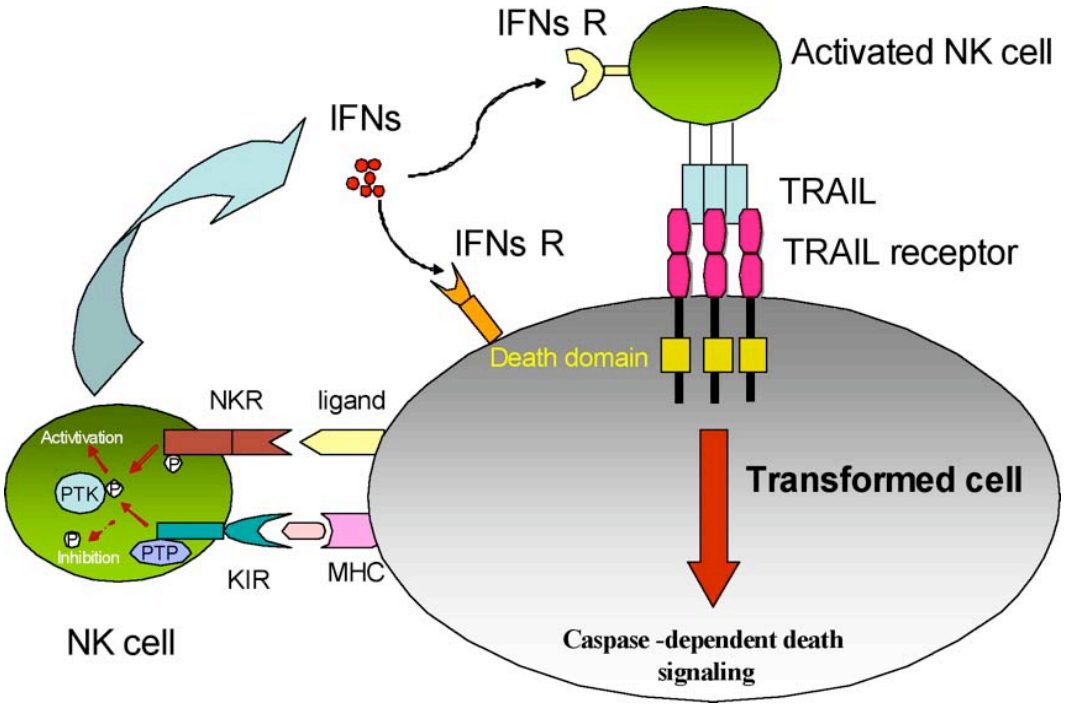

Figure 1.5. **The model indicates the role of TRAIL in immunosurveillance hindering tumor development.** Natural killer cell activating receptors (NKR) recognize ligands on tumor cells and activate protein tyrosine kinase (PTK), whose activity is inhibited by killer inhibitory receptors (KIR) that recognize MHC class I antigens and activate protein tyrosine phosphatases (PTP). The activated NK cells produce IFN-γ, which subsequently activates expression of TRAIL on activated NK cells. As a result, activated NK cells eliminate the transformed cells in a TRAIL-dependent manner.

1.6. References

1. Jemal A, Siegel R, Ward E, Hao Y, Xu J, Thun MJ. Cancer statistics, 2009. CA Cancer J Clin 2009 Jul-Aug;59(4):225-49.

2. Landen CN, Jr., Birrer MJ, Sood AK. Early events in the pathogenesis of epithelial ovarian cancer. J Clin Oncol 2008 Feb 20;26(6):995-1005.

3. Wong AS, Auersperg N. Ovarian surface epithelium: family history and early events in ovarian cancer. Reprod Biol Endocrinol 2003 Oct 7;1:70.

4. Fathalla MF. Factors in the causation and incidence of ovarian cancer. Obstet Gynecol Surv 1972 Nov;27(11):751-68.

5. Wajant H, Pfizenmaier K, Scheurich P. TNF-related apoptosis inducing ligand (TRAIL) and its receptors in tumor surveillance and cancer therapy. Apoptosis 2002 Oct;7(5):449-59.

6. Wiley SR, Schooley K, Smolak PJ, et al. Identification and characterization of a new member of the TNF family that induces apoptosis. Immunity 1995 Dec;3(6):673-82.

7. Pitti RM, Marsters SA, Ruppert S, Donahue CJ, Moore A, Ashkenazi A. Induction of apoptosis by Apo-2 ligand, a new member of the tumor necrosis factor cytokine family. J Biol Chem 1996 May 31;271(22):12687-90.

8. Hymowitz SG, O'Connell MP, Ultsch MH, et al. A unique zinc-binding site revealed by a high-resolution X-ray structure of homotrimeric Apo2L/TRAIL. Biochemistry 2000 Feb 1;39(4):633-40.

9. Cha SS, Kim MS, Choi YH, et al. 2.8 A resolution crystal structure of human TRAIL, a cytokine with selective antitumor activity. Immunity 1999 Aug;11(2):253-61.

10. Ashkenazi A. Targeting death and decoy receptors of the tumour-necrosis factor superfamily. Nat Rev Cancer 2002 Jun;2(6):420-30.

11. Clancy L, Mruk K, Archer K, et al. Preligand assembly domain-mediated ligand-independent association between TRAIL receptor 4 (TR4) and TR2 regulates TRAIL-induced apoptosis. Proc Natl Acad Sci U S A 2005 Dec 13;102(50):18099-104.

12. Degli-Esposti MA, Dougall WC, Smolak PJ, Waugh JY, Smith CA, Goodwin RG. The novel receptor TRAIL-R4 induces NF-kappaB and protects against TRAIL-mediated apoptosis, yet retains an incomplete death domain. Immunity 1997 Dec;7(6):813-20.

13. Degli-Esposti MA, Smolak PJ, Walczak H, et al. Cloning and characterization of TRAIL-R3, a novel member of the emerging TRAIL receptor family. J Exp Med 1997 Oct 6;186(7):1165-70.

14. Walczak H, Degli-Esposti MA, Johnson RS, et al. TRAIL-R2: a novel apoptosis-mediating receptor for TRAIL. EMBO J 1997 Sep 1;16(17):5386-97.

15. Truneh A, Sharma S, Silverman C, et al. Temperature-sensitive differential affinity of TRAIL for its receptors. DR5 is the highest affinity receptor. J Biol Chem 2000 Jul 28;275(30):23319-25.

16. Schneider P, Olson D, Tardivel A, et al. Identification of a new murine tumor necrosis factor receptor locus that contains two novel murine receptors for tumor necrosis factor-related apoptosis-inducing ligand (TRAIL). J Biol Chem 2003 Feb 14;278(7):5444-54.

17. Wang S, El-Deiry WS. TRAIL and apoptosis induction by TNF-family death receptors. Oncogene 2003 Nov 24;22(53):8628-33.

18. Pai SI, Wu GS, Ozoren N, et al. Rare loss-of-function mutation of a death receptor gene in head and neck cancer. Cancer Res 1998 Aug 15;58(16):3513-8.

19. Lee SH, Shin MS, Kim HS, et al. Alterations of the DR5/TRAIL receptor 2 gene in non-small cell lung cancers. Cancer Res 1999 Nov 15;59(22):5683-6.

20. Shin MS, Kim HS, Lee SH, et al. Mutations of tumor necrosis factor-related apoptosis-inducing ligand receptor 1 (TRAIL-R1) and receptor 2 (TRAIL-R2) genes in metastatic breast cancers. Cancer Res 2001 Jul 1;61(13):4942-6.

21. Arai T, Akiyama Y, Okabe S, Saito K, Iwai T, Yuasa Y. Genomic organization and mutation analyses of the DR5/TRAIL receptor 2 gene in colorectal carcinomas. Cancer Lett 1998 Nov 27;133(2):197-204.

22. Jeng YM, Hsu HC. Mutation of the DR5/TRAIL receptor 2 gene is infrequent in hepatocellular carcinoma. Cancer Lett 2002 Jul 26;181(2):205-8.

23. Yagita H, Takeda K, Hayakawa Y, Smyth MJ, Okumura K. TRAIL and its receptors as targets for cancer therapy. Cancer Sci 2004 Oct;95(10):777-83.

24. Peter ME. The TRAIL DISCussion: It is FADD and caspase-8! Cell Death Differ 2000 Sep;7(9):759-60.

25. Scaffidi C, Fulda S, Srinivasan A, et al. Two CD95 (APO-1/Fas) signaling pathways. Embo J 1998 Mar 16;17(6):1675-87.

26. Bertin J, Armstrong RC, Ottilie S, et al. Death effector domain-containing herpesvirus and poxvirus proteins inhibit both Fas- and TNFR1-induced apoptosis. Proc Natl Acad Sci U S A 1997 Feb 18;94(4):1172-6.

27. Hu S, Vincenz C, Buller M, Dixit VM. A novel family of viral death effector domain-containing molecules that inhibit both CD-95- and tumor necrosis factor receptor-1-induced apoptosis. J Biol Chem 1997 Apr 11;272(15):9621-4.

28. Thome M, Schneider P, Hofmann K, et al. Viral FLICE-inhibitory proteins (FLIPs) prevent apoptosis induced by death receptors. Nature 1997 Apr 3;386(6624):517-21.

29. Goltsev YV, Kovalenko AV, Arnold E, Varfolomeev EE, Brodianskii VM, Wallach D. CASH, a novel caspase homologue with death effector domains. J Biol Chem 1997 Aug 8;272(32):19641-4.

30. Han DK, Chaudhary PM, Wright ME, et al. MRIT, a novel death-effector domain-containing protein, interacts with caspases and BclXL and initiates cell death. Proc Natl Acad Sci U S A 1997 Oct 14;94(21):11333-8.

31. Hu S, Vincenz C, Ni J, Gentz R, Dixit VM. I-FLICE, a novel inhibitor of tumor necrosis factor receptor-1- and CD-95-induced apoptosis. J Biol Chem 1997 Jul 11;272(28):17255-7.

32. Inohara N, Koseki T, Hu Y, Chen S, Nunez G. CLARP, a death effector domain-containing protein interacts with caspase-8 and regulates apoptosis. Proc Natl Acad Sci U S A 1997 Sep 30;94(20):10717-22.

33. Irmler M, Thome M, Hahne M, et al. Inhibition of death receptor signals by cellular FLIP. Nature 1997 Jul 10;388(6638):190-5.

34. Rasper DM, Vaillancourt JP, Hadano S, et al. Cell death attenuation by 'Usurpin', a mammalian DED-caspase homologue that precludes caspase-8 recruitment and activation by the CD-95 (Fas, APO-1) receptor complex. Cell Death Differ 1998 Apr;5(4):271-88.

35. Shu HB, Halpin DR, Goeddel DV. Casper is a FADD- and caspase-related inducer of apoptosis. Immunity 1997 Jun;6(6):751-63.

36. Srinivasula SM, Ahmad M, Ottilie S, et al. FLAME-1, a novel FADD-like anti-apoptotic molecule that regulates Fas/TNFR1-induced apoptosis. J Biol Chem 1997 Jul 25;272(30):18542-5.

37. Djerbi M, Darreh-Shori T, Zhivotovsky B, Grandien A. Characterization of the human FLICE-inhibitory protein locus and comparison of the anti-apoptotic activity of four different flip isoforms. Scand J Immunol 2001 Jul-Aug;54(1-2):180-9.

38. Yang JK. FLIP as an anti-cancer therapeutic target. Yonsei Med J 2008 Feb 29;49(1):19-27.

39. Scaffidi C, Schmitz I, Krammer PH, Peter ME. The role of c-FLIP in modulation of CD95-induced apoptosis. J Biol Chem 1999 Jan 15;274(3):1541-8.

40. Krueger A, Schmitz I, Baumann S, Krammer PH, Kirchhoff S. Cellular FLICE-inhibitory protein splice variants inhibit different steps of caspase-8 activation at the CD95 death-inducing signaling complex. J Biol Chem 2001 Jun 8;276(23):20633-40.

41. Krueger A, Baumann S, Krammer PH, Kirchhoff S. FLICE-inhibitory proteins: regulators of death receptor-mediated apoptosis. Mol Cell Biol 2001 Dec;21(24):8247-54.

42. Kayagaki N, Yamaguchi N, Nakayama M, et al. Involvement of TNF-related apoptosis-inducing ligand in human CD4+ T cell-mediated cytotoxicity. J Immunol 1999 Mar 1;162(5):2639-47.

43. Kayagaki N, Yamaguchi N, Nakayama M, Eto H, Okumura K, Yagita H. Type I interferons (IFNs) regulate tumor necrosis factor-related apoptosis-inducing ligand (TRAIL) expression on human T cells: A novel mechanism for the antitumor effects of type I IFNs. J Exp Med 1999 May 3;189(9):1451-60.

44. Kayagaki N, Yamaguchi N, Nakayama M, et al. Expression and function of TNF-related apoptosis-inducing ligand on murine activated NK cells. J Immunol 1999 Aug 15;163(4):1906-13.

45. Griffith TS, Wiley SR, Kubin MZ, Sedger LM, Maliszewski CR, Fanger NA. Monocyte-mediated tumoricidal activity via the tumor necrosis factor-related cytokine, TRAIL. J Exp Med 1999 Apr 19;189(8):1343-54.

46. Nakayama M, Kayagaki N, Yamaguchi N, Okumura K, Yagita H. Involvement of TWEAK in interferon gamma-stimulated monocyte cytotoxicity. J Exp Med 2000 Nov 6;192(9):1373-80.

47. Fanger NA, Maliszewski CR, Schooley K, et al. Human dendritic cells mediate cellular apoptosis via tumor necrosis factor-related apoptosis-inducing ligand (TRAIL)

Monocyte-mediated tumoricidal activity via the tumor necrosis factor-related cytokine, TRAIL. J Exp Med 1999 Oct 18

Apr 19;190(8):1155-64.

48. Koga Y, Matsuzaki A, Suminoe A, Hattori H, Hara T. Neutrophil-derived TNF-related apoptosis-inducing ligand (TRAIL): a novel mechanism of antitumor effect by neutrophils. Cancer Res 2004 Feb 1;64(3):1037-43.

49. Cretney E, Takeda K, Yagita H, Glaccum M, Peschon JJ, Smyth MJ. Increased susceptibility to tumor initiation and metastasis in TNF-related

apoptosis-inducing ligand-deficient mice. J Immunol 2002 Feb 1;168(3):1356-61.

50. Sedger LM, Glaccum MB, Schuh JC, et al. Characterization of the in vivo function of TNF-alpha-related apoptosis-inducing ligand, TRAIL/Apo2L, using TRAIL/Apo2L gene-deficient mice. Eur J Immunol 2002 Aug;32(8):2246-54.

51. Lamhamedi-Cherradi SE, Zheng SJ, Maguschak KA, Peschon J, Chen YH. Defective thymocyte apoptosis and accelerated autoimmune diseases in TRAIL-/- mice. Nat Immunol 2003 Mar;4(3):255-60.

52. Takeda K, Smyth MJ, Cretney E, et al. Critical role for tumor necrosis factor-related apoptosis-inducing ligand in immune surveillance against tumor development. J Exp Med 2002 Jan 21;195(2):161-9.

53. Smyth MJ, Hayakawa Y, Takeda K, Yagita H. New aspects of natural-killer-cell surveillance and therapy of cancer. Nat Rev Cancer 2002 Nov;2(11):850-61.

54. Takeda K, Smyth MJ, Cretney E, et al. Involvement of tumor necrosis factor-related apoptosis-inducing ligand in NK cell-mediated and IFN-gamma-dependent suppression of subcutaneous tumor growth. Cell Immunol 2001 Dec 15;214(2):194-200.

55. Kelly JM, Darcy PK, Markby JL, et al. Induction of tumor-specific T cell memory by NK cell-mediated tumor rejection. Nat Immunol 2002 Jan;3(1):83-90.

56. Takeda K, Hayakawa Y, Smyth MJ, et al. Involvement of tumor necrosis factor-related apoptosis-inducing ligand in surveillance of tumor metastasis by liver natural killer cells. Nat Med 2001 Jan;7(1):94-100.

57. Smyth MJ, Cretney E, Takeda K, et al. Tumor necrosis factor-related apoptosis-inducing ligand (TRAIL) contributes to interferon gamma-dependent natural killer cell protection from tumor metastasis. J Exp Med 2001 Mar 19;193(6):661-70.

58. Taieb J, Chaput N, Menard C, et al. A novel dendritic cell subset involved in tumor immunosurveillance. Nat Med 2006 Feb;12(2):214-9.

59. Seki N, Hayakawa Y, Brooks AD, et al. Tumor necrosis factor-related apoptosis-inducing ligand-mediated apoptosis is an important endogenous mechanism for resistance to liver metastases in murine renal cancer. Cancer Res 2003 Jan 1;63(1):207-13.

60. Hayakawa Y, Takeda K, Yagita H, et al. Critical contribution of IFN-gamma and NK cells, but not perforin-mediated cytotoxicity, to anti-metastatic effect of alpha-galactosylceramide. Eur J Immunol 2001 Jun;31(6):1720-7.

61. Cretney E, Shanker A, Yagita H, Smyth MJ, Sayers TJ. TNF-related apoptosis-inducing ligand as a therapeutic agent in autoimmunity and cancer. Immunol Cell Biol 2006 Feb;84(1):87-98.

62. Smyth MJ, Takeda K, Hayakawa Y, Peschon JJ, van den Brink MR, Yagita H. Nature's TRAIL--on a path to cancer immunotherapy. Immunity 2003 Jan;18(1):1-6.

2. Aim of my PhD thesis

The overall aim of my PhD study was to decipher the key role of the TRAIL signaling pathway in terms of DR5 and c-FLIP$_L$ in inhibiting OC development. Moreover, I also aimed to shed some light on the mechanisms by which OC cells escape the natural immunosurveillance and subsequently acquire the potential to develop overt malignancy.

In the course of my PhD thesis I used two different animal models that made it possible to investigate different aspects of TRAIL-mediated cytotoxicity in protecting the host from ovarian tumor formation *in vivo*:

The xenograft mouse model reflects similarities with human OC but tumorigenesis can only be studied in immune deficient animals providing a strategy to model late stages of OC progression. I prepared and inoculated parental and genetically modified human OC cells in nude mice which lack T cell lympocytes and therefore prevent xenograft rejection of the introduced tumors. This model offered an ideal environment to perform *in vivo* functional analysis of the role of DR5 and c-FLIP$_L$ in human ovarian tumor development, which is not possible in an immunocompetent mouse model.

The syngeneic mouse model naturally displays species differences with human cancer, but tumorigenesis can be studied in an immunocompetent setting, which reflects both early and late stages of the disease. I applied this model in pathogen-free C57BL/6 mice.

To provide a clear layout of my PhD thesis, two specific aims were defined:

Specific Aim-I. Functional analysis of TRAIL signaling pathway in OC progression. In particular, my aim was to describe the molecular basis of DR5 and c-$FLIP_L$ on the outgrowth of ovarian tumor *in vitro* and *in vivo.* Moreover, I also aimed to study the role of NK-mediated tumor immunity against OC.

Specific Aim-II. Characterisation of the TRAIL pathway in a syngeneic mouse model of OC. Specifically, I aimed to analyze the expression of mDR5, c-FLIP, and caspase-8 in ten established transformed mouse ovarian surface epithelial (MOSE) cell lines and to compare their expression to normal (non-tumorigenic) MOSE cells, as well as to measure their sensitivity to TRAIL-induced apoptosis. Furthermore, I aimed to apply loss of function approach to analyze the influence of DR5 on the development of OC in immunocompetent mice.

3. Results and Discussion

3.1. Natural immunity enhances the activity of a DR5 agonistic antibody and carboplatin in the treatment of ovarian cancer (manuscript submitted)

Ahmed El-Gazzar [1], Paul Perco [2], Eva Eckelhart [3], Mariam Anees [1], Veronika Sexl [3], Bernd Mayer [2], Yanxin Liu [4], Wolfgang Mikulits [5], Reinhard Horvat [6], Thomas Pangerl [1], Dexian Zheng [4], Michael Krainer [1]

[1] Division of Oncology, Department of Medicine I, Medical University of Vienna, Waehringer Guertel 18-20, 1090 Vienna, Austria; [2] Institute for Theoretical Chemistry, University of Vienna, Waehringerstrasse 17, 1090 Vienna, Austria; [3] Institute of Pharmacology, Medical University of Vienna, Waehringerstrasse 13A, 1090 Vienna, Austria; [4] National Laboratory of Medical Molecular Biology, Institute of Basic Medical Sciences, Chinese Academy of Medical Sciences and Peking Union Medical College, 5 Dong Dan San Tiao, Beijing 100005, China; [5] Institute of Cancer Research, Department of Medicine I, Medical University of Vienna, Borschkegasse 8a, 1090 Vienna, Austria; [6] Department of Pathophysiology, Medical University of Vienna, Waehringer Guertel 18-20, 1090 Vienna, Austria.

Running title: Natural immunity enhances activity of AD5-10.

Key words: ovarian cancer; TRAIL; apoptosis; immunosurveillance; DR5 agonistic antibody.

Correspondence to:

Michael Krainer, MD

Division of Oncology

Department of Medicine I

Medical University of Vienna

Waehringer Guertel 18-20, 1090 Vienna, Austria

Phone: +43 1 40400 7572

Fax: +43 1 40400 4687

E-mail: michael.krainer@meduniwien.ac.at

Funding: This work was supported by the Austrian Science Fund (FWF) (grant number P20715).

Disclosure of potential conflicts of interest: No potential conflicts of interest were disclosed.

Abstract

The TNF-related apoptosis-inducing ligand (TRAIL) induces apoptosis specifically in cancer cells with little effect on normal cells. We have previously demonstrated that TRAIL signaling is altered in most ovarian cancer (OC) patients, and that resistance to TRAIL contributes to OC progression. In this study we investigated whether resistance to TRAIL may be overcome by a monoclonal TRAILR2 (DR5) agonistic antibody (AD5-10). We found that the joint presence of AD5-10 with TRAIL and NK-cells expressed TRAIL resensitizes OC cells to apoptosis *in vitro* and *in vivo* respectively. The combination of AD5-10 with carboplatin exerts a more than additive effect *in vitro*, which may at least partially be explained by the fact that carboplatin triggers DR5 expression on OC cells. Moreover, AD5-10 restores the sensitivity of platin-resistant OC to carboplatin *in vivo*. In addition, we found that TRAIL expression and natural killer (NK) cells are abundant in the tumor microenvironment, and that depletion of NK cells abolishes the antitumor activity of AD5-10. This indicates that NK-mediated immunosurveillance against OC might be mediated by TRAIL and that apoptosis-induced by AD5-10 requires the presence of NK cells. In conclusion, this study indicates a key role and strong antitumorigenic effect of DR5, and highlights a novel link between NK-mediated immunosurveillance and activation of DR5-mediated apoptosis in OC.

Introduction

Ovarian cancer (OC) is the most lethal gynaecological cancer and the fifth leading cause of cancer-related deaths among women in western industrialized countries (1, 2). OC originating from the ovarian surface epithelium (OSE) is the most common form and displays a range of histological subtypes (3). While most OCs are sensitive to platin-based chemotherapy at the time of diagnosis, recurrence of the disease is frequent, and ultimately platin-resistant disease develops in all patients.

Apoptosis is important for maintaining cellular homeostasis in normal tissues by eliminating disordered cells, and defects in the apoptosis pathway may lead to cancer (4). The apoptotic cascade can be stimulated by death receptors, resulting in activation of caspases (5). Trimerization of TRAIL (tumor necrosis factor related apoptosis-inducing ligand) functional receptors TRAILR1 (DR4) or TRAILR2 (DR5) by their ligands leads to assembly of the death-inducing signaling complex (DISC), which initiates the apoptotic cascade (6). DR4 and DR5 are characterized by an extracellular cystein-rich domain and an intracellular death domain, giving them the ability to trigger the assembly of the DISC. We have previously found that TRAIL is highly expressed in the human OC microenvironment, but that tumor tissues display a reduced number of TRAIL functional receptors (7).

One major physiological role of TRAIL is the mediation of natural immunity and the elimination of developing tumors (8, 9). Previous studies have shown that soluble TRAIL, or agonistic monoclonal antibodies specific for functional TRAIL receptors, exhibit tumoricidal activities, a phenomenon that has been tested in clinical trials (10). The agonistic human DR5 specific

monoclonal antibody AD5-10 used in this study was reported to mediate antitumor effects in various tumor cells and due to its unique binding site does not compete with TRAIL for binding to DR5 in contrast to other agonistic DR5 antibodies (11).

In the current study, we identified the functional role of DR5 in OC progression, and shed light on a novel strategy to eliminate OC in a preclinical mouse model. Moreover, we show for the first time that the function of NK cells is necessary for the activation of DR5-mediated apoptosis and that the presence of NK cells is highly correlated with a longer life span in xenograft mice.

Material and methods

Drugs

Carboplatin, paclitaxel (both EBEWE), bevacizumab (Roche), lapatinib (GlaxoSmithKline), agonistic DR5 monoclonal antibody (AD5-10) prepared as described previously (11), and recombinant human soluble TRAIL (Alexis) were used for stimulation of OC cell lines at various concentrations.

Cell culture

The human OC cell lines MDAH-2774 (ovarian endometroid adenocarcinoma (OEA)-derived cell line, originating from ascitic fluid of a patient (12)), and a platin resistant sub-line of the OC cell line A2780 (human epithelial OC cell line established from tumor tissue (13)) were cultured in RPMI 1640 medium (Invitrogen). The OC cell line ES-2 (human ovarian clear cell carcinoma cell line taken from a 47-year-old woman (14)) was cultured in McCoy's medium (Invitrogen). Medium was supplemented with 10% FCS (PAA Laboratories GmbH), 1 mmol/L glutamine, and 1% penicillin/streptomycin (PAA Laboratories GmbH). MDAH-2774 and ES-2 cell lines were obtained from the American Type Culture Collection (ATCC, Manassas, VA), and the cell line A2780 was obtained from the European Collection of Cell Cultures (ECACC, Salisbury, Wiltshire, UK).

Determination of apoptosis

MDAH-2774, A2780, and ES-2 OC cell lines were plated at a density of 5 x 10^4 cells/well in 24-well plates and incubated for 24 h prior to stimulation. Then cells were treated with either AD5-10 (1 µg/ml) or carboplatin (100

µg/ml), paclitaxel (0.05 µM), bevacizumab (100 ng/ml), lapatinib (4 µM) or with an antibody–drug combination for 24 h. Cells were harvested by trypsinization using 0.05% trypsin and 0.02% EDTA without Ca^{2+} and Mg^{2+} (PAA Laboratories GmbH). Apoptosis was determined by an annexin V-FITC apoptosis detection kit (Alexis) according to the manufacturer's instructions. Flow cytometry of annexin V-FITC and Pidium Iodide (PI) staining was performed using FACScan (Becton Dickinson) with CELLQuest Pro software.

Immunoblotting analysis

Western blot analysis was performed according to the standard protocol. Briefly, proteins were extracted from cells lysed for 30 min at 4^{o}C in RIPA+ buffer supplemented with complete protease inhibitor (Roche) and 1 mM orthovanadat, followed by high speed centrifugation. Protein concentration was determined according to the method of Bradford (Sigma-Aldrich). Equal amounts of protein (~ 50 µg protein per lane) were separated by 12% SDS-PAGE gel and electroblotted onto PVDF membranes (GE Healthcare). The membrane proteins were incubated with the following primary antibodies: mouse anti-caspase-8 monoclonal antibody, 12F5 (recognizes human procaspase-8 and active human caspase-8, Alexis), mouse anti-caspase-3 monoclonal antibody, 31A1067 (recognizes human procaspase-3 and active human caspase-3, Imgenex), mouse anti-p53 monoclonal antibody (Cell Signaling), and goat anti-actin polyclonal antibody (Santa Cruz). Detection was performed with the appropriate peroxidase-conjugated (HRP) secondary antibody (Santa Cruz). The membranes were developed using enhanced chemoluminescence (ECL, Amersham).

Detection of TRAIL ligand and its functional receptor expression by flow cytometry

MDAH-2774, A2780, and ES-2 OC cell lines were collected and washed in PBS. The cells were then incubated with mouse monoclonal antibodies against human TRAILR1, HS101 (Alexis), human TRAILR2, HS201 (Alexis), or mouse IgG1 isotype control (Ancell) for 1 h at 4^{o}C. Afterwards, cells were washed in PBS, incubated with goat anti-mouse IgG-FITC (Santa Cruz) for 1 h at 4^{o}C in the dark and washed with PBS and analysed by flow cytometry. TRAIL intracellular staining was performed as described previously (15). Briefly, cells were washed with PBS and resuspended in 2% formaldehyde and incubated for 10 min at 4^{o}C. Afterwards, cells were washed with PBS and resuspended in blocking solution (0.1% Saponin and 20% serum) and incubated for 20 min at room temperature. Cells were then stained with mouse monoclonal antibody against human TRAIL, III6F (Alexis) or mouse IgG2b isotype control (Ancell) for 30 min at room temperature in staining buffer (0.1% Saponin, 2% FCS serum). After that, cells were washed three times with staining buffer, resuspended in secondary antibody goat anti-mouse IgG-FITC (Santa Cruz), and incubated for 1 h at 4^{o}C in staining buffer. Then, cells were washed three times with staining buffer and analysed by flow cytometry. Flow cytometric analysis was performed using FACScan (Becton Dickinson) and the resulting data were analysed with CELLQuest Pro software.

Immunohistochemistry

Immunohistochemical analysis was performed using paraffin embedded sections as described previously (7). Briefly, tissue sections were deparaffinized and rehydrated. For epitope retrieval, specimens were incubated in 96°C pre-warmed 10 mM citrate buffer (pH 6.0) for 20 min. Slides were then incubated with 0.3% H_2O_2/PBS for 10 min at room temperature to block endogenous peroxidase. After blocking the background staining with serum of the secondary antibody (diluted 1:10 in PBS), tissues were incubated for 1 h at room temperature with primary antibody diluted in serum/PBS. The following primary antibodies were used: rabbit anti-human cleaved caspase-3 monoclonal antibody, Asp175 (dilution 1:50, Cell Signaling); mouse anti-human Ki-67 monoclonal antibody (dilution 1:200, Dako); goat anti-mouse TRAIL polyclonal antibody, AF1121 (dilution 1:100, R&D Systems); rabbit anti-human TRAILR1 polyclonal antibody, H130, (dilution 1:200, Santa Cruz); rat anti-mouse Ly-49G2 monoclonal antibody, 4D11 (16) (dilution 1:400, eBioscience). The appropriate secondary biotinylated antibodies (Vector Laboratories) were diluted with the serum/PBS-buffer (dilution 1:200) and incubated for 30 min at room temperature. Tissue sections were incubated with StreptABComplex/HRP (Dako) for 45 min at room temperature and then visualized with DAB (Dako) and counterstained with Mayer's Haematoxyline. Tissue sections were analysed on an Olympus BX50 upright light microscope (Olympus Europe) equipped with the Soft Imaging system CC12.

Apoptosis was measured by using an *in situ* cell death detection kit (Roche) according to the manufacturer's instructions. Afterwards the cells

were analysed on a fluorescence microscope (Nikon Eclipse 800) equipped with a Nikon DS-R1 camera, using the NIS-Elements software.

Negative controls were performed by excluding incubation with primary antibody, and yielded negative results. The percentage of positive cells was determined by a blinded operator.

Xenograft mouse model

Four to six week-old female athymic nude-Foxn1 nu/nu mice were obtained from Harlan (Italy) and maintained under specific pathogen-free conditions at the animal resource service of the Medical University of Vienna. Mice were subcutaneously inoculated with A2780 OC cells on both sides. Treatment started on day 2 by intraperitoneal injection of PBS, AD5-10, carboplatin, or the latter two in combination. Tumor size was measured every second day by calipers. The tumor volume was calculated according to the formula $V=4/3 \times \pi \times (L/2 \times W/2 \times W/2)$; L, length; W, width (17). At the end of the experiment, tumors were recovered and weighed and then prepared for histological and pathological analysis. Animal experiments were performed according to protocols approved by the Austrian Federal Ministry for Education, Science and Art. For NK depletion experiments, mice were treated with 20 µl anti-asialo GM1 antibody (Wako) and 100 µ g NK1.1 antibody (prepared as described previously (18)) 3 days before inoculation, and then every 4 days.

Generation of splenocytes and analysis of NK cells

The spleen was removed from sacrificed mice and placed into 60 mm tissue culture dishes. A single cell suspension was made by passing the tissue through a 70 µm nylon cell strainer (BD Bioscience) in PBS containing 2% FCS. Cells were centrifuged and hypotonic lysis of red blood cells was performed using ACK lysis buffer (0.15 M NH_4Cl, 1 mM $KHCO_3$, and 0.1 mM Na_2EDTA, pH 7.2), followed by resuspension in an appropriate volume of PBS containing 2% FCS. Cells were incubated at 4^oC with Fc-block (BD Bioscience) for 5 min, and then stained with PerCP Hamster anti-mouse CD3e, APC mouse anti-mouse NK-1.1, and FITC rat anti-mouse CD49b (BD Bioscience) antibodies for 30 min at 4^oC in PBS. After that, cells were washed three times with PBS and analysed by flow cytometry. Flow cytometric analysis was performed on FACSCalibur (BD Biosciences). Data were analysed using the CellQuest Pro software.

Statistical analysis

Two-sided Student's t-tests were used to detect statistically significant differences between study groups and controls, using R and Statstoft's Statistica software. Data were visualized with box plots or bar plots. *P* values below 0.05 were considered statistically significant, and *P* values below 0.005 were considered highly significant. The correlation between variables was estimated using the Pearson correlation coefficient.

Results

In vitro effect of combining AD5-10 with cytotoxic drugs

We have previously demonstrated that the TRAIL signaling pathway plays a fundamental role in OC progression (7, 19). In this study, we addressed the functional role of human DR5 using three distinct OC cell lines (MDAH-2774, A2780, ES-2). The selected OC cell lines have accumulated different mutational and epigenetic changes that alter normal cell growth and survival pathway e.g. mutated p53 in MDAH-2774 and ES-2, epigenetic silencing of DR4 in A2780, as well as upregulation of c-FLIP in most of them (19-22). Moreover, they express different levels of DR5 (Fig. 3.1.1*A*) and all of them were resistant to TRAIL-induced apoptosis. We found that AD5-10 triggered tumor cell apoptosis to a detectable extent and had an additive effect when combined with different pharmacological and cellular anticancer agents (paclitaxel, bevacizumab, and lapatinib; Fig. 3.1.1*B*). In combination with carboplatin, AD5-10 showed a more than additive effect (Fig. 3.1.1*B*), illustrated by comparing the sum effect of AD5-10 and carboplatin to a combination of both**.** This particular effect was observed in three different carboplatin-resistant OC cell lines and was confirmed by detection of active caspase cleavage fragments (Fig. 3.1.1*B* and *C*). The dose response curves for carboplatin in the presence of AD5-10 confirmed the observed effects (Fig. 3.1.1*D*). Together, these findings suggest that AD5-10-mediated stimulation of DR5 in the presence of carboplatin efficiently sensitizes OC cell lines to apoptosis.

A)

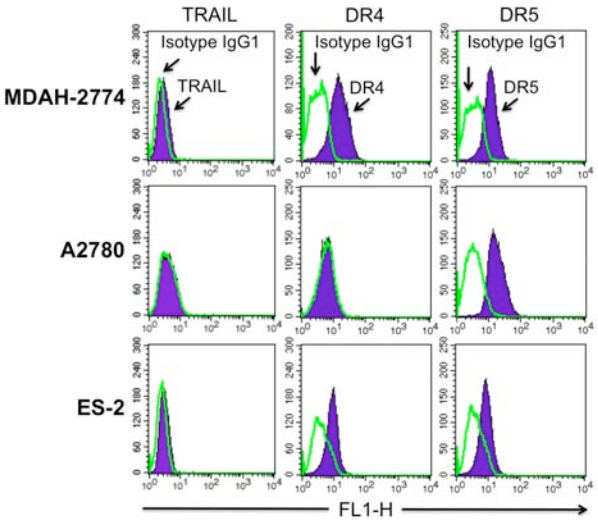
TRAIL
DR4
DR5
Isotype IgG1
Isotype IgG1
Isotype IgG1
TRAIL
DR4
DR5
MDAH-2774
A2780
ES-2
FL1-H

B)

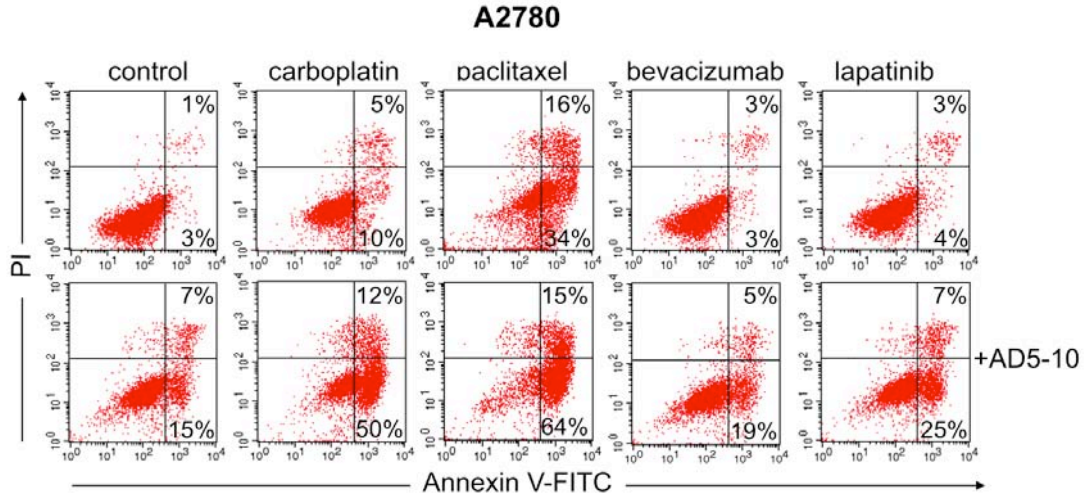
A2780
control
carboplatin
paclitaxel
bevacizumab
lapatinib
1%
3%
5%
10%
16%
34%
3%
3%
3%
4%
7%
15%
12%
50%
15%
64%
5%
19%
7%
25%
+AD5-10
PI
Annexin V-FITC

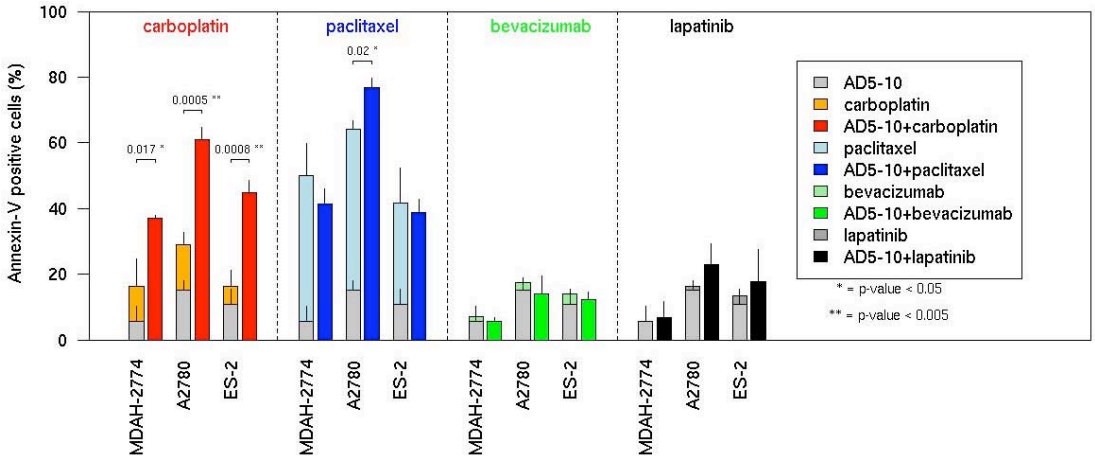
carboplatin
paclitaxel
bevacizumab
lapatinib
Annexin-V positive cells (%)
0.017 *
0.0005 **
0.0008 **
0.02 *
AD5-10
carboplatin
AD5-10+carboplatin
paclitaxel
AD5-10+paclitaxel
bevacizumab
AD5-10+bevacizumab
lapatinib
AD5-10+lapatinib
* = p-value < 0.05
** = p-value < 0.005
MDAH-2774
A2780
ES-2

C)

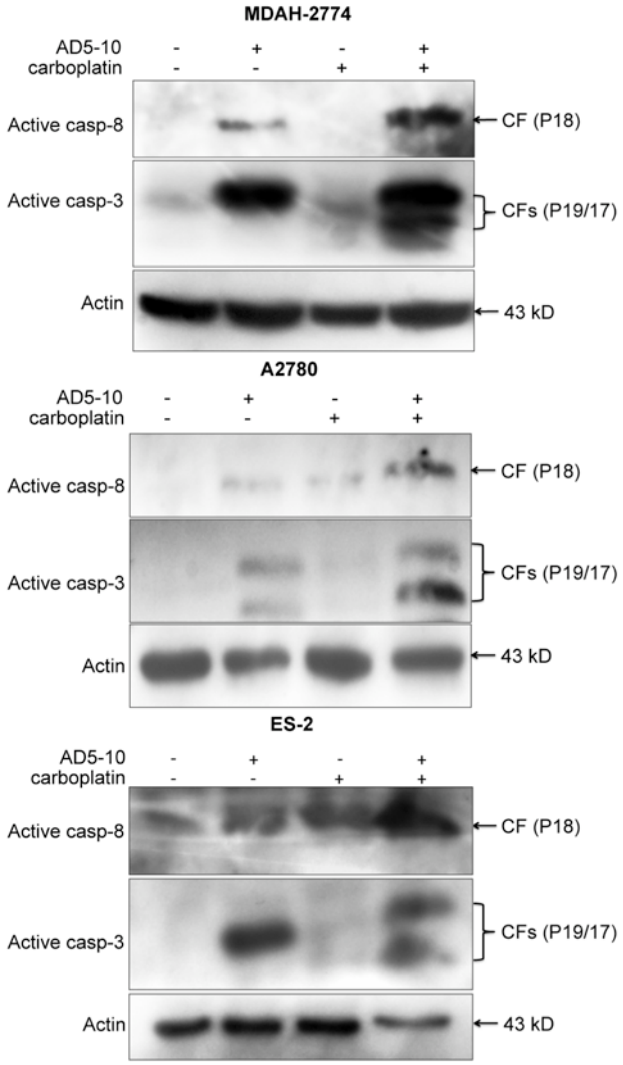
MDAH-2774
AD5-10
carboplatin
Active casp-8
Active casp-3
Actin
CF (P18)
CFs (P19/17)
43 kD
A2780
AD5-10
carboplatin
Active casp-8
Active casp-3
Actin
CF (P18)
CFs (P19/17)
43 kD
ES-2
AD5-10
carboplatin
Active casp-8
Active casp-3
Actin
CF (P18)
CFs (P19/17)
43 kD

D)

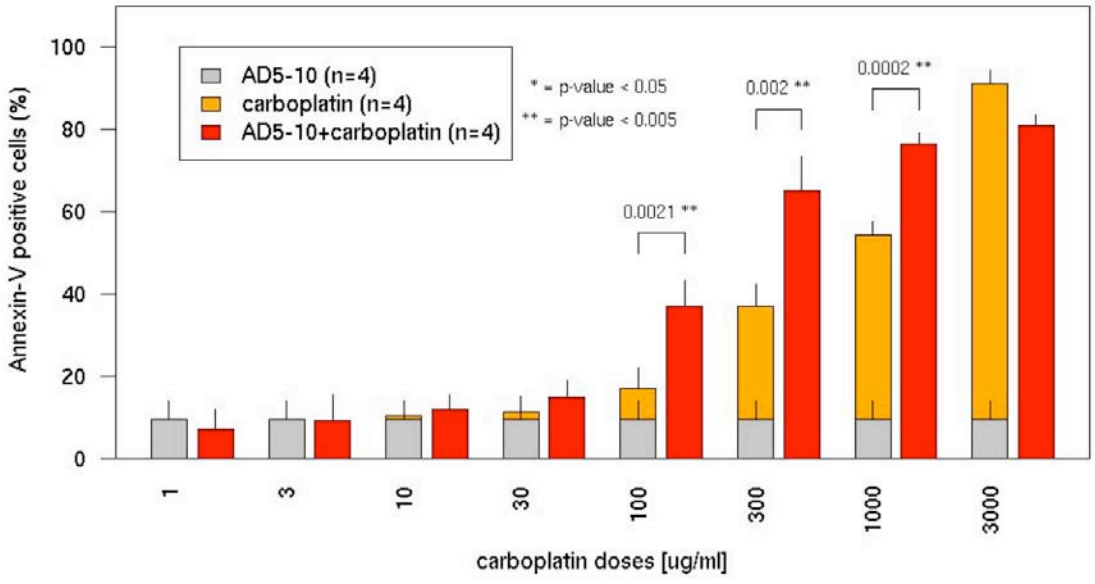
AD5-10 (n=4)
carboplatin (n=4)
AD5-10+carboplatin (n=4)
* = p-value < 0.05
** = p-value < 0.005
0.0021 **
0.002 **
0.0002 **
Annexin-V positive cells (%)
100
80
60
40
20
0
1
3
10
30
100
300
1000
3000
carboplatin doses [ug/ml]

Figure 3.1.1. Effect of combining AD5-10 with carboplatin *in vitro*. A) Histogram showing expression of the TRAIL ligand as well as its functional receptors DR4 and DR5 on the surface of selected OC cell lines as determined by flow cytometry. Selected OC cell lines were stained with either TRAIL ligand (III6F, Alexis), anti-DR4 (HS101, Alexis), anti-DR5 (HS201, Alexis) monoclonal antibody (coloured histogram), or isotype control IgG1 monoclonal antibody (unfilled histogram). Data represent three independent experiments. **B)** *Upper panel,* the A2780 OC cell line was treated with either AD5-10 (1 µg/ml), carboplatin (100 µg/ml), paclitaxel (0.05 µM), bevacizumab (100 ng/ml), lapatinib (4 µM) or with an antibody-drug combination for 24 h. Apoptosis was determined by annexin-V and PI staining. Numbers in dot plot quadrants represent the percentage of stained apoptotic cells. *Lower panel,* quantitative evaluation of upper panel as well as the apoptosis rate of MDAH-2774 and ES-2 OC cell lines. Columns represent the mean of three independent experiments; bars, ±S.E.M. (the standard error of the mean); *statistically significant (P<0.05), or **highly significant (P<0.005) differences obtained by comparing the sum effect of AD5-10 and carboplatin to a combination of both. **C)** Expression levels of activated caspase-8 and caspase-3 were determined by immunoblotting in untreated and treated OC cells using AD5-10 (1 µg/ml), carboplatin (100 µg/ml), or both. Data represent two independent experiments. CF, cleavage form. **D)** Dose response curve of carboplatin is presented using MDAH-2774 cells. MDAH-2774 OC cell line was incubated with the specified concentration of carboplatin, AD5-10 (1 µg/ml), or both for 24 h, and apoptosis was determined. Columns represent the mean of four independent experiments; bars, ±SE; **statistically highly significant (P<0.005) differences obtained by comparing the sum effect of AD5-10 and carboplatin to a combination of both. EC50 values of carboplatin shifted from 105.5 µg/ml to 172.6 µg/ml (95% confidence interval) in the presence of 1 µg/ml AD5-10.

Carboplatin cooperates with AD5-10 to trigger apoptosis in OC cells by upregulation of DR5

We then focused on the mechanism by which carboplatin cooperates with AD5-10 signaling to mediate enhanced tumor cell death. DR5 is a transcriptional target of p53 (23), and carboplatin has been shown to induce the p53 tumor suppressor pathway (24). In order to identify whether carboplatin cooperates with AD5-10 via upregulation of DR5 expression, we treated MDAH-2774 cells (overexpressing a mutated form of p53; Arg273His, (22)), A2780 cells (expressing wt p53, (20)), and ES-2 cells (expressing a mutated form of p53; S241F, (21)) with carboplatin and analysed the expression of p53 and DR5 by immunoblotting and flow cytometry, respectively (Fig. 3.1.2). The p53 status in selected OC cell lines was

confirmed by sequencing p53 in all three selected cell lines (data not shown). While DR5 expression levels were increased in all cell lines after carboplatin treatment, p53 expression was only increased in some (Fig. 3.1.2). Notably, DR5 expression (after treatment with carboplatin) and the apoptosis rate (after treatment with a combination of AD5-10 with carboplatin) in wt p53 cells were higher than in cells with mutant p53 (Fig. 3.1.2*B* and 3.1.1*B* respectively). These observations indicate that carboplatin forces expression of DR5 on OC cells, thereby enhancing their susceptibility to AD5-10-mediated apoptosis. In addition, MDAH-2774 harboured a mutant p53 allele; nevertheless, it showed a clear dose-dependent effect *in vitro* (Fig. 3.1.1*B* and *D*), illustrating that carboplatin also cooperates with AD5-10 regardless of the p53 status in OC cells. Thus, carboplatin treatment induced an increase in the expression of DR5 irrespective of the p53 status; hence, p53 mutations do not limit the therapeutic usefulness of combining AD5-10 with carboplatin.

A)

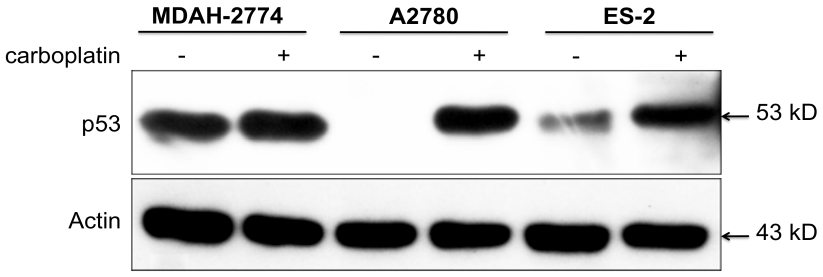

B)

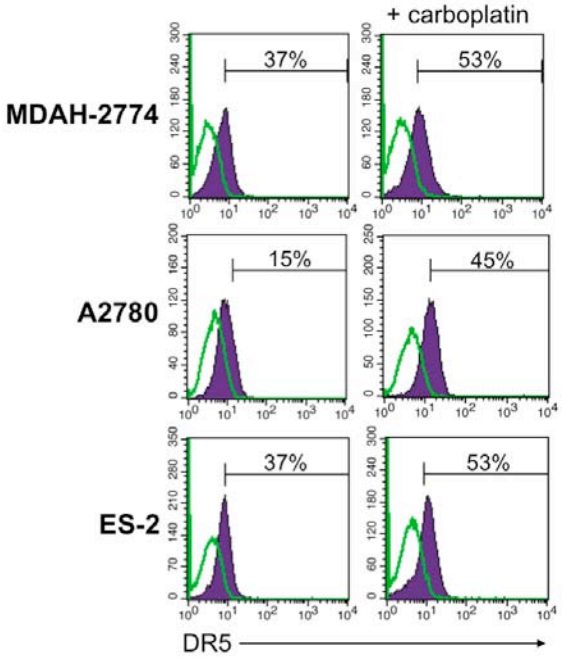

Figure 3.1.2. Carboplatin cooperates with AD5-10 to trigger apoptosis in OC cells by upregulation of DR5. A) Selected OC cell lines were either untreated or treated with carboplatin (100 µg/ml) for 24 h. Expression of p53 was determined by immunoblotting; data represent two independent experiments. **B)** Flow cytometry analysis of DR5 expression on OC cell lines either untreated or treated with carboplatin (100 µg/ml) for 24 h; data represent three independent experiments.

Combination of AD5-10 and carboplatin eradicates tumors in a xenograft OC mouse model

To assess the antitumor efficacy of AD5-10 alone and/or in combination with carboplatin, we applied a tumor model of OC in xenograft-bearing mice. In this model, mice bearing subcutaneously established tumors were randomly grouped for treatment with vehicle, AD5-10, carboplatin, or a combination of AD5-10 and carboplatin. Treatment started on day 2, and tumor size was measured every second day after tumor inoculation. After two weeks, all tumor-bearing mice were sacrificed and tumor-free mice were maintained for another two weeks (Table 3.1.1).

Mice treated with AD5-10 showed a clear reduction in tumor

progression compared to untreated mice (Fig. 3.1.3*A* and *B*). As expected, the treatment with carboplatin alone had no significant effect on tumor growth. In contrast, the combination of AD5-10 with carboplatin significantly suppressed tumor growth. Six out of seven treated mice (86%) remained tumor-free at the time of sacrificing (day 14^{th}). After 28 days, >50% of mice (n=4) remained tumor-free following combined AD5-10 and carboplatin treatment (Table 3.1.1). Overall, our data suggest that AD5-10 in combination with carboplatin induces a high apoptosis rate in OC cells *in vitro,* and OC rejection in a significant number of mice in a xenograft model, whereas carboplatin alone has no significant effect (Fig. 3.1.1*B* and 3.1.3, and Table 3.1.1).

Significant differences in tumor volume between control and AD5-10 treated mice were also observed. The largest reduction in tumor volume compared to the control group of untreated mice was observed in the group treated with AD5-10 in combination with carboplatin (Fig. 3.1.3*A* and *C*, and Table 3.1.1). Similar results were obtained for tumor weight (Fig. 3.1.3*B*). In contrast, mice receiving carboplatin alone did not display any statistically significant differences in tumor volume or tumor weight. Clearly, the tumor suppressive effect of AD5-10 alone and the elimination effect of AD5-10 in combination with carboplatin suggest that DR5 plays a strong antitumor role in carboplatin-resistant OC.

Table 3.1.1. Antitumorigenic effect of AD5-10 alone and/or in combination with carboplatin in a xenograft nude OC mouse model.

	Number of mice sacrificed upon tumor development				
Group	**14th day**	**23rd day**	**25th day**	**28th day**	**tumor-free mice after observation period**
control (n=7)	7*	-	-	-	0 (0%)
AD5-10 (n=5)	3	1	-	-	1 (20%)
carboplatin (n=6)	4	1***	-	-	1 (16.7%)
AD5-10+carboplatin (n=7)	1	1	1	-	4** (57.2%)

* one tumor-bearing mouse died before sacrificing.
** one mouse without tumor was sacrificed for the photograph in Fig. 3*C* on day 14.
*** sacrificed due to subcutaneous tumor development and ascites.
Note: (I) Two mice in the AD5-10 and one mouse in the carboplatin treated group were excluded from the statistical analysis due to inoculation resulting in intraperitoneal tumor.
(II) On day 14, all tumor-bearing mice were sacrificed, the remaining mice were sacrificed upon reaching the final tumor volume of ~4000 mm^3.

A)

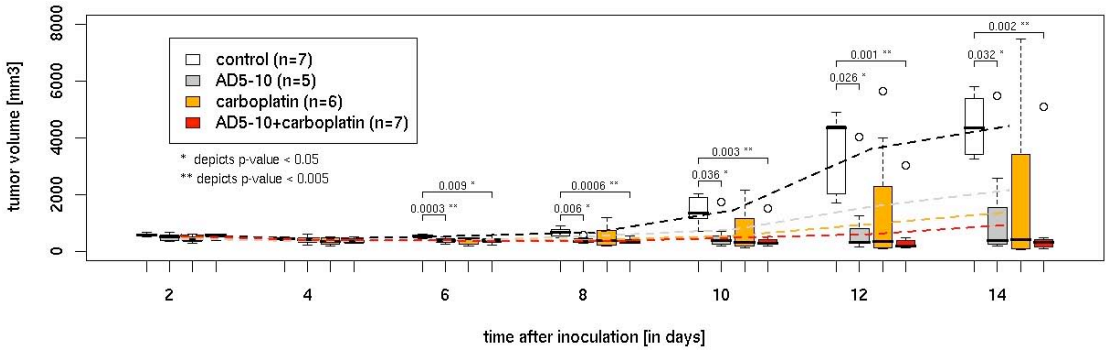

B)

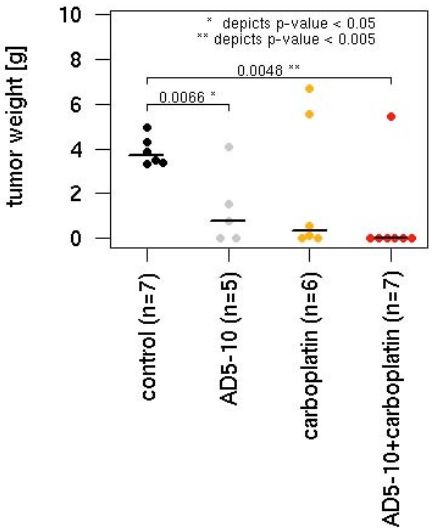

C)

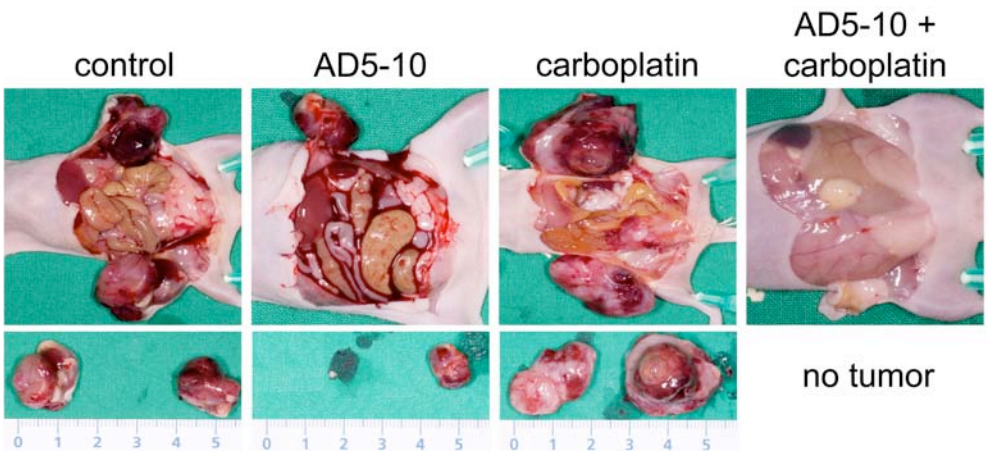

Figure 3.1.3. Combination of AD5-10 with carboplatin eradicates large, established tumors in a xenograft OC mouse model. A) 28 nude/nude mice were inoculated subcutaneously with $1.5x10^7$ A2780 OC cell line into the left and right hind ventral flank (day 0). Random groups of seven mice each were then treated intraperitoneally with either saline (control tumor) or AD5-10 (10 mg/kg) on days 2, 6, 9, 13, 16, and 20; carboplatin (100 mg/kg) on day 2; or a combination of AD5-10 and carboplatin at the respective doses and time as indicated above. Tumor volumes were measured every second day and on day 14 all tumor-bearing mice were sacrificed. Each measurement in each group is the sum of both left and right tumor volumes per animal and is included in the box plots. Box plots depict median values and the interquartile range, whereas dotted lines depict mean values in each group. Statistically significant differences * $P<0.05$, ** $P<0.005$ were determined by comparing tumor volume in the control group with treated groups. **B)** Tumor weight (after 14 days) in the four different groups; the median is indicated by a horizontal line. Each measurement in each group is the sum of both left and right tumor weight per animal. **C)** Representative mice and tumors of the indicated groups were assessed on day 14.

AD5-10 enhances antitumor activity against OC *in vivo*

We then evaluated the cytotoxic effect of administered substances on tumor tissues by immunohistochemical analysis. We observed a significant increase in caspase-3 activation and consequently in the apoptosis rate (measured by terminal deoxynucleotidyltransferase-mediated dUTP nick-end-labeling, TUNEL, assay) for AD5-10, but not for carboplatin, when compared to a control group (Fig. 3.1.4*A* and *B*). No significant differences in proliferation were observed for AD5-10 or carboplatin treatment (Fig. 3.1.3*C*). These data indicate that AD5-10 treatment induces apoptosis, consequently inhibiting the

growth of ovarian tumor tissue.

DR4 is epigenetically silenced in the A2780 cells *in vitro* (19). To determine whether the observed effects are due to DR5 and not to DR4 e.g. by demethylation of the DR4 promoter and reconstitution of DR4 expression *in vivo*, we analysed the expression of DR4 in tumor tissues. Immunohistochemical and immunoblotting analysis showed no reconstitution of DR4 expression *in vivo* (Fig. 3.1.4*D*), indicating that TRAIL-induced apoptosis is only mediated by DR5. Furthermore, we analyzed the immunohistochemical expression of murine TRAIL using anti-mouse TRAIL antibody. Interestingly, we found that murine TRAIL to be highly expressed in tumor tissues (Fig. 3.1.4*D*). Remarkably, selected human OC cells do not express human TRAIL (Fig. 3.1.1*A*) and murine TRAIL was shown to have some cross-reactivity with human tumor cells (25). This finding might support our previous observation in humans that TRAIL is highly expressed in the tumor microenvironment of OC patients (7). TRAIL is a key mediator of cytotoxic activity of activated NK cells and CD8+ lymphocytes (26), and is at least in part responsible for antimetastatic activities *in vivo* (27, 28). Immunohistochemical analysis revealed a dense infiltration of the tumor tissues with NK cells (Fig. 3.1.4*D*), suggesting that NK cells mediate cytotoxicity in OC by TRAIL-induced death.

A)

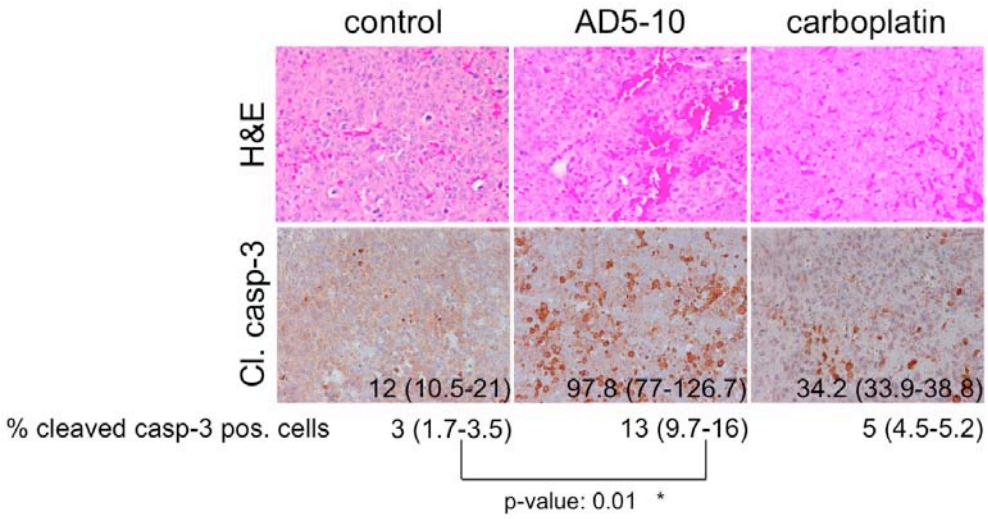
control
AD5-10
carboplatin
H&E
Cl. casp-3
12 (10.5-21)
97.8 (77-126.7)
34.2 (33.9-38.8)
% cleaved casp-3 pos. cells
3 (1.7-3.5)
13 (9.7-16)
5 (4.5-5.2)
p-value: 0.01 *

B)

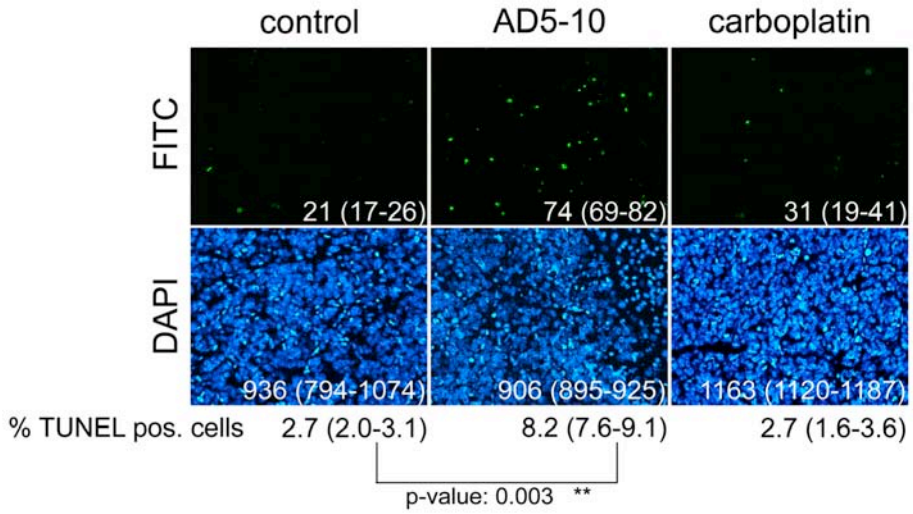
control
AD5-10
carboplatin
FITC
DAPI
21 (17-26)
74 (69-82)
31 (19-41)
936 (794-1074)
906 (895-925)
1163 (1120-1187)
% TUNEL pos. cells
2.7 (2.0-3.1)
8.2 (7.6-9.1)
2.7 (1.6-3.6)
p-value: 0.003 **

C)

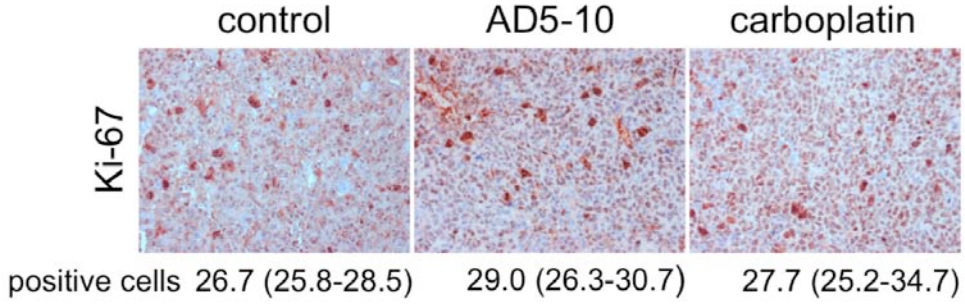
control
AD5-10
carboplatin
Ki-67
positive cells
26.7 (25.8-28.5)
29.0 (26.3-30.7)
27.7 (25.2-34.7)

D)

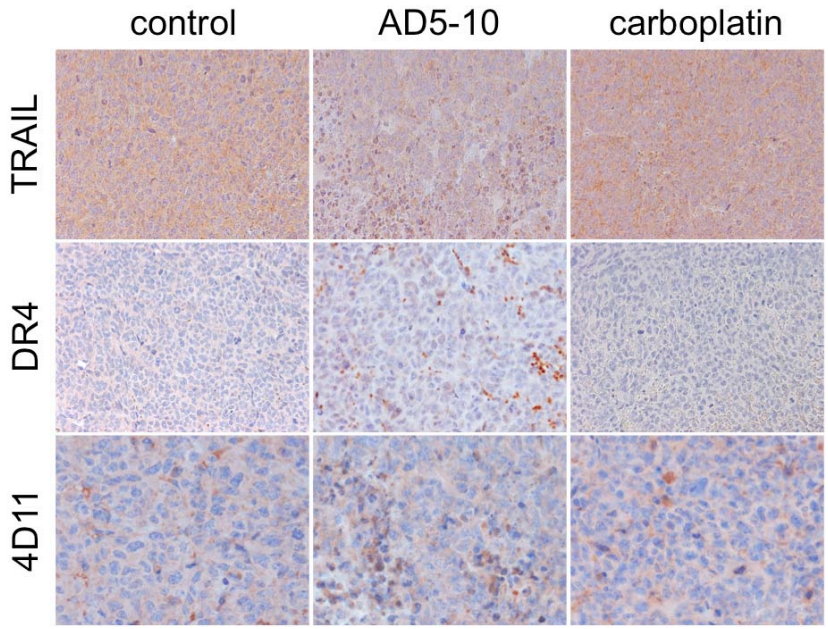

Figure 3.1.4. AD5-10 enhances sensitivity of ovarian tumors to apoptosis. Immunohistochemical analysis of tumors obtained from mice inoculated with A2780 OC cell line and sacrificed on day 14 (Fig. 3.1.3) for **A)** H&E and caspase-3 staining; **B)** Tunel assay; **C)** Ki-67 staining; and **D)** TRAIL ligand, DR4, and NK cell staining; magnification 20x. **A)** H&E staining showed vital solid intact tumor tissues in control and carboplatin-treated mice. In contrast, tumor cells from AD5-10 treated mice appeared damaged, leading to structural alteration and secondary bleeding. **A and B)** Proportional cell numbers in each micrograph (in caspase-3 staining, numbers of cleaved caspase-3 positive cells) are given as median values, and the interquartile range of 12 subsections of four different tumor sections per group is indicated within brackets. The median and interquartile range of the percentage of cleaved caspase-3 and TUNEL positive cells are given below micrographs. Significant differences between the control group and the various treated groups are indicated: * $P<0.05$, ** $P<0.005$. **C)** Numbers given in the lower section show Ki-67-positive cells of nine subsections of three different tumor sections per group. Statistically significant differences are given as *$P<0.05$, comparing the control tumor group with the various treated groups. **D)** *TRAIL staining (*performed using goat anti-mouse TRAIL polyclonal antibody, AF1121 (R&D Systems))*:* vital tumor cells with weak diffused background staining of murine TRAIL, probably representing the soluble form of the molecule in control and carboplatin-treated tumor tissues. However, damaged tumor cells were observed in TRAIL positive AD5-10 treated tumor tissue. *DR4 staining*: tumor cells were consistently negative for DR4 in all tumor sections. Tissues from animal treated with AD5-10 showed granular-intercellular staining, which probably represents unspecific staining of degenerated apoptotic tumor cells. *4D11 staining:* monoclonal antibody 4D11 (anti-Ly-49G2) revealed specific reactivity for mouse NK cells (16). Specific staining for NK cells was observed in all tumor sections. Damaged tumor cells were observed close to positive NK cells staining in AD5-10-treated but not in control or carboplatin-treated tumors.

AD5-10 cooperates with NK cells to suppress tumor growth of established OC in a xenograft mouse model

We further explored the antitumor effect of AD5-10 in combination with TRAIL. Combination of TRAIL with AD5-10 enhances A2780 cellular sensitivity to TRAIL-induced apoptosis *in vitro* (Fig. 3.1.5*A*). Notably, AD5-10 antibody has been shown to bind to a different binding site than TRAIL (11). Therefore, AD5-10 does not compete with the TRAIL-binding site, which may explain a significantly increased rate of apoptosis observed after treatment with the combination of AD5-10 and human soluble TRAIL.

Finally, we determined whether NK cell-mediated cytotoxicity is involved in AD5-10-induced effects. To do so, we made use of NK-cell-depleting antibodies. Four groups of nude mice were subcutaneously inoculated with A2780 cells and were either left untreated or treated with AD5-10 and/or NK1.1- and anti-asialo-depleting antibodies (Fig. 3.1.5*B*). Tumor development was observed for a period of 4 weeks. In NK-cell-depleted mice, AD5-10 had only a minimal effect on tumor growth (Fig. 3.1.5*C*), whereas AD5-10 significantly reduced tumor volume in the presence of NK cells (Fig. 3.1.3*A* and 3.1.5*C*). This suggests that TRAIL expressed by active NK cells is required for AD5-10-induced apoptosis. This finding is in line with the fact that DR5 is more efficiently activated by secondary cross-linked trimers of TRAIL (29, 30). NK cell depletion alone had only a small effect on tumor growth, which might reflect the fact that A2780 cells are resistant to TRAIL-induced apoptosis (expressed via NK cells). Moreover, we found that NK cell numbers correlate with the survival of the animal, with a high NK cell number being

protective (Fig. 3.1.5*D*). In summary, these data suggest that the antitumor activity of AD5-10 depends on NK in OC.

A)

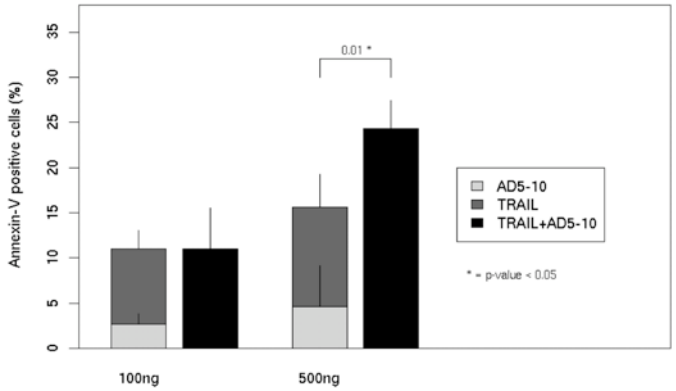

B)

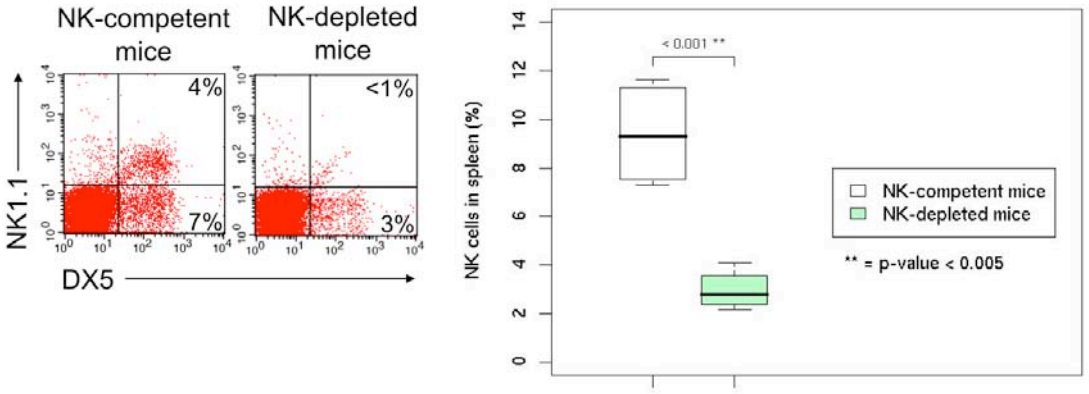

C)

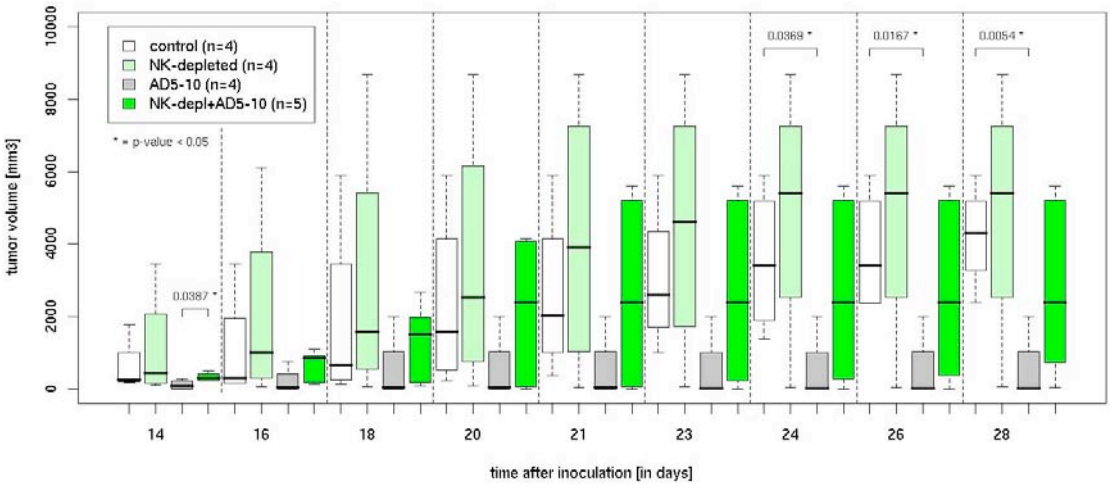

D)

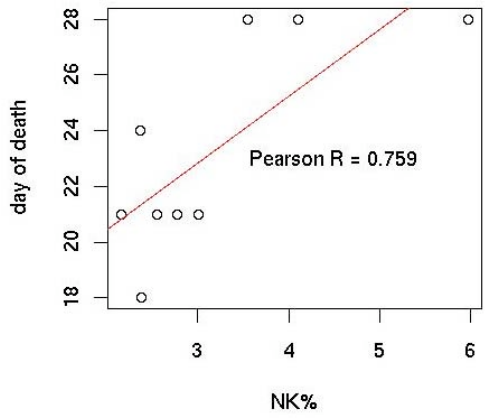

Figure 3.1.5. Depletion of NK cells suppresses the tumoricidal effect of AD5-10 on tumor outgrowth. A) A2780 OC cell line was incubated with the specified concentration of TRAIL, AD5-10 (1 µg/ml), or both for 24 h, and the apoptosis rate was measured. Columns represent the mean of three independent experiments; bars, ±SE; *statistically significant (*P*<0.05) difference obtained by comparing the sum effect of AD5-10 and TRAIL to a combination of both. **B)** Two groups of mice were depleted of NK cells by administration of polyclonal rabbit anti-asialo GM1 antibody at a dose of 20 µl intraperitoneally every 4 days starting on day 3, and NK1.1 antibody 100 µg intraperitoneally every third day starting at day 3. A total of $1x10^7$ A2780 cells were inoculated subcutaneously into the left and right dorsal sides of the mice. Mice were treated intraperitoneally with AD5-10 or saline as indicated in Fig. 3.1.3*A*. *Left panel:* Histograms showing analysis of NK expression on splenocytes from NK-competent and NK-depleted mice. Numbers in dot plot quadrants indicate the percentage of NK-positive staining. *Right panel:* numbers of NK cells in NK-competent and NK-depleted mice are indicated. Each measurement in each group is included in the box plots showing the median; 25^{th} and 75^{th} percentiles; statistically highly significant differences **p<0.005 were determined by comparing the number of NK cells in NK-competent and NK-depleted groups. **C)** Tumor volumes in the four different groups were measured every second day. Mice were sacrificed when tumor size (at least in one flank) reached the required volume (~ 4000 mm^3). Each measurement in each group is the sum of both left and right tumor volumes per animal. Data are represented as indicated in Fig. 3.1.3*A*. **D)** Correlation between NK cells (%) in depleted mice and life span.

Discussion

The TRAIL pathway has been extensively studied *in vitro* and *in vivo*, and molecules targeting this pathway have become attractive candidates for anticancer treatment (10). Preclinical studies in mice provided the first evidence that the soluble form of recombinant TRAIL (rTRAIL) suppresses the growth of human tumor xenografts with no apparent systemic toxicity (31, 32). More recently, rTRAIL has also entered clinical trials for the treatment of various malignancies (33). Although published phase 1 and 2 studies have indicated tolerated toxicity, the therapeutic efficiency is variable. In addition to the soluble ligand, several agonistic antibodies to the TRAIL functional receptors (DR4 or DR5) have been developed and entered into clinical trials in parallel (10). These agonistic antibodies may be more effective than the ligand at eradicating tumors for several reasons, one of them being the prolonged half-life time *in vivo* when compared to the recombinant proteins. Furthermore, the decoy receptors, which have been implicated in modulating the response to TRAIL, are not targeted by these ligands. Cross linking therapeutic antibodies might also overcome the resistance mechanisms to TRAIL-induced apoptosis observed in OC (5,13) according to the data in our study, which provides a novel link between NK-mediated immunosurveillance and activation of DR5-mediated apoptosis.

DR5 was identified in 1997 (23, 34) and several DR5 agonistic antibodies exhibit a potent antitumor effect against TRAIL-sensitive tumor cells, but not against TRAIL-resistant tumor cells. These are currently in phase II evaluations in patients with advanced malignancies (35, 36). In the present study we used a DR5 agonistic antibody AD5-10 against TRAIL-

resistant OC cells, and our results shed light on the postulated critical role of DR5 and NK-mediated immunosurveillance in OC progression. As expected, we observed limited cytotoxic effects on OC cells resistant to TRAIL-induced apoptosis *in vitro* upon stimulation with AD5-10 alone (Fig. 3.1.1*B* and *C*). We hypothesized that combined therapy with anti-DR5 and different pharmacological anticancer agents might induce more than additive antitumor activity. Our results showed that out of a number of agents used in the standard treatment of OC only the combination of AD5-10 with carboplatin displayed more than additive effect *in vitro* (Fig. 3.1.1*B*). This phenotype stimulated our interest in the nature of this mechanism. Consequently, we determined the cytotoxic effect of AD5-10 alone or in combination with carboplatin in a platin-resistant OC mouse model. While there was, as expected, no effect of carboplatin alone, an effect of AD5-10 was observed. Importantly, the combination of AD5-10 with carboplatin eventually eliminated OC (Fig. 3.1.3*A*, *B*, and *C*; and Table 3.1.1) in a significant number of animals. Chemotherapeutic agents have been shown to cooperate with the TRAIL ligand to enhance apoptosis (37). However, the molecular basis behind such cooperation has not yet been elucidated. One mechanism (probably not the only one) is based on our observation that carboplatin cooperates with AD5-10 by upregulating DR5 expression regardless of the p53 status (Fig. 3.1.2). However, this finding does not fully explain the exceptional activity of AD5-10 and carboplatin *in vivo* and makes it necessary to consider the activity of these substances in the context of the immune system.

As postulated previously the TRAIL pathway plays a key role in tumor surveillance (7, 26-28). Understanding the activity of a potential agent

targeting this pathway requires putting a spotlight on the activity of the hosts' immune system as reflected in the tumor microenvironment. Our previously published data support a key role of TRAIL and the functional TRAIL receptors in OC, showing increased survival in patients expressing a high level of TRAIL in tissue adjacent to the tumor (7, 19). However, the origin of this expression has not been fully evaluated to date. In our current study we addressed the role of NK cell-mediated effects of DR5-induced apoptosis. We recorded that AD5-10 alone did not have a significant effect on apoptosis; however, it had a more than additive effect when combined with human soluble TRAIL *in vitro* to enhance TRAIL-mediated cytotoxicity (Fig. 3.1.5*A*). Moreover, we observed that TRAIL and NK cells are highly expressed in the tumor microenvironment (Fig. 3.1.4*D*), and that depletion of NK cells from mice bearing tumors led to increased tumor growth and also abolished the cytotoxic effect of AD5-10 (Fig. 3.1.5*C* and *D*). These findings indicate that TRAIL expressed on active NK cells might cross link AD5-10, suggesting that DR5 is more efficiently activated by secondary cross-linked trimers of soluble TRAIL than by non-cross-linked molecules (Fig. 3.1.5*A*, and (29, 30)). Notably, AD5-10 antibody binds to a different binding site than TRAIL cells (11), and murine TRAIL was shown to have some cross-reactivity with human tumor cells (25). However, other mechanisms like upregulation of DR5 on OC cells by carboplatin and targeting by AD5-10 efficiently activated cell killing without the need for secondary cross linking (Fig. 3.1.1*B* and *C*). In fact, according to our data, forced expression of DR5 in the presence of TRAIL-expressing NK cells provides an ideal environment for highly efficient activation of DR5 by AD5-10. This fact is supported by eradication of

implanted tumors in an NK-competent xenograft OC mouse model (Fig. 3.1.3*A* and Table 3.1.1), and by the abolished cytotoxic activity of AD5-10 in NK-depleted mice (Fig. 3.1.5*C* and *D*). This finding clearly confirms the importance of NK-mediated immunosurveillance in OC in a preclinical mouse model. Agonistic DR5 antibodies probably act together with naturally occurring TRAIL ligand to overcome the resistance mechanisms that develop during tumorigenesis.

Our study highlights the lack of knowledge regarding the interplay between therapeutic agents, host immunity, and the evasion mechanisms developed by individual tumors. Only an improved understanding of these basic mechanisms will ultimately lead to tailored patient selection and the choice of combination partners for drugs targeting the TRAIL pathway. Carboplatin and AD5-10 seem to be a promising regimen for future clinical trials in platin-resistant OC.

Acknowledgments

We would like to thank Prof. U. Losert and his colleagues in the animal facility for taking good care of our mice. We would also like to thank Mrs. Bettina Pichlhoefer (Department of Pathology, Medical University of Vienna) for sequencing p53 in our OC cell lines.

References

1. Guppy AE, Nathan PD, Rustin GJ. Epithelial ovarian cancer: a review of current management. Clin Oncol (R Coll Radiol) 2005 Sep;17(6):399-411.
2. Jemal A, Siegel R, Ward E, Murray T, Xu J, Thun MJ. Cancer statistics, 2007. CA Cancer J Clin 2007 Jan-Feb;57(1):43-66.
3. Wong AS, Auersperg N. Ovarian surface epithelium: family history and early events in ovarian cancer. Reprod Biol Endocrinol 2003 Oct 7;1:70.
4. Hengartner MO. The biochemistry of apoptosis. Nature 2000 Oct 12;407(6805):770-6.
5. Fulda S, Debatin KM. Extrinsic versus intrinsic apoptosis pathways in anticancer chemotherapy. Oncogene 2006 Aug 7;25(34):4798-811.
6. Ashkenazi A. Targeting death and decoy receptors of the tumour-necrosis factor superfamily. Nat Rev Cancer 2002 Jun;2(6):420-30.
7. Horak P, Pils D, Kaider A, et al. Perturbation of the tumor necrosis factor--related apoptosis-inducing ligand cascade in ovarian cancer: overexpression of FLIPL and deregulation of the functional receptors DR4 and DR5. Clin Cancer Res 2005 Dec 15;11(24 Pt 1):8585-91.
8. Lamhamedi-Cherradi SE, Zheng SJ, Maguschak KA, Peschon J, Chen YH. Defective thymocyte apoptosis and accelerated autoimmune diseases in TRAIL-/- mice. Nat Immunol 2003 Mar;4(3):255-60.
9. Cretney E, Takeda K, Yagita H, Glaccum M, Peschon JJ, Smyth MJ. Increased susceptibility to tumor initiation and metastasis in TNF-

related apoptosis-inducing ligand-deficient mice. J Immunol 2002 Feb 1;168(3):1356-61.

10. Johnstone RW, Frew AJ, Smyth MJ. The TRAIL apoptotic pathway in cancer onset, progression and therapy. Nat Rev Cancer 2008 Oct;8(10):782-98.

11. Guo Y, Chen C, Zheng Y, et al. A novel anti-human DR5 monoclonal antibody with tumoricidal activity induces caspase-dependent and caspase-independent cell death. J Biol Chem 2005 Dec 23;280(51):41940-52.

12. Freedman RS, Pihl E, Kusyk C, Gallager HS, Rutledge F. Characterization of an ovarian carcinoma cell line. Cancer 1978 Nov;42(5):2352-9.

13. Behrens BC, Hamilton TC, Masuda H, et al. Characterization of a cis-diamminedichloroplatinum(II)-resistant human ovarian cancer cell line and its use in evaluation of platinum analogues. Cancer Res 1987 Jan 15;47(2):414-8.

14. Lau DH, Lewis AD, Ehsan MN, Sikic BI. Multifactorial mechanisms associated with broad cross-resistance of ovarian carcinoma cells selected by cyanomorpholino doxorubicin. Cancer Res 1991 Oct 1;51(19):5181-7.

15. Liabakk NB, Sundan A, Torp S, Aukrust P, Froland SS, Espevik T. Development, characterization and use of monoclonal antibodies against sTRAIL: measurement of sTRAIL by ELISA. J Immunol Methods 2002 Jan 1;259(1-2):119-28.

16. Dokun AO, Chu DT, Yang L, Bendelac AS, Yokoyama WM. Analysis of in situ NK cell responses during viral infection. J Immunol 2001 Nov 1;167(9):5286-93.

17. Esumi H, Lu J, Kurashima Y, Hanaoka T. Antitumor activity of pyrvinium pamoate, 6-(dimethylamino)-2-[2-(2,5-dimethyl-1-phenyl-1H-pyrrol-3-yl)ethenyl]-1-methyl-qu inolinium pamoate salt, showing preferential cytotoxicity during glucose starvation. Cancer Sci 2004 Aug;95(8):685-90.

18. Zebedin E, Simma O, Schuster C, et al. Leukemic challenge unmasks a requirement for PI3Kdelta in NK cell-mediated tumor surveillance. Blood 2008 Dec 1;112(12):4655-64.

19. Horak P, Pils D, Haller G, et al. Contribution of epigenetic silencing of tumor necrosis factor-related apoptosis inducing ligand receptor 1 (DR4) to TRAIL resistance and ovarian cancer. Mol Cancer Res 2005 Jun;3(6):335-43.

20. Brown R, Clugston C, Burns P, et al. Increased accumulation of p53 protein in cisplatin-resistant ovarian cell lines. Int J Cancer 1993 Oct 21;55(4):678-84.

21. Concin N, Stimpfl M, Zeillinger C, et al. Role of p53 in G2/M cell cycle arrest and apoptosis in response to gamma-irradiation in ovarian carcinoma cell lines. Int J Oncol 2003 Jan;22(1):51-7.

22. Santoso JT, Tang DC, Lane SB, et al. Adenovirus-based p53 gene therapy in ovarian cancer. Gynecol Oncol 1995 Nov;59(2):171-8.

23. Wu GS, Burns TF, McDonald ER, 3rd, et al. KILLER/DR5 is a DNA damage-inducible p53-regulated death receptor gene. Nat Genet 1997 Oct;17(2):141-3.

24. Koivusalo R, Krausz E, Ruotsalainen P, Helenius H, Hietanen S. Chemoradiation of cervical cancer cells: targeting human papillomavirus E6 and p53 leads to either augmented or attenuated apoptosis depending on the platinum carrier ligand. Cancer Res 2002 Dec 15;62(24):7364-71.

25. Wiley SR, Schooley K, Smolak PJ, et al. Identification and characterization of a new member of the TNF family that induces apoptosis. Immunity 1995 Dec;3(6):673-82.

26. Takeda K, Smyth MJ, Cretney E, et al. Critical role for tumor necrosis factor-related apoptosis-inducing ligand in immune surveillance against tumor development. J Exp Med 2002 Jan 21;195(2):161-9.

27. Smyth MJ, Hayakawa Y, Takeda K, Yagita H. New aspects of natural-killer-cell surveillance and therapy of cancer. Nat Rev Cancer 2002 Nov;2(11):850-61.

28. Takeda K, Smyth MJ, Cretney E, et al. Involvement of tumor necrosis factor-related apoptosis-inducing ligand in NK cell-mediated and IFN-gamma-dependent suppression of subcutaneous tumor growth. Cell Immunol 2001 Dec 15;214(2):194-200.

29. Kelley RF, Totpal K, Lindstrom SH, et al. Receptor-selective mutants of apoptosis-inducing ligand 2/tumor necrosis factor-related apoptosis-inducing ligand reveal a greater contribution of death receptor (DR) 5

than DR4 to apoptosis signaling. J Biol Chem 2005 Jan 21;280(3):2205-12.

30. Muhlenbeck F, Schneider P, Bodmer JL, et al. The tumor necrosis factor-related apoptosis-inducing ligand receptors TRAIL-R1 and TRAIL-R2 have distinct cross-linking requirements for initiation of apoptosis and are non-redundant in JNK activation. J Biol Chem 2000 Oct 13;275(41):32208-13.
31. Ashkenazi A, Pai RC, Fong S, et al. Safety and antitumor activity of recombinant soluble Apo2 ligand. J Clin Invest 1999 Jul;104(2):155-62.
32. Walczak H, Miller RE, Ariail K, et al. Tumoricidal activity of tumor necrosis factor-related apoptosis-inducing ligand in vivo. Nat Med 1999 Feb;5(2):157-63.
33. Kimberley FC, Screaton GR. Following a TRAIL: update on a ligand and its five receptors. Cell Res 2004 Oct;14(5):359-72.
34. Screaton GR, Mongkolsapaya J, Xu XN, Cowper AE, McMichael AJ, Bell JI. TRICK2, a new alternatively spliced receptor that transduces the cytotoxic signal from TRAIL. Curr Biol 1997 Sep 1;7(9):693-6.
35. Estes JM, Oliver PG, Straughn JM, Jr., et al. Efficacy of anti-death receptor 5 (DR5) antibody (TRA-8) against primary human ovarian carcinoma using a novel ex vivo tissue slice model. Gynecol Oncol 2007 May;105(2):291-8.
36. Hotte SJ, Hirte HW, Chen EX, et al. A phase 1 study of mapatumumab (fully human monoclonal antibody to TRAIL-R1) in patients with advanced solid malignancies. Clin Cancer Res 2008 Jun 1;14(11):3450-5.

37. Tomek S, Horak P, Pribill I, et al. Resistance to TRAIL-induced apoptosis in ovarian cancer cell lines is overcome by co-treatment with cytotoxic drugs. Gynecol Oncol 2004 Jul;94(1):107-14.

3.2. The role of c-FLIP$_L$ in ovarian cancer: chaperoning tumor cells from immunosurveillance and increasing their invasive potential (manuscript submitted)

Ahmed El-Gazzar[1], Michael Wittinger[1, 5], Paul Perco[2], Mariam Anees[1], Reinhard Horvat[3], Wolfgang Mikulits[4], Thomas W. Grunt[1], Bernd Mayer[2], Michael Krainer[1, *]

[1] Division of Oncology, Department of Medicine I, Medical University of Vienna, Austria.

[2] Institute for Theoretical Chemistry, University of Vienna, Vienna, Austria.

[3] Department of Pathology, Medical University of Vienna, Vienna, Austria.

[4] Institute of Cancer Research, Department of Medicine I, Medical University of Vienna, Vienna, Austria.

[5] Present address: Cold Spring Harbor Laboratory, Cold Spring Harbor, NY, USA.

*** Correspondence to**:

Michael Krainer, MD

Division of Oncology

Department of Medicine I

Medical University of Vienna

Waehringer Guertel 18-20, 1090 Vienna, Austria

Phone: +43 1 40400 7572

Fax: +43 1 40400 4687

E-mail: michael.krainer@meduniwien.ac.at

Running title: c-FLIP$_L$ depletion inhibits OC progression

Key words: ovarian cancer; c-FLIP$_L$; apoptosis; immunosurveillance

Funding: This work was supported by the Austrian Science Fund (FWF) (grant number P20715).

Disclosure of potential conflicts of interest: No potential conflicts of interest were disclosed.

Abstract

Activation of tumor necrosis factor (TNF)-related apoptosis-inducing ligand (TRAIL) functional receptors by their ligand induces apoptosis through activation of caspase-8. Cellular Fas-associated death domain-like interleukin-1β-converting enzyme (FLICE)-like inhibitory protein (c-FLIP) blocks TRAIL-mediated apoptosis through inhibition of caspase-8 activation. The current study is based on our previous observations that about 40% of OC patients express high levels of c-$FLIP_L$, and that natural killer (NK) cells mediated immunosurveillance in OC. In the present study, we observed that the knockdown of c-$FLIP_L$ in human OC cell lines not only enhanced their sensitivity to TRAIL mediated-apoptosis, but also inhibited their migratory phenotype in a TRAIL-dependent manner *in vitro*. Shutdown of c-$FLIP_L$ in OC cells significantly decreased tumor development by induction of apoptosis and reduction of proliferation *in vivo*. Importantly, the knockdown of c-$FLIP_L$ particularly inhibited the invasion of OC cells into the peritoneal cavity, which might be due to high expression of TRAIL by NK cells and NK-cell mediated immunosurveillance. These data demonstrate that c-$FLIP_L$ exhibits multiple functions in OC cells: first by concomitantly evading the natural immunity mediated by TRAIL-induced cell death, second by augmenting cell motility and invasion *in vivo*. Our findings indicate that c-$FLIP_L$ regulates sensitivity of OC to TRAIL-mediated apoptosis and offers possible therapeutical implications for OC in the future.

Introduction

Apoptosis is a physiological process playing a fundamental role not only in controlling cell differentiation and tissue homeostasis, but also in eliminating cells that undergo uncontrolled cellular proliferation [1-4]. Caspases, a family of cysteine proteinases, are key elements in apoptosis [5, 6]. So far, at least 10 caspases have been reported [5], each encoding sequences essential for proteolytic activity and induction of apoptosis. Activation of the caspase cascade is triggered by various death signals, subsequently leading to apoptotic cell death.

Death receptors such as APO-1/FAS or functional tumor necrosis factor (TNF)-related apoptosis-inducing ligand (TRAIL) receptors exhibit an intracellular sequence denoted as death domain (DD). The adaptor protein Fas-associated death domain protein (FADD) is recruited to the death receptors by homotypic DD interaction [7]. Ligation of death receptors by their cognate ligands leads to recruitment of FADD, which in turn leads to activation of caspase-8, further resulting in assembly of the death-inducing signaling complex (DISC) initiating the apoptotic cascade [8].

The apoptosis signaling pathway induced by death receptors is regulated by inhibitor proteins at distinct steps. Among these proteins is the cellular Fas-associated death domain-like interleukin-1β-converting enzyme (FLICE)-like inhibitory protein (c-FLIP). c-FLIP interferes with activation of pro-caspase-8 most proximal to the plasma membrane [9, 10]. Eleven distinct isoforms of c-FLIP produced by alternative splicing at the RNA level have been described. Of these, two splice variants, the long c-$FLIP_L$ and the short isoform c-$FLIP_S$, were found to exhibit different molecular mechanisms for

inhibiting the activation of pro-caspase-8 at the protein level [10-13]. While c-FLIP$_S$ inhibits activation of pro-caspase-8 by blocking cleavage for processing the active form, c-FLIP$_L$ triggers the first cleavage of pro-caspase-8 resulting in the large and small subunit [14]. c-FLIP was found to be highly expressed in various human tumors such as melanoma [10, 15, 16] and ovarian cancer (OC) [17]. c-FLIP$_L$ was shown to prevent natural killer (NK) cells and cytolytic T lymphocytes (CTLs)-mediated cell killing via Fas ligand (FasL), resulting in escape of immunosurveillance and establishment of aggressive tumors *in vivo* [18-20]. In this regard, we have shown recently that NK cells play an essential role in immunosurveillance of OC [21], and that c-FLIP$_L$ is upregulated in OC patients [17].

So far, several intracellular signaling pathways, including ERK, AKT/PI3K, and NF-κB pathways [22-24] were shown to regulate c-FLIP transcription and posttranslational regulation. Moreover, p53 was shown to inhibit c-FLIP expression [25, 26].

In the present study, we deciphered the role of c-FLIP$_L$ in OC. We report that removal of c-FLIP$_L$ from TRAIL-resistant OC cells not only enhances sensitivity to TRAIL-induced apoptosis, but also inhibits tumor growth *in vitro* as well as *in vivo*. We found that downregulation of c-FLIP$_L$ inhibits migration of OC cells in presence of soluble TRAIL *in vitro*, and abolishes the invasive behaviour of ovarian tumors *in vivo*. Altogether, our data highlight c-FLIP$_L$ as a key regulatory protein in ovarian tumor progression.

Material and Methods

Cell lines

Human OC cell lines MDAH-2774 (ovarian endometroid adenocarcinoma (OEA)-derived cell line, derived from the ascitic fluid of a patient [27], and a platin resistant sub-line of the OC cell line A2780 (human epithelial OC cell line established from tumor tissue [28]) were used in our study. Cell lines were cultured in RPMI medium supplemented with 10% fetal calf serum (FCS) (PAA Laboratories GmbH, Pasching, Austria) and 0.1% penicillin/streptomycin (PAA Laboratories GmbH). The cell line MDAH-2774 was obtained from the American Type Culture Collection (ATCC, VA, USA), and the cell line A2780 was obtained from the European Collection of Cell Cultures (ECACC, Wiltshire, UK).

RNA interference (RNAi)

Oligonucleotides encoding short hairpin RNAs (shRNAs) targeting c-FLIP were designed (Sigma-Aldrich, MO, USA) to hold restriction sites for BamH1 and HindIII at their 5' and 3' end, respectively. The annealed oligonucleotides were cloned into BamH1 and HindIII of pSilencer 4.1-CMV neo vector (Applied Biosystems, CA, USA). Cloning of resulting vectors was verified by sequencing. The specificity of the shRNA was confirmed using two oligonucleotides targeted to different regions of the mRNA: oligo 1 (nucleotides 514-534 ORF): 5'-GATCCGCAGTCTGTTCAAGGAGCATTCAAGAGATGCTCCTTGAACAGAC TGCTTA-3' [29]. Oligo 2 (nucleotides 29-49) 5'-GATCCGAAGCACTTGATACAGATGTTCAAGAGACATCTGTATCAAGTGCT

TCTTA-3' [30]. Each of the shRNA suppressed the encoded protein and exerting the same effects. shRNA control was used to confirm that the observed effects are indeed specific and due to c-FLIP$_L$ suppression by RNAi. The control was designed in a way to avoid targeting of any protein coding gene product.

Selected OC cell lines were transfected with the corresponding vectors utilizing the Lipofectamine method according to the manufacturer's instructions (Lipofectamine 2000; Invitrogen, CA, USA). Stable clonal transfectants were generated, and the efficiency of downregulation was confirmed by quantitative reverse transcription-polymerase chain reaction and Western blot.

Quantitative Reverse Transcription-Polymerase Chain Reaction (qRT-PCR)

Total RNA was isolated from parental and genetically manipulated OC cell lines by RNeasy Mini Kit (Qiagen, Hilden, Germany) according to the manufacturer's instructions. RNAs were then quantified by Nano Chips (Lab-on-a-Chip, Agilent Technologies, CA, USA). Subsequently, cDNAs were generated by reverse transcription of isolated mRNAs using SuperScript II RNase H- Reverse Transcriptase (Invitrogen, CA, USA) according to the manufacturer's instruction. Quantitative real time PCR was performed using the following Assay On Demand probes: c-FLIP, Hs00153439_m1; HPRT1, Hs99999909_m1 purchased from Applied Biosystem (CA, USA). qRT-PCR Master MIX (Eurogentec, CA, USA) was used to perform the qRT-PCR. The qRT-PCR was performed on a 7900HT Sequence Detection System (Applied

Biosystems) applying the following program: 50°C for 2 minutes and 95°C for 10 minutes, followed by 40 cycles of 95°C for 15 seconds and 60°C for 1 minute. Relative expression was calculated from the threshold cycles (Ct) obtained with the SDS 2.2 Software (Applied Biosystems) as follows: 2^–[(Ct_{gene} mean of duplicated probes – Ct_{gene} mean of duplicated calibrator) – (Ct_{HPRT1} mean of duplicated probes – Ct_{HPRT1} mean of duplicated calibrator)].

Western blot

Western blot was performed as described previously [21] using the following primary antibodies: mouse monoclonal anti-human c-FLIP (NF6; dilution 1:500; Alexis, Lausen, Switzerland), and goat anti-actin polyclonal antibody (dilution 1:500; Santa Cruz, CA, USA).

Determination of apoptosis

Parental as well as genetically manipulated MDAH-2774 and A2780 OC cell lines were plated at a density of 5 x 10^4 cells/well in 24-well plates and incubated for 24 hours prior to stimulation. Then cells were treated with soluble TRAIL (Alexis) 100 ng/ml for 24 hours. Cells were harvested by trypsinization using 0.05% trypsin and 0.02% EDTA without Ca^{2+} and Mg^{2+} (PAA Laboratories GmbH). Apoptosis was measured by an annexin V-FITC apoptosis detection kit (Alexis) according to the manufacturer's instructions. Flow cytometry of annexin V-FITC and Propidium Iodide (PI) staining was performed using FACScan (Becton Dickinson, Heidelberg, Germany) with CELLQuest Pro software.

Proliferation assay

Selected OC cell lines were plated at a density of 5 x 10^3 in 100 µl of culture medium in a 96-well plate and were left to adhere. Cells were then incubated for 24 to 72 hours. Cell viability was measured by CellTiter-Blue® Assay (Promega, WI, USA) according to the manufacturer's instructions. The fluorescence signal was recorded using a Wallac 1420 VICTOR2 fluorescence plate reader (Perkin Elmer, MA, USA). Three independent experiments, each in triplicate, were performed.

***In vitro* migration assay**

Migration assays were performed using a 24-well trans-well cell culture chamber (BD Biosciences, CA, USA) according to the manufacturer's instructions. Briefly, 500 µl of selected OC cells were suspended in the upper chamber at a final concentration of $5x10^4$ cells/ml in duplicate. One group was left untreated and the other was supplemented with 100 ng/ml medium of soluble TRAIL. The lower chamber contained 30% FCS/culture medium. After 24 hours incubation, the OC cells on the upper surface were removed by wiping with cotton swabs, and the migrated cell on the lower surface were stained with mounting medium for fluorescence with DAPI (Vector Laboratories, Inc., CA, USA). The number of cells on the lower surface of the filters was counted under a fluorescence microscope (Nikon Eclipse 800, Tokyo, Japan) equipped with a Nikon DS-R1 camera, using the NIS-Elements software. Three independent experiments, each in duplicate, were performed.

Xenograft animal model

4-6 week-old female athymic nude-Foxn1 nu/nu mice were obtained from Harlan (Udine, Italy) and maintained under specific pathogen-free conditions at the animal resource service of the Medical University of Vienna. Mice were subcutaneously inoculated with 1.5 x 10^7 A2780 OC cells on both ventral hind flanks. Tumor size was measured every second day by calipers. The tumor volume was calculated according to the formula V=4/3 x π x (L/2 x W/2 x W/2); L, length; W, width [31]. Mice were sacrificed two weeks after inoculation. Tumors were recovered, weighed and further processed for histological and pathological analysis. Animal experiments were performed according to protocols approved by the Austrian Federal Ministry for Education, Science and Art.

Immunohistochemistry

Formalin fixed, paraffin embedded sections were deparaffinized, rehydrated and cooked in 10 mmol citrate buffer (pH 6,0) for 20 minutes. To inhibit endogenous peroxidase, slides were incubated in 0.3% hydrogen peroxide. Serum was used to block background staining. Sections were subsequently incubated with the following primary antibodies: anti-human Ki-67 (clone MIB-1; dilution 1:200; Dako, CA, USA) for 1 hour, c-$FLIP_L$ (C-19; dilution 1:25; Santa Cruz; this antibody shows non cross-reactivity with $FLIP_S$) for 1 hour. The secondary biotinylated antibody was applied corresponding to the source of the primary antibody. Then the Strep-ABComplex (Dako) was added for 45 minutes and DAB (Dako) was used for color development and Mayer's hematoxylin for counterstaining. Tissue sections were analyzed on an

Olympus BX50 upright light microscope (Olympus Europe, Hamburg, Germany) equipped with the Soft Imaging system CC12.

Tunel Assay

Apoptosis was determined by terminal deoxynucleotidyltransferase-mediated dUTP nick end labeling (TUNEL; Roche, Manchester, UK) according to the manufacturer's instructions. Cells were analyzed on a fluorescence microscope (Nikon Eclipse 800) equipped with a Nikon DS-R1 camera, using the NIS-Elements software.

Positive and negative controls were performed by treating samples with DNase I or excluding incubation with primary antibody, and yielded positive and negative results, respectively. The percentage of positive cells was determined by a blinded operator.

Statistical analysis

Statistical significance was assessed by two-sided Student's t-tests using R and Statstoft's Statistica software (Hamburg, Germany). Data were visualized with box plots or bar plots. *P* values below 0.05 were considered as statistically significant, and *P* values below 0.005 were considered highly significant. The correlation between variables was estimated using the Pearson correlation coefficient.

Results

c-FLIP$_L$ depletion sensitizes OC cells for TRAIL-induced apoptosis

We previously showed that more than two third of OC patients display defects in the TRAIL pathway, including downregulation of TRAIL functional receptors DR4 and/or DR5, as well as upregulation of c-FLIP$_L$ [17]. Based on these finding we intended to decipher the physiological function and intracellular regulation of c-FLIP$_L$ in OC development. We applied a loss of function approach via expressing shRNA for depleting c-FLIP$_L$ expression in OC cell lines. We expressed shRNA from two different c-FLIP$_L$ sequences (shRNA1 or shRNA2) in two human OC cell lines, namely MDAH-2774 and A2780. These cell lines are highly resistant to TRAIL-induced apoptosis, and harbor various alterations ranging from non-functional p53 in MDAH-2774 [32], and silencing of DR4 expression in A2780 (Supplementary Fig. 3.2.1) [33]. The shRNA reduced the expression of c-FLIP$_L$ protein significantly, as demonstrated by immunoblotting (Fig. 3.2.1*A*). Respective mRNA expression levels were reduced by 61% and 55% in MDAH-2774, and by 63% and 46% in A2780 in both c-FLIP shRNA1 and c-FLIP shRNA2 when compared to control shRNA (Fig. 3.2.1*B* and Supplementary Fig. 3.2.2*A*). c-FLIP$_L$ expression remained unaltered in MDAH-2774 and A2780 cell lines expressing a control shRNA not targeting a protein coding transcript when compared to parental cells (Fig. 3.2.1*A* and *B*).

We found that depletion of c-FLIP$_L$ increased the apoptosis rate of c-FLIP shRNA1 and c-FLIP shRNA2 in MDAH-2774 and A2780 OC cell lines significantly when compared with parental and control shRNA cells in a TRAIL-dependent manner *in vitro* (Fig. 3.2.1*C* and *D,* and Supplementary Fig.

3.2.2*B*). Next, we wanted to determine whether the genetic alterations introduced into OC cells affected their proliferation. c-FLIP shRNA1, c-FLIP shRNA2, control shRNA and parental cells from MDAH-2774 and A2780 OC cells were seeded into 24-well plate and the proliferation rate was determined every 24 hours for 4 days. No significant differences were found in c-FLIP$_L$ depleted cells compared to either control shRNA or parental counterparts *in vitro* (Fig. 3.2.1*E*).

Together, these data show that downregulation of c-FLIP$_L$ significantly enhanced the susceptibility of OC cells to TRAIL-induced apoptosis *in vitro*.

A)

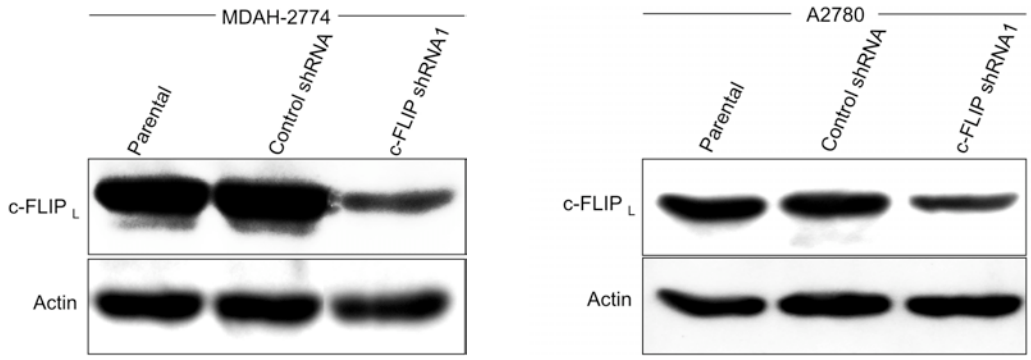

B)

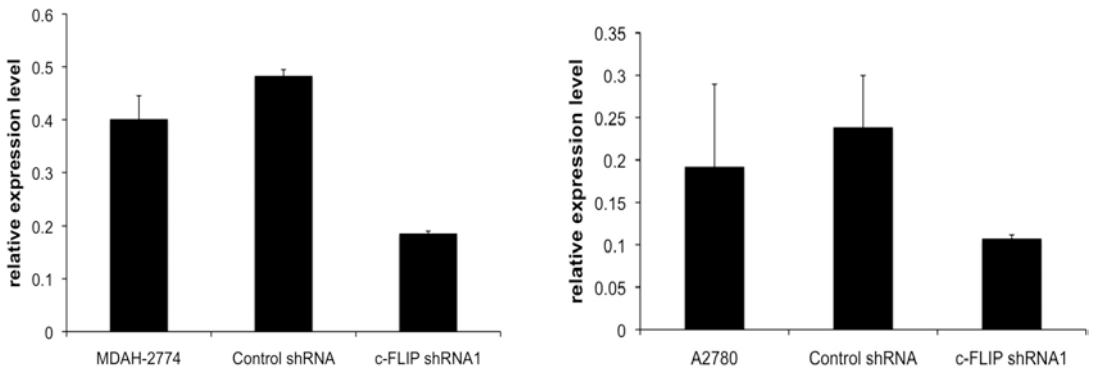

C)

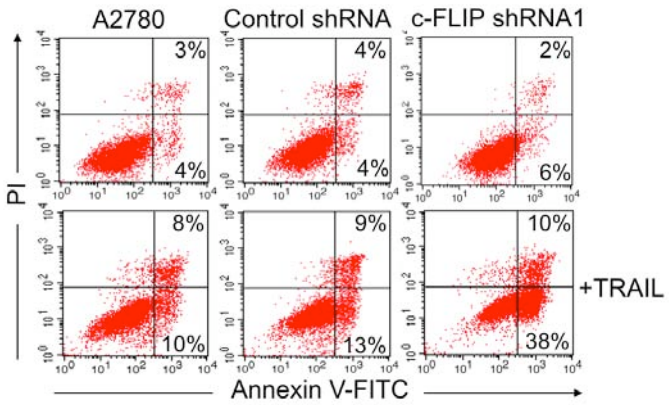

D)

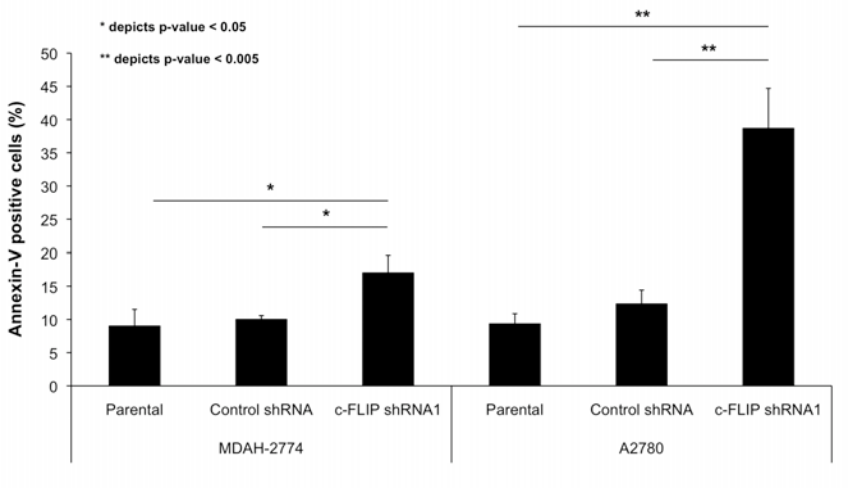

E)

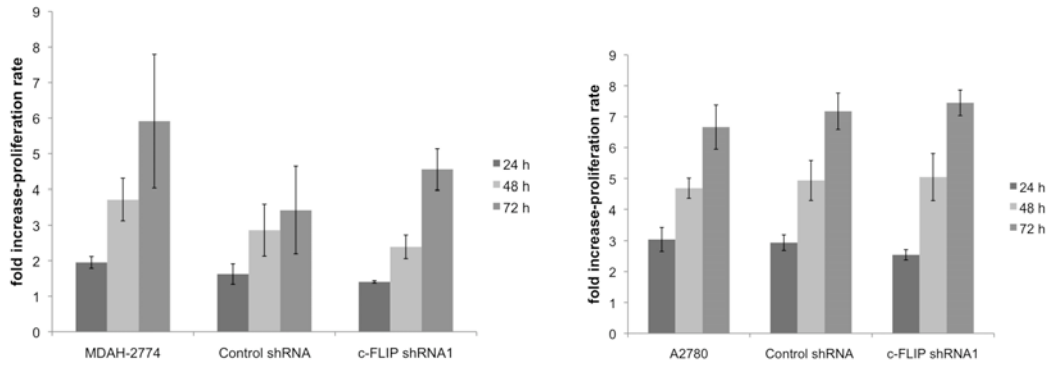

Figure 3.2.1. c-FLIP$_L$ depletion sensitizes OC cells for TRAIL-induced apoptosis. A) MDAH-2774 and A2780 OC cells were either left untransfected or were transfected with a vector encoding control shRNA or c-FLIP shRNA1. Protein expression of c-FLIP$_L$ and actin, used as housekeeping protein, were assessed by Western blot. A representative experiment for two independent experiments is shown. **B)** RNAs were isolated from untransfected MDAH-2774 and A2780 OC cells and those transfected with a vector encoding control shRNA or c-FLIP shRNA1.

qRT-PCR was performed using specific primers for c-FLIP and HPRT1, used as housekeeping gene. Columns represent the mean of duplicate of one experiment; bars, ±S.E.M. (standard error of the mean). Data represent three independent experiments. **C)** Parental A2780 cells or those transfected with control shRNA or c-FLIP shRNA1 were either left untreated or treated with soluble TRAIL (100 ng/ml) for 24 hours. Apoptosis was determined by annexin-V and PI staining. The percentage of apoptotic cells in the respective quadrant is given. **D)** Parental MDAH-2774 and A2780 OC cells or those transfected with control shRNA or c-FLIP shRNA1 were either left untreated or treated with soluble TRAIL (100 ng/ml) for 24 hours, and apoptosis was measured as indicated above. *Columns* hold the mean of three independent experiments: *bars*, ±S.E.M.; *statically significant (P<0.05), or **highly significant (P<0.005) differences obtained by comparing c-FLIP shRNA1 transfected cells to either parental or control shRNA transfected cells. **E)** *In vitro* cell proliferation assay. The proliferation rate of MDAH-2774 and A2780 parental cells or those transfected with control shRNA or c-FLIP shRNA1 was determined by Cell Titer-Blue for 24, 48 and 72 hours. The experiment was performed in triplicate, columns represent the mean of triplicate of one experiment; bars ±S.E.M. Data represent three independent experiments.

c-FLIP$_L$ depletion causes regression of OC in a xenograft mouse model

We next evaluated the effects of c-FLIP$_L$ depletion on OC progression *in vivo*. We used the A2780 human epithelial OC cell line, representing the most common category of human OC, to establish a xenograft OC mouse model. We subcutaneously implanted c-FLIP shRNA1, control shRNA expressing cells, or parental cells (1.5×10^7) into 6 to 8-week-old female athymic mice, and monitored tumor growth. All mice were sacrificed after 2 weeks and tumor weights were determined. We observed that both parental (n=5) and control shRNA cells (n=8) formed very large tumors within 2 weeks, whereas mice injected with c-FLIP shRNA1 cells showed either no tumor (n=4) or reduced tumor formation (n=4) (Fig. 3.2.2*A*, and Supplementary Fig. 3.2.3*A*). These results were obtained from two independent experiments. In contrast to both parental and control shRNA cells, which showed large tumor weight, c-FLIP shRNA1 cells resulted in significantly reduced tumor weight (Fig. 3.2.2*C* and Supplementary Fig. 3.2.3*C*). The correlation between tumor volume (day 14) and tumor weight was high (Pearson r=0.84 and 0.87, Fig. 3.2.2*B* and

Supplementary Fig. 3.2.3*B* respectively). These results indicate that c-FLIP$_L$ expression promotes OC development *in vivo*, giving new insights about the physiological role of c-FLIP$_L$ in ovarian tumor progression *in vivo*.

A)

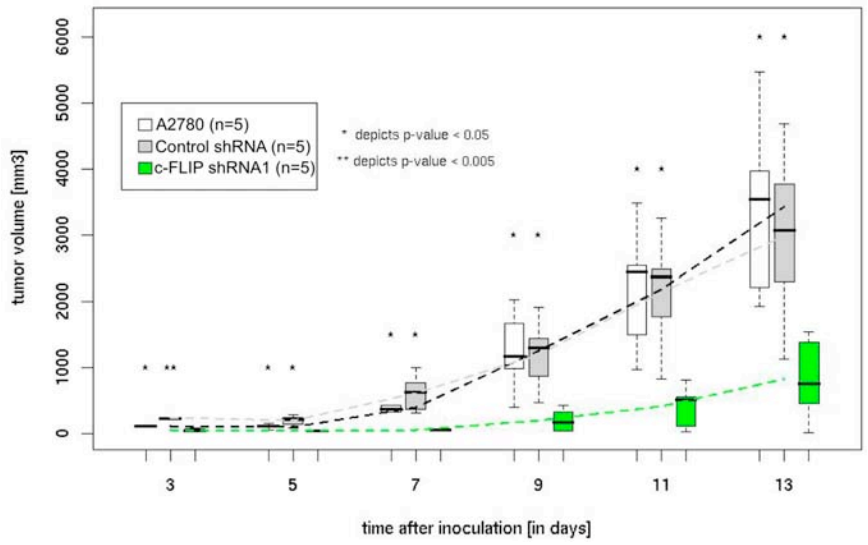

B)

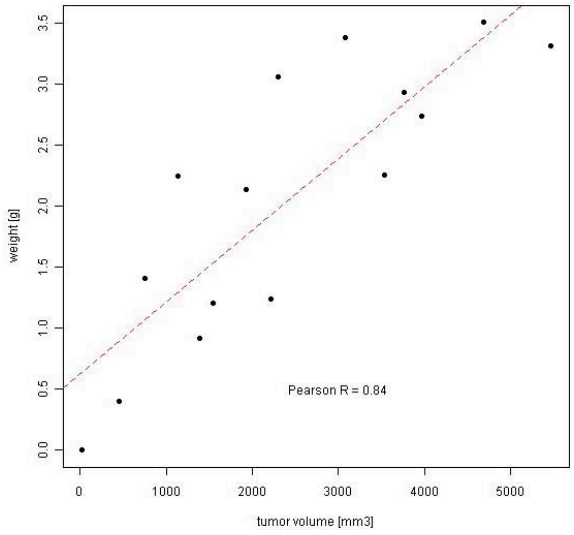

C)

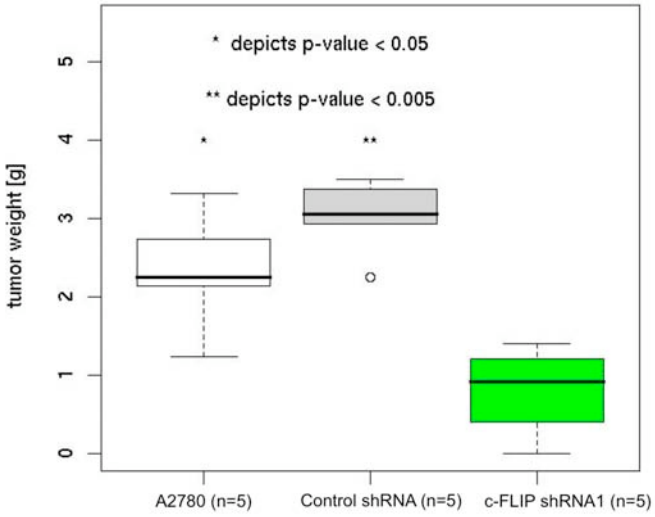

Figure 3.2.2. c-FLIP$_L$ depletion causes regression of OC in a xenograft mouse model. A) Groups of five female nude/nude mice were subcutaneously inoculated with 1.5 x 10^7 of either parental A2780 ovarian tumor cells or those transfected with control shRNA1 or c-FLIP shRNA1 into left and right ventral hind flanks (day 0). Tumor volumes were measured every second day for a period of 14 days. Every measurement in each group represents the sum of both left and right tumor volumes per animal and is depicted by box plots; the line inside each boxplot indicates median, and the boxes at the 25th and 75th percentiles indicate error bars at minimum and maximum, respectively. * P<0.05, ** P<0.005, comparing tumor volume in c-FLIP shRNA1 group with either parental or control shRNA groups. **B)** Correlation between tumor volume on day 14 and tumor weight. **C)** The tumor weight of the given groups after 14 days is depicted by box plots; * P<0.05, ** P<0.005, comparing the c-FLIP shRNA1 group with parental or control shRNA groups. Weight measurement in each group is represented by the sum of both left and right tumors per animal.

c-FLIP$_L$ depletion enhances sensitivity of ovarian tumors to apoptosis and inhibits proliferation *in vivo*

We analyzed whether the suppressive effect of c-FLIP$_L$ depletion on ovarian tumor growth *in vivo* is due to increased apoptosis or reduced proliferation. Histological analyses confirmed that the number of vital, intact cells was markedly reduced in mice injected with c-FLIP shRNA1 when compared to control shRNA or parental cells, indicating that c-FLIP$_L$ depletion influenced tumor cell survival (Fig. 3.2.3*A*). c-FLIP$_L$ was markedly reduced in c-FLIP

shRNA1 compared to control or parental tumor tissues, again confirming effective depletion of c-FLIP$_L$ (Fig. 3.2.3*A*).

Interestingly, immunohistochemical analysis of tumor tissues showed that c-FLIP shRNA1 expressing tumors displayed a reduction in Ki-67 (indicator for cell proliferation) positive cells when compared to control shRNA and parental cells (Fig. 3.2.3*A* and *B*). Moreover, the apoptosis rate was significantly increased from 4% in parental and control shRNA to 27% in c-FLIP shRNA1 expressing cells (Fig. 3.2.3*A* and *C*). This observation reflects the finding mentioned above that c-FLIP$_L$ restores sensitivity of OC to TRAIL-induced apoptosis (Fig. 3.2.1*C* and *D,* and Supplementary Fig. 3.2.2*B*). Taken together, these data indicate that the antitumorigenic effects observed in mice implanted with c-FLIP shRNA1 are in fact not only due to induction of apoptosis, but also due to inhibition of proliferation. Our finding indicates that c-FLIP$_L$ is indeed an apoptosis inhibitor as well as a proliferation mediator *in vivo*.

A)

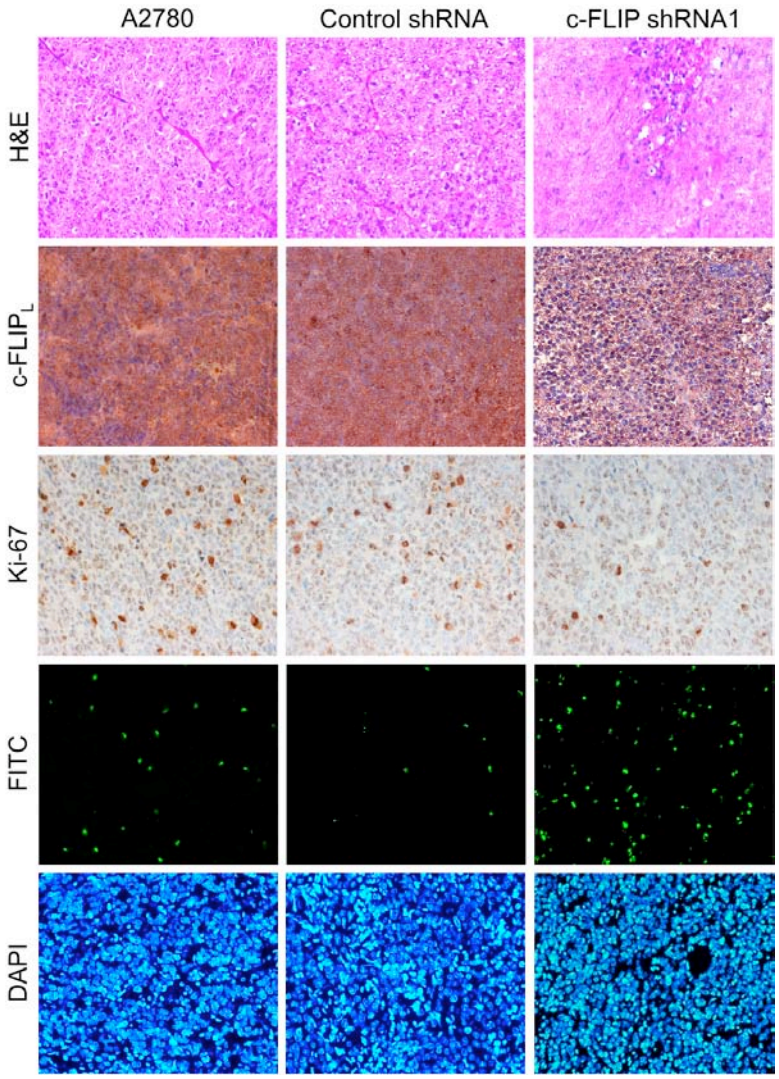
A2780
Control shRNA
c-FLIP shRNA1
H&E
c-FLIP$_L$
Ki-67
FITC
DAPI

B)

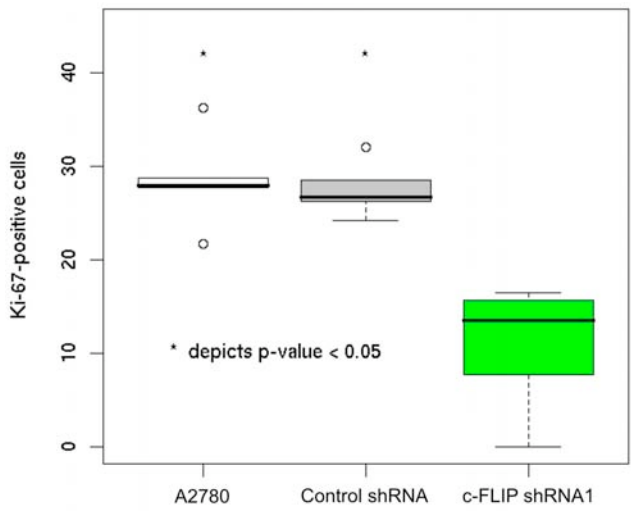
Ki-67-positive cells
0
10
20
30
40
* depicts p-value < 0.05
A2780
Control shRNA
c-FLIP shRNA1

C)

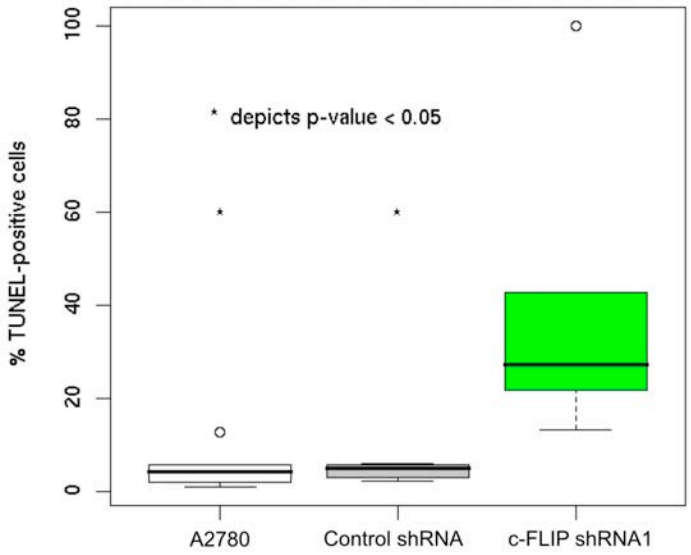

Figure 3.2.3. c-FLIP$_L$ depletion enhances sensitivity of ovarian tumors to apoptosis and inhibits proliferation *in vivo.* Immunohistochemical analysis of tumors obtained from mice on day 14 transplanted with either parental A2780 cells or cells transfected with control shRNA or c-FLIP shRNA1 for **A)** H&E, c-FLIP$_L$, Ki-67 staining, and Tunel assay; magnification 200x. **B and C)** Proportional cell numbers of positive staining of 9 subsections of three different tumor sections per group are depicted by box plot; *statistically significant (P<0.05), or **highly significant (P<0.005) differences when comparing the c-FLIP shRNA1 group with parental or control shRNA groups.

c-FLIP$_L$ depletion inhibits migration and the invasive behavior of OC cells

We examined whether c-FLIP$_L$ depletion has an effect on the migratory phenotype of OC cells *in vitro*. c-FLIP shRNA1, control shRNA, and parental A2780 cells were grown in absence or presence of 100 ng/ml TRAIL for 24 hours, and the number of migrated cells through chambers was determined. We found that the depletion of c-FLIP$_L$ by shRNA completely inhibited migration of OC cells (98.7%), whereas cells treated with control shRNA or parental cells were not inhibited in presence of soluble TRAIL (38%) (Fig. 3.2.4*A* and *B*). Importantly, no differences in migration were observed between the tested groups in absence of TRAIL (Fig. 3.2.4*A* and *B*), which

might suggest that the observed inhibitory effects are indeed due to the increase of apoptosis upon downregulation of c-FLIP$_L$. Moreover, this result confirms the increase in apoptosis rate which was observed after c-FLIP$_L$ depletion and treatment with soluble TRAIL (Fig. 3.2.1*C* and *D,* and Supplementary Fig. 3.2.2*B*). Together, these data indicate that c-FLIP$_L$ inhibits TRAIL-induced apoptosis, and also permits migration of OC cells in presence of TRAIL.

We finally examined whether c-FLIP$_L$-mediated tumor growth is required for the invasive phenotype of OC *in vivo.* We subcutaneously inoculated control shRNA and c-FLIP shRNA1 expressing cells into athymic nude mice. Two weeks after inoculation we observed that control shRNA tumors inoculated into mice (n=4) invaded the peritoneal cavity, whereas no invasive tumors were observed in mice inoculated with c-FLIP shRNA1 expressing tumors (n=3) (Fig. 3.2.4*C*). This finding is in line with our observation outlined above that c-FLIP$_L$ depletion inhibits migration of OC cells in the presence of soluble TRAIL (Fig. 3.2.4*A* and *B*). Taken together, these results indicate that the expression of c-FLIP$_L$ promotes tumor development, furthermore acquiring the ability to invade the peritoneal cavity.

A)

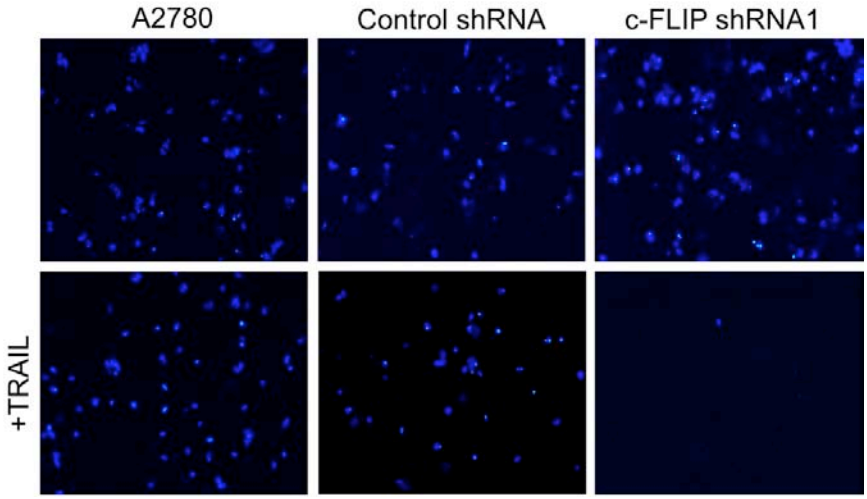

B)

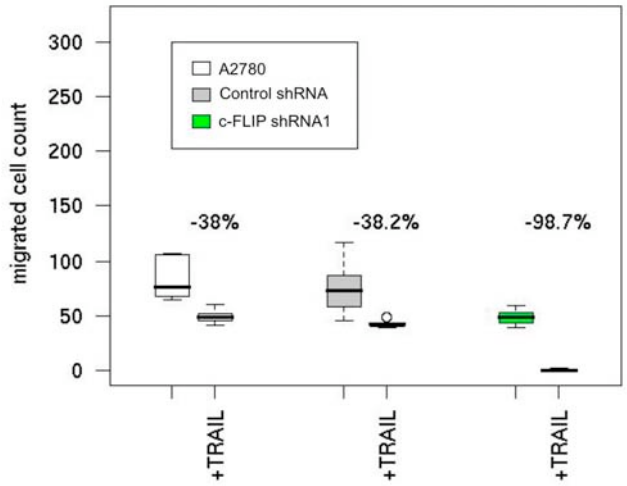

C)

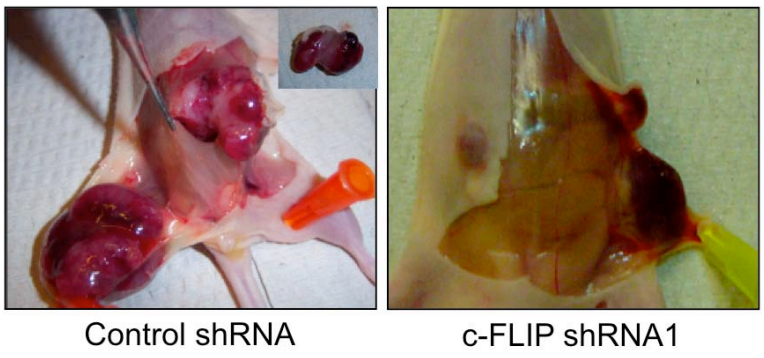

Figure 3.2.4. c-FLIP$_L$ depletion inhibits migration and the invasive behavior of OC cells. A) *In vitro* migration assay. Parental A2780 cells, transfected with control shRNA, or with c-FLIP shRNA1 were either left untreated or treated with soluble TRAIL (100 ng/ml), and their migratory potential was assessed in 24-well transwell cell culture chambers for 24 hours. Migrated cells were counted by staining the lower surface of the membrane with DAPI. Data represent three independent experiments. **B)** The number of migrated cells is shown in presence or absence of soluble TRAIL.

Data represent three independent experiments. **C)** Groups of five female nude/nude mice were subcutaneously inoculated with 1.5 x 10^7 A2780 ovarian tumor cells expressing either control shRNA or c-FLIP shRNA1 into left and right ventral hind flanks (two mice of the group inoculated with c-FLIP shRNA1 were excluded from the analysis as inoculation resulted in intraperitoneal tumors). In contrast to A2780 OC cells transfected with c-FLIP shRNA1, cells transfected with control shRNA invaded the peritoneal cavity of nude mice.

Discussion

TRAIL is known to induce apoptosis in transformed cells but not in normal cells. There are several potential resistance mechanisms that protect normal cells from the cytotoxic effect of TRAIL, including expression of decoy receptors (DCR1 and DCR2), or the presence of apoptosis inhibitor proteins such as c-FLIP. The expression of functional TRAIL protein appears to be restricted to immune cells. Moreover, TRAIL-deficient mice do not show large abnormalities, except for impaired tumor immunosurveillance and higher sensitivity to experimental autoimmune diseases [34]. These findings provide strong evidence for the physiological role of TRAIL in the immune system. NK cells and CTLs both have the ability to destroy tumor cells by various mechanisms; one of them is the production of death ligands such as FasL and TRAIL. As published previously, c-FLIP$_L$ prevents NK cells and CTLs-mediated immunosurveillance, resulting in aggressive tumors *in vivo* [18-20]. We have recently shown that TRAIL is highly expressed in the ovarian tumor microenvironment, and NK-mediated immunosurveillance in OC might be mediated by TRAIL [21]. We further wanted to investigate the role of c-FLIP$_L$ in inhibiting TRAIL-induced apoptosis and in mediating OC progression. Initially, we examined expression values of c-FLIP in gene expression datasets in human primary ovarian tumors as stored in the Oncomine database [35]. The expression level of c-FLIP was found to be upregulated in various ovarian tumors (endometrioid, serous, mucinous, and clear cell carcinomas) when compared to normal ovarian tissue samples in a dataset published by Lu [36]. These observations in human primary ovarian carcinoma are in line with previous findings that c-FLIP$_L$ is highly expressed in

primary ovarian tumors [17, 37]. Actually, c-FLIP has been suggested to mediate proapoptotic as well as antiapoptotic effects [9, 10, 13, 38, 39]. Nonetheless, proapoptotic effects were observed mainly upon transient, forced expression, which may have been due to high cytoplasmic levels of c-FLIP. This in turn may have mediated activation of procaspase-8 [40]. Results from stably forced expression of c-FLIP and from c-FLIP knockout mice supported the anti-apoptotic effect [10, 41]. In the current study, we showed that c-$FLIP_L$ mediates anti-apoptotic signals in ovarian tumor malignancy using OC cell lines resistant to TRAIL-mediated apoptosis. We found that depletion of c-$FLIP_L$ in OC cell lines breaks the resistance mechanism to TRAIL-induced apoptosis *in vitro*. We observed that depletion of c-$FLIP_L$ in MDAH-2774 cells enhanced sensitivity to TRAIL-induced apoptosis to about 25%, and in A2780 cells to about 45% (Fig. 3.2.1 and Supplementary Fig. 3.2.2).

In the preclinical xenograft mouse model we found that the shut down of c-$FLIP_L$ reduced tumor development (Fig. 3.2.2*A* and *C*, and Supplementary Fig. 3.2.3*A* and *C*). Tumor volume and tumor weight were dramatically reduced in c-$FLIP_L$ depleted cells when compared to cells given control shRNA, or parental cells. Moreover, we found that c-$FLIP_L$ depletion increased the rate of apoptosis in tumor cells implanted in mice (Fig. 3.2.3*A* and *C*). These *in vivo* results, next to our *in vitro* data, indicate the key role of c-$FLIP_L$ in inhibiting apoptosis in OC via mediating the escape of ovarian tumors from immunosurveillance. Remarkably, nude mice are characterized by a higher cytotoxic activity of NK cells and macrophages than their euthymic counterparts [42, 43]. Therefore we preferred nude mice for our studies over

other immune deficient animal models. The homology between the human and murine TRAIL ligand is only 65%; however, murine TRAIL was shown to have some cross-reactivity with the receptors on human tumor cells [44].

Interestingly, we found that c-FLIP$_L$ depletion has no effect on proliferation and migration of OC cell lines in absence of soluble TRAIL *in vitro*. However, our *in vivo* results showed that depletion of c-FLIP$_L$ decreased the rate of proliferation in ovarian tumor tissues (Fig. 3.2.3*A* and *B*). Several lines of evidence support such a role for c-FLIP$_L$ in induction of proliferation: First, studies applying gain of function showed that c-FLIP$_L$ activates ERK and NF-κB -mediated T-cell proliferation [45-47]. Second, conditional removal of c-FLIP in mouse T-cells displayed a decrease in TCR-activated proliferation and IL-2 production, which has been linked to a defect in NF-κB signaling [45, 48]. Third, c-FLIP$_L$ has been shown to mediate T-cell proliferation through an NF-κB -independent mechanism, which still needs to be further illustrated [49]. In our study, we did not observe any alterations in proliferation of c-FLIP$_L$ depleted OC cells *in vitro* (Fig. 3.2.1*E*), which might be explained by the fact that the specific microenvironment is absent *in vitro*. We noted that in the presence of soluble TRAIL, c-FLIP$_L$ depletion completely inhibited the migratory behavior of OC cells (Fig. 3.2.4*A* and *B*), and inhibited the invasive behavior *in vivo*. This observation indicates that c-FLIP$_L$ depletion induces apoptosis in OC cells (Fig. 3.2.4), which might be the reason that these cells do not go through the peritoneal cavity and therefore inhibits their invasive behavior. Additionally, c-FLIP$_L$ has been shown to regulate ERK and NF-κB pathways [46], which might explain why c-FLIP$_L$ induces OC invasion. Notably, OC in humans metastasizes in most cases into the free peritoneal

cavity and is restricted to the peritoneal cavity. Metastases at other sites are a rare event, which is in line with our observations in the xenograft mouse model that also showed invasion restricted to the peritoneal cavity and not other sites.

In conclusion, our *in vitro* and *in vivo* data indicate that c-FLIP$_L$ depletion inhibits tumor growth through induction of apoptosis and inhibition of proliferation, indicating that c-FLIP$_L$ plays a key role in ovarian tumor progression. Our study highlights c-FLIP$_L$ as a central switch between cell proliferation and cell death at the DISC level in OC, suggesting that c-FLIP$_L$ is a potential target for OC therapy.

Acknowledgement

We thank Prof. Losert and his colleagues in the animal facility for taking care of mice. We would also like to acknowledge Thomas Pangerl and Sabine Strommer for excellent assistance in the mice experiments.

References

[1] Green DR, Evan GI. A matter of life and death. Cancer Cell 2002;1: 19-30.

[2] Hengartner MO. The biochemistry of apoptosis. Nature 2000;407: 770-6.

[3] Thompson CB. Apoptosis in the pathogenesis and treatment of disease. Science 1995;267: 1456-62.

[4] Vaux DL, Strasser A. The molecular biology of apoptosis. Proc Natl Acad Sci U S A 1996;93: 2239-44.

[5] Alnemri ES, Livingston DJ, Nicholson DW, Salvesen G, Thornberry NA, Wong WW, Yuan J. Human ICE/CED-3 protease nomenclature. Cell 1996;87: 171.

[6] Kumar S. ICE-like proteases in apoptosis. Trends Biochem Sci 1995;20: 198-202.

[7] Chinnaiyan AM, O'Rourke K, Tewari M, Dixit VM. FADD, a novel death domain-containing protein, interacts with the death domain of Fas and initiates apoptosis. Cell 1995;81: 505-12.

[8] Ashkenazi A. Targeting death and decoy receptors of the tumour-necrosis factor superfamily. Nat Rev Cancer 2002;2: 420-30.

[9] Inohara N, Koseki T, Hu Y, Chen S, Nunez G. CLARP, a death effector domain-containing protein interacts with caspase-8 and regulates apoptosis. Proc Natl Acad Sci U S A 1997;94: 10717-22.

[10] Irmler M, Thome M, Hahne M, Schneider P, Hofmann K, Steiner V, Bodmer JL, Schroter M, Burns K, Mattmann C, Rimoldi D, French LE,

Tschopp J. Inhibition of death receptor signals by cellular FLIP. Nature 1997;388: 190-5.

[11] Djerbi M, Darreh-Shori T, Zhivotovsky B, Grandien A. Characterization of the human FLICE-inhibitory protein locus and comparison of the anti-apoptotic activity of four different flip isoforms. Scand J Immunol 2001;54: 180-9.

[12] Scaffidi C, Schmitz I, Krammer PH, Peter ME. The role of c-FLIP in modulation of CD95-induced apoptosis. J Biol Chem 1999;274: 1541-8.

[13] Shu HB, Halpin DR, Goeddel DV. Casper is a FADD- and caspase-related inducer of apoptosis. Immunity 1997;6: 751-63.

[14] Krueger A, Schmitz I, Baumann S, Krammer PH, Kirchhoff S. Cellular FLICE-inhibitory protein splice variants inhibit different steps of caspase-8 activation at the CD95 death-inducing signaling complex. J Biol Chem 2001;276: 20633-40.

[15] Chawla-Sarkar M, Bae SI, Reu FJ, Jacobs BS, Lindner DJ, Borden EC. Downregulation of Bcl-2, FLIP or IAPs (XIAP and survivin) by siRNAs sensitizes resistant melanoma cells to Apo2L/TRAIL-induced apoptosis. Cell Death Differ 2004;11: 915-23.

[16] Song JH, Song DK, Herlyn M, Petruk KC, Hao C. Cisplatin down-regulation of cellular Fas-associated death domain-like interleukin-1beta-converting enzyme-like inhibitory proteins to restore tumor necrosis factor-related apoptosis-inducing ligand-induced apoptosis in human melanoma cells. Clin Cancer Res 2003;9: 4255-66.

[17] Horak P, Pils D, Kaider A, Pinter A, Elandt K, Sax C, Zielinski CC, Horvat R, Zeillinger R, Reinthaller A, Krainer M. Perturbation of the

tumor necrosis factor--related apoptosis-inducing ligand cascade in ovarian cancer: overexpression of FLIPL and deregulation of the functional receptors DR4 and DR5. Clin Cancer Res 2005;11: 8585-91.

[18] Kataoka T, Schroter M, Hahne M, Schneider P, Irmler M, Thome M, Froelich CJ, Tschopp J. FLIP prevents apoptosis induced by death receptors but not by perforin/granzyme B, chemotherapeutic drugs, and gamma irradiation. J Immunol 1998;161: 3936-42.

[19] Medema JP, de Jong J, van Hall T, Melief CJ, Offringa R. Immune escape of tumors in vivo by expression of cellular FLICE-inhibitory protein. J Exp Med 1999;190: 1033-8.

[20] Screpanti V, Wallin RP, Ljunggren HG, Grandien A. A central role for death receptor-mediated apoptosis in the rejection of tumors by NK cells. J Immunol 2001;167: 2068-73.

[21] Ahmed El-Gazzar, Paul Perco, Eva Eckelhart, Mariam Anees, Veronika Sexl, Bernd Mayer, Yanxin Liu, Wolfgang Mikulits, Reinhard Horvat, Thomas Pangerl, Dexian Zheng, Michael Krainer. Natural immunity enhances the activity of a DR5 agonistic antibody and carboplatin in the treatment of ovarian cancer. Submitted 2009.

[22] Micheau O, Lens S, Gaide O, Alevizopoulos K, Tschopp J. NF-kappaB signals induce the expression of c-FLIP. Mol Cell Biol 2001;21: 5299-305.

[23] Panka DJ, Mano T, Suhara T, Walsh K, Mier JW. Phosphatidylinositol 3-kinase/Akt activity regulates c-FLIP expression in tumor cells. J Biol Chem 2001;276: 6893-6.

[24] Wang W, Prince CZ, Mou Y, Pollman MJ. Notch3 signaling in vascular smooth muscle cells induces c-FLIP expression via ERK/MAPK activation. Resistance to Fas ligand-induced apoptosis. J Biol Chem 2002;277: 21723-9.

[25] Abedini MR, Muller EJ, Brun J, Bergeron R, Gray DA, Tsang BK. Cisplatin induces p53-dependent FLICE-like inhibitory protein ubiquitination in ovarian cancer cells. Cancer Res 2008;68: 4511-7.

[26] Fukazawa T, Fujiwara T, Uno F, Teraishi F, Kadowaki Y, Itoshima T, Takata Y, Kagawa S, Roth JA, Tschopp J, Tanaka N. Accelerated degradation of cellular FLIP protein through the ubiquitin-proteasome pathway in p53-mediated apoptosis of human cancer cells. Oncogene 2001;20: 5225-31.

[27] Freedman RS, Pihl E, Kusyk C, Gallager HS, Rutledge F. Characterization of an ovarian carcinoma cell line. Cancer 1978;42: 2352-9.

[28] Behrens BC, Hamilton TC, Masuda H, Grotzinger KR, Whang-Peng J, Louie KG, Knutsen T, McKoy WM, Young RC, Ozols RF. Characterization of a cis-diamminedichloroplatinum(II)-resistant human ovarian cancer cell line and its use in evaluation of platinum analogues. Cancer Res 1987;47: 414-8.

[29] Longley DB, Wilson TR, McEwan M, Allen WL, McDermott U, Galligan L, Johnston PG. c-FLIP inhibits chemotherapy-induced colorectal cancer cell death. Oncogene 2006;25: 838-48.

[30] Banno T, Gazel A, Blumenberg M. Pathway-specific profiling identifies the NF-kappa B-dependent tumor necrosis factor alpha-regulated genes in epidermal keratinocytes. J Biol Chem 2005;280: 18973-80.

[31] Esumi H, Lu J, Kurashima Y, Hanaoka T. Antitumor activity of pyrvinium pamoate, 6-(dimethylamino)-2-[2-(2,5-dimethyl-1-phenyl-1H-pyrrol-3-yl)ethenyl]-1-methyl-qu inolinium pamoate salt, showing preferential cytotoxicity during glucose starvation. Cancer Sci 2004;95: 685-90.

[32] Santoso JT, Tang DC, Lane SB, Hung J, Reed DJ, Muller CY, Carbone DP, Lucci JA, 3rd, Miller DS, Mathis JM. Adenovirus-based p53 gene therapy in ovarian cancer. Gynecol Oncol 1995;59: 171-8.

[33] Horak P, Pils D, Haller G, Pribill I, Roessler M, Tomek S, Horvat R, Zeillinger R, Zielinski C, Krainer M. Contribution of epigenetic silencing of tumor necrosis factor-related apoptosis inducing ligand receptor 1 (DR4) to TRAIL resistance and ovarian cancer. Mol Cancer Res 2005;3: 335-43.

[34] Yagita H, Takeda K, Hayakawa Y, Smyth MJ, Okumura K. TRAIL and its receptors as targets for cancer therapy. Cancer Sci 2004;95: 777-83.

[35] Rhodes DR, Kalyana-Sundaram S, Mahavisno V, Varambally R, Yu J, Briggs BB, Barrette TR, Anstet MJ, Kincead-Beal C, Kulkarni P, Varambally S, Ghosh D, Chinnaiyan AM. Oncomine 3.0: genes, pathways, and networks in a collection of 18,000 cancer gene expression profiles. Neoplasia 2007;9: 166-80.

[36] Lu KH, Patterson AP, Wang L, Marquez RT, Atkinson EN, Baggerly KA, Ramoth LR, Rosen DG, Liu J, Hellstrom I, Smith D, Hartmann L, Fishman D, Berchuck A, Schmandt R, Whitaker R, Gershenson DM, Mills GB, Bast RC, Jr. Selection of potential markers for epithelial ovarian cancer with gene expression arrays and recursive descent partition analysis. Clin Cancer Res 2004;10: 3291-300.

[37] Hendrix ND, Wu R, Kuick R, Schwartz DR, Fearon ER, Cho KR. Fibroblast growth factor 9 has oncogenic activity and is a downstream target of Wnt signaling in ovarian endometrioid adenocarcinomas. Cancer Res 2006;66: 1354-62.

[38] Goltsev YV, Kovalenko AV, Arnold E, Varfolomeev EE, Brodianskii VM, Wallach D. CASH, a novel caspase homologue with death effector domains. J Biol Chem 1997;272: 19641-4.

[39] Srinivasula SM, Ahmad M, Ottilie S, Bullrich F, Banks S, Wang Y, Fernandes-Alnemri T, Croce CM, Litwack G, Tomaselli KJ, Armstrong RC, Alnemri ES. FLAME-1, a novel FADD-like anti-apoptotic molecule that regulates Fas/TNFR1-induced apoptosis. J Biol Chem 1997;272: 18542-5.

[40] Siegel RM, Martin DA, Zheng L, Ng SY, Bertin J, Cohen J, Lenardo MJ. Death-effector filaments: novel cytoplasmic structures that recruit caspases and trigger apoptosis. J Cell Biol 1998;141: 1243-53.

[41] Yeh WC, Itie A, Elia AJ, Ng M, Shu HB, Wakeham A, Mirtsos C, Suzuki N, Bonnard M, Goeddel DV, Mak TW. Requirement for Casper (c-FLIP) in regulation of death receptor-induced apoptosis and embryonic development. Immunity 2000;12: 633-42.

[42] Budzynski W, Radzikowski C. Cytotoxic cells in immunodeficient athymic mice. Immunopharmacol Immunotoxicol 1994;16: 319-46.

[43] Radzikowski C, Rygaard J, Budzynski W, Stenvang JP, Schou M, Vangsted A, Zeuthen J. Strain- and age-dependent natural and activated in vitro cytotoxicity in athymic nude mice. APMIS 1994;102: 481-8.

[44] Wiley SR, Schooley K, Smolak PJ, Din WS, Huang CP, Nicholl JK, Sutherland GR, Smith TD, Rauch C, Smith CA, et al. Identification and characterization of a new member of the TNF family that induces apoptosis. Immunity 1995;3: 673-82.

[45] Dohrman A, Kataoka T, Cuenin S, Russell JQ, Tschopp J, Budd RC. Cellular FLIP (long form) regulates CD8+ T cell activation through caspase-8-dependent NF-kappa B activation. J Immunol 2005;174: 5270-8.

[46] Kataoka T, Budd RC, Holler N, Thome M, Martinon F, Irmler M, Burns K, Hahne M, Kennedy N, Kovacsovics M, Tschopp J. The caspase-8 inhibitor FLIP promotes activation of NF-kappaB and Erk signaling pathways. Curr Biol 2000;10: 640-8.

[47] Kataoka T, Tschopp J. N-terminal fragment of c-FLIP(L) processed by caspase 8 specifically interacts with TRAF2 and induces activation of the NF-kappaB signaling pathway. Mol Cell Biol 2004;24: 2627-36.

[48] Chau H, Wong V, Chen NJ, Huang HL, Lin WJ, Mirtsos C, Elford AR, Bonnard M, Wakeham A, You-Ten AI, Lemmers B, Salmena L, Pellegrini M, Hakem R, Mak TW, Ohashi P, Yeh WC. Cellular FLICE-

inhibitory protein is required for T cell survival and cycling. J Exp Med 2005;202: 405-13.

[49] Zhang N, Hopkins K, He YW. The long isoform of cellular FLIP is essential for T lymphocyte proliferation through an NF-kappaB-independent pathway. J Immunol 2008;180: 5506-11.

Supplementary data

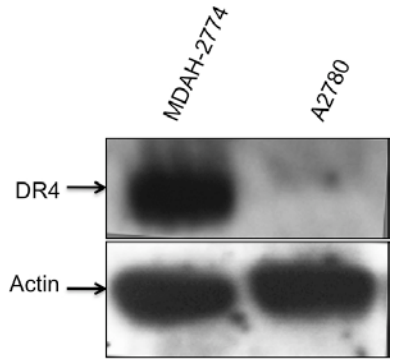

Supplementary figure 3.2.1. Expression of DR4 in selected OC cell lines. Immunoblotting analysis of DR4 and actin expression in MDAH-2774 and A2780 OC cell lines.

A)

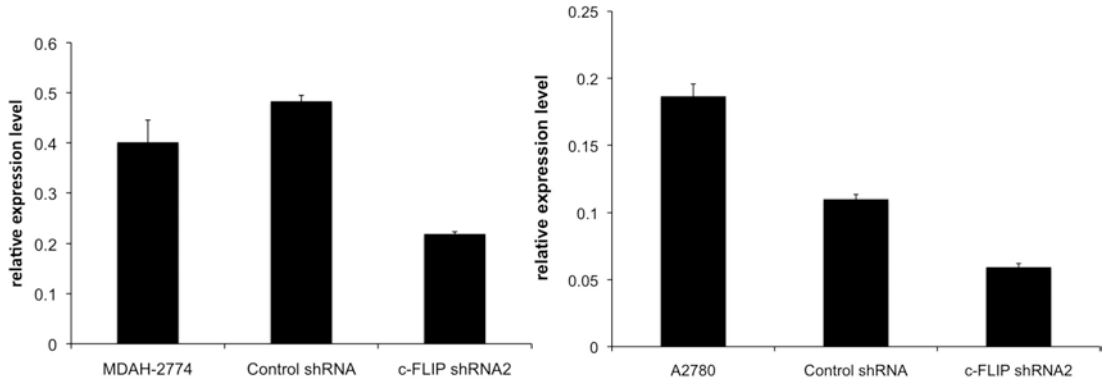

B)

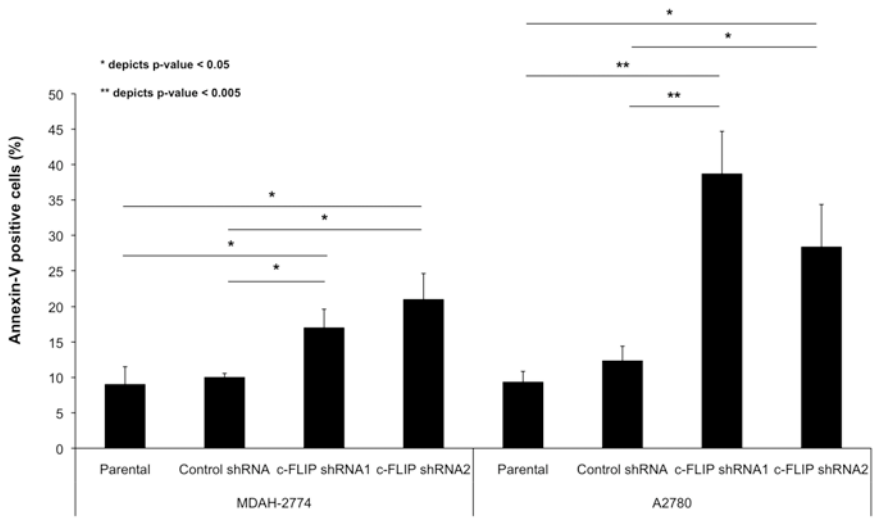

Supplementary figure 3.2.2. c-FLIP$_L$ depletion sensitizes OC cells for TRAIL-induced apoptosis. A) RNAs were isolated from untransfected MDAH-2774 and A2780 OC cells and those transfected with a vector encoding control shRNA or c-FLIP shRNA2. qRT-PCR was performed using specific primers for c-FLIP and HPRT1. Columns represent the mean of duplicate of one experiment; bars, ±S.E.M. Data represent three independent experiments. **B)** Parental MDAH-2774 and A2780 cell lines or those transfected with control shRNA, c-FLIP shRNA1, or c-FLIP shRNA2 were either left untreated or treated with soluble TRAIL (100 ng/ml) for 24 hours. Apoptosis was determined by annexin-V and PI staining. *Columns* hold the mean of three independent experiments: *bars*, ±S.E.M.; *statically significant (P<0.05), or **highly significant (P<0.005) differences obtained by comparing c-FLIP shRNA1/2 transfected cells to either parental or control shRNA transfected cells.

A)

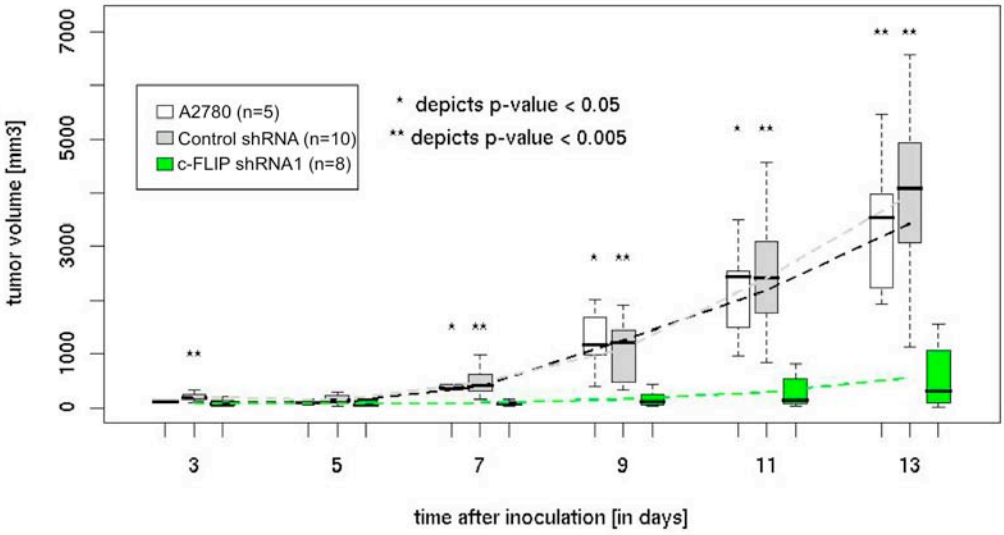

B)

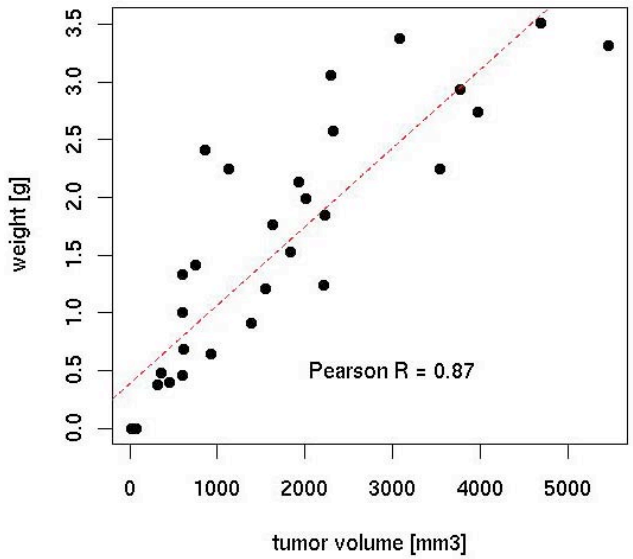

C)

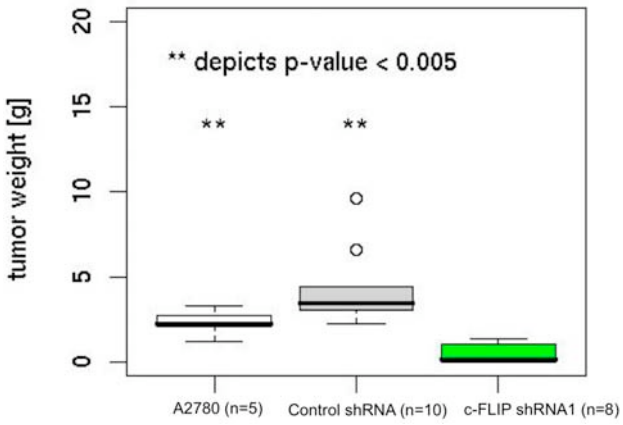

Supplementary figure 3.2.3. c-FLIP$_L$ depletion causes regression of OC in a xenograft mouse model. A) For each experimental group, holding five female nude/nude mice, the animals were inoculated subcutaneously with 1.5x10^7 A2780 ovarian tumor cells either as parental or transfected with control shRNA1 or c-FLIP shRNA1 into left and right ventral flank (day 0). Tumor volumes were measured every second day for a period of 14 days. Each measurement in each group represents the sum of both left and right tumor volumes per animal and is depicted by box plot; the line inside each boxplot indicates the median, and boxes at 25th and 75th percentiles indicate error bars at minimum and maximum, respectively (results are based on two independent experiments). * P<0.05, ** P<0.005, comparing tumor volume in c-FLIP shRNA1 group with either parental or control shRNA groups. Two mice in the c-FLIP shRNA1 inoculated group were excluded from the analysis due to inoculation resulting in intraperitoneal tumors. **B)** Correlation between tumor volume on day 14 and tumor weight in all mice as found in two independent experiments. **C)** Tumor weight of the given (two independent experiments) as found after 14 days is depicted by box plots; *statistically significant (P<0.05), or **highly significant (P<0.005) differences comparing the c-FLIP shRNA1 group with parental or control shRNA groups. Every weight measurement in each group is represented by the sum of both left and right tumor per animal.

3.3. Characterization of the TRAIL pathway in a syngeneic mouse model of ovarian cancer

Introduction

Most human tumors eventually continue to grow independently of spontaneous or therapy induced immune responses, a process described as escape from tumor surveillance. There is ample evidence that this rests on the ability of a fraction of cancer cells to continuously evade potentially effective immune recognition and destruction (1-3). Immunosurveillance against tumors is mediated by both innate and adaptive components of cellular immunity. Endogenous TRAIL protein expressed mainly on a variety of cells of innate and adaptive immune cells, and its expression depends on the stimulation status (4-10). IFN-γ can induce expression of TRAIL on dendritic cells (DCs) and NK cells (4, 5). Increased expression of TRAIL was detected on monocytes and macrophages after stimulation with lipopolysaccharide (LPS) and interferon-β (11, 12). Moreover, TRAIL is upregulated on the surface of CD4+ and CD8+ human T cells after T-cell receptor stimulation, in presence of type I IFNs. TRAIL has been shown to suppress tumor growth of various types such as B-cell lymphoma (13) and breast and renal carcinoma cells (14-16). However, the role of TRAIL-mediated tumor surveillance in the context of ovarian tumors is unclear. As mentioned before, human TRAIL has two known functional receptors DR4 and DR5 and two additional decoy receptors (cell-bound receptors incapable of driving apoptosis signals) DCR1 and DCR2. In addition, human TRAIL can bind with OPG (17, 18). By contrast, in mice there is only one death-inducing receptor homologous to human DR5 (mTRAIL-R2/mDR5), and two potential

decoy receptors (mDcTRAIL-R1 and mDcTRAIL-R2) specific for mouse TRAIL (19). Even though, the homology between the human and murine TRAIL ligands is only 65%, murine TRAIL has been shown to have some cross-reactivity with human tumor cells (20). Mouse DR5 (mDR5) contains the death domain and apoptosis can be induced in response to both mouse and human TRAIL (21). Interestingly, the overall sequence structures of mDcTRAIL-R1 and mDcTRAIL-R2 are distinct from those of the known human decoy TRAIL receptors. OPG can also bind to mouse TRAIL, and might act as soluble decoy receptor for TRAIL (21).

Although both subcutaneous and intraperitoneal xenograft OC mouse models have provided useful insights into clinical treatment (22-29), understanding early events in the establishment and progression of OC is not possible in immunodeficient mice. The immunocompetent mouse model I applied in this study (30) is based on established models utilizing human and rat ovarian surface epithelial cells and tumor cell lines (25, 29, 31-33). Rat ovarian surface epithelial cells become transformed after multiple passages *in vitro* and have been shown to develop tumors in athymic mice (32, 33). The hypothesis is that multiple passages of ovarian surface epithelial cells might cause transformation, which is in line with the theory of incessant ovulation and development of OC (32, 34).

In this part of my PhD thesis I utilized a syngeneic mouse model using ten transformed mouse ovarian surface epithelial (MOSE) cell lines derived from C57BL/6 mice to assess the implications of TRAIL in OC. I characterized all tumorigenic MOSE cell lines in terms of the most relevant players in the TRAIL signaling pathway (mDR5, c-FLIP and caspase-8), and measured their

sensitivity to TRAIL-induced apoptosis. Interestingly, I observed that all tumorigenic MOSE cell lines showed a downregulation of mDR5 when compared with normal (non-tumorigenic) MOSE cells. Additionally, seven out of ten cell lines were resistant to TRAIL-induced apoptosis. I subsequently focused on the well-characterized MOSE ID8 cell line. *In vivo* preliminary data showed that the knockdown of mDR5 by shRNA in the selected ID8 cells accelerated the development of ascites compared to control shRNA and parental cells. Moreover, the downregulation of mDR5 inhibited significantly the apoptosis rate. *In vitro* data as well as preliminary *in vivo* results clearly suggest that the TRAIL/TRAIL-R2 system plays a fundamental role in tumor progression in an accepted immunocompetent OC mouse model.

Material and Methods

Tumorigenic MOSE cell lines

Tumorigenic MOSE cell lines have been kindly provided by Dr Kathy Roby from the University of Kansas, USA. These cell lines were isolated from C57BL/6 mice, cultured *in vitro*, and underwent spontaneous transformation after multiple passages. The parental cell line was cloned and ten tumorigenic MOSE cell lines were established (Fig. 3.3.1).

Tumorigenic MOSE cells (greater than pass 20) were subcultured at 1-2 week intervals in complete medium (DMEM supplemented with 4% FCS (Gibco), 100 U/ml penicillin, 100 µg/ml streptomycin, 5 µg/ml insulin, 5 µg/ml transferring, and 5 ng/ml sodium selenite (Sigma)) and split at ratios of 1:10.

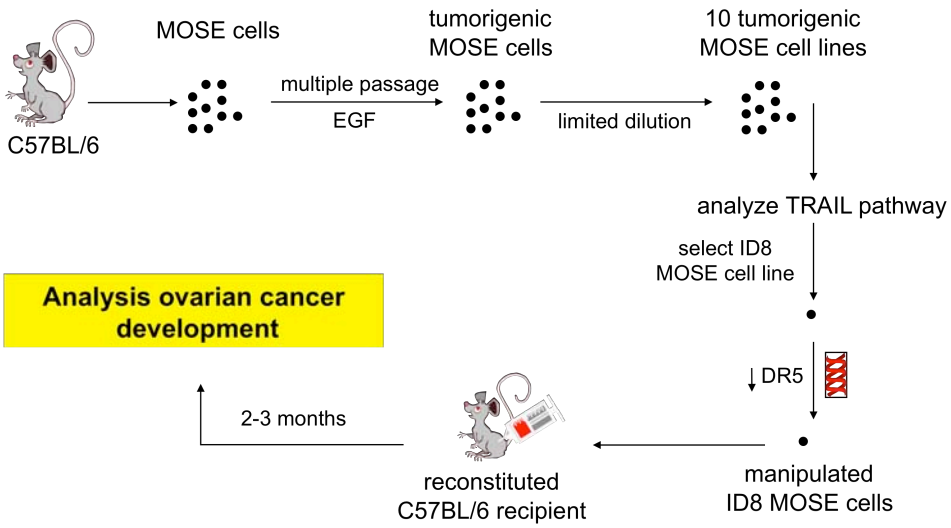

Figure 3.3.1. Schematic map of applying the syngeneic OC mouse model. Tumorigenic MOSE cell lines enriched by mouse ovarian surface epithelial cells were isolated from C57BL/6 donor mice. Proliferation of MOSE cells was induced by adding murine epidermal growth factor (EGF), and cells became transformed after multiple passages. The ID8 MOSE cell line was selected and genetically manipulated by downregulating mDR5. Parental and manipulated cells were subsequently transplanted individually into immunocompetent C57BL/6 recipient mice. Eight weeks after tumorigenic MOSE cells reconstitution, the development of OC cells was analyzed.

Isolation and culturing of normal (non-tumorigenic) ovarian epithelial cells

Ovaries were isolated from five female C57BL/6 mice (eight weeks old; Charles River) and placed in a culture dish containing 1xPBS (Gibco) at 4ºC, under sterile conditions. The ovaries were washed with 1xPBS and placed in a 15 ml conical culture tube containing 10 ml 1xPBS with 0.2% trypsin. The ovaries were incubated in a horizontal position in a tube containing trypsin solution at 37ºC in a humidified atmosphere of 5% CO_2 and air for 30 minutes. After 30 minutes, the media containing epithelial cells was transferred to a fresh tube and 5 ml complete medium was added. The epithelial cells (approximately 100.000 per 10 ovaries) were harvested by centrifugation (1000g for 10 minutes at 22ºC), and were resuspended in 2 ml complete medium and placed in a single well of a 6-well culture dish (all cells were subcultured with trypsin (0.2%) at near confluent). 2 ng/ml murine epidermal growth factor (EGF, Sigma) was added to the medium during the early passage growth.

RNA isolation, cDNA synthesis, and qRT-PCR

RNA isolation, cDNA synthesis and qRT-PCR were performed as described in sections 3.1 and 3.2. For quantitative real time PCR, the following mouse assay-on-Demand probes were used: Mm00457866_m1 DR5, Mm01255578_m1 c-FLIP, Mm00437174_m1 TRAIL, and Mm01545399_m1 HPRT1.

Protein preparation and Western blot analysis

Protein preparation and Western blot were performed as described before in sections 3.1 and 3.2. The following primary antibodies were used: monoclonal anti-mouse TRAIL-R2 (DR5)/TNFRSF10B antibody (dilution 1:250; R&D systems), monoclonal anti-mouse FLIP antibody (Dave-2, dilution 1:1000, Alexis), monoclonal anti-mouse caspase-8 antibody (1G12; dilution 1:1000; Alexis), and goat polyclonal actin HRP (dilution 1:500; Santa Cruz) antibody. The protein bands were quantified using Epi Chemi II Darkroom chamber (UVP laboratory products) and LabWork Gel-Pro Application software.

Apoptosis Assay

Apoptosis assay was performed as decribed before in sections 3.1 and 3.2. Briefly, MOSE cell lines were treated with recombinant mouse soluble TRAIL (Alexis) at final concentrations of 100, 500 and 1000 ng/ml and incubated for 24 hours. Cells were harvested by trypsinization and assessed for apoptosis by a propidium iodide and annexin-V staining assays according to the manufacturer's instruction. The degree of apoptosis was calculated by subtracting measured apoptosis in treated cells from untreated controls.

Generation of RNAi

Oligonucleotides encoding shRNA targeting mDR5 were designed by using Ambion's online Target Finder (Fig. 3.3.2). The specific target sequence for mDR5 (accession number: AF176833) are shown in Table 3.3.1. Control shRNA was used to confirm the specificity of selected shRNAs. Oligonucleotides were annealed by mixing 10 μg of each oligonucleotide

(forward and reverse) with 2 μl 10x annealing buffer (1 M NaCl and 100 mM Tris HCl 'pH 7.4') in a total volume of 20 μ l. The reaction mixture was incubated at 95ºC for 5 minutes and then cooled down slowly at room temperature.

The oligonucleotides were designed to contain restriction sites BamHI and HindIII at 5' and 3' respectively. 1 μg/μl pSilencer 4.1-CMV neo vector (Applied Biosystems) was linearized by digestion with BamH1/HindIII, followed by gel purification on a 1% agarose gel. The annealed oligonucleotides were cloned into a pSilencer 4.1-CMV neo vector and sequences of the resulting vectors were verified by sequencing.

ID8 MOSE cell line was then transfected with the according vectors (encoded shRNA oligonucleotide) by the lipofecatmine transfection method (Invitrogen) according to the manufacturer's instructions. To measure the suppression level of the mDR5 target gene mRNA and protein were isolated, and qRT-PCR and Western blot were performed respectively.

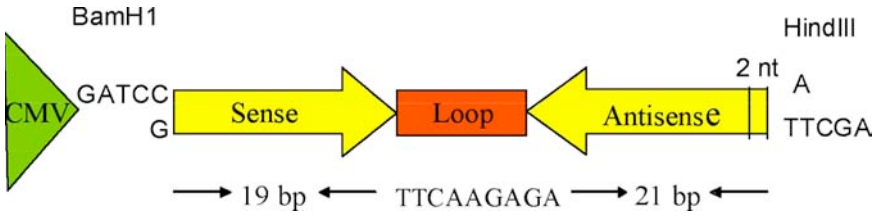

Figure 3.3.2. Schematic map of the design of the shRNA target sequence. A prototypical shRNA is comprised of two hybridized RNA molecules with 19 complementary nucleotides (derived from mRNA sequence), a loop sequence separating the two complementary domains, and 3′ polythymidine tract to terminate transcription. Transcription is regulated by the CMV promoter.

Target name	Oligonucleotide sequence
A	**Forward:** 5'-GATCC GCGCAGACTTCTATATAGC TTCAAGAGA GCTATATAGAAGTCTGCGCTTA-3' **Reverse:** 5'-AGCTTAAGCGCAGACTTCTATATAGCTCTCTTGAA GCTATATAGAAGTCTGCGCG-3'
B	**Forward:** 5'-GATCCATACGGTGTGTCGATGCAATTCAAGAGA TTGCATCGACACACCGTATTTA-3' **Reverse:** 5'-AGCTTAAATACGGTGTGTCGATGCAATCTCTTGAA TTGCATCGACACACCGTATG-3'
C	**Forward:** 5'-GATCCCCGGAAGTGTGTCTCCAAATTCAAGAGA TTTGGAGACACACTTCCGGTTA-3' **Reverse:** 5'-AGCTTAACCGGAAGTGTGTCTCCAAATCTCTTGAA TTTGGAGACACACTTCCGGG-3'
D	**Forward:** 5'-GATCCAGTGCGAACTCTGTGCATTTTCAAGAGA AATGCACAGAGTTCGCACTTTA-3' **Reverse:** 5'-AGCTTAAAGTGCGAACTCTGTGCATTTCTCTTGAA AATGCACAGAGTTCGCACTG-3'
E	**Forward:** 5'-GATCCCCTGGCAAGACTCAGAAAATTCAAGAGA TTTTCTGAGTCTTGCCAGGTTA-3' **Reverse:** 5'-AGCTTAACCTGGCAAGACTCAGAAAATCTCTTGAA TTTTCTGAGTCTTGCCAGGG-3'

Table 3.3.1. Oligonucleotide sequences of the various hairpins used for the knockdown of mDR5. The sequences of the forward and reverse primers are shown. Five oligonucleotides were designed (A, B, C, D, and E). The underlined sequences were added for cloning purposes and contain restriction sites (BamHI or HindIII) required for cloning. The red sequence indicates the hairpin.

Immunocompetent OC mouse model

Female immunocompetent C57BL/6 mice, eight weeks of age, were injected intraperitoneally with a single-cell suspension ($5x10^6$ cells in 0.2 ml DMEM containing no additives) of the individual parental or manipulated ID8 MOSE cell line. Observation and measurement of the tumor development were performed by weighting mice every 2-3 days after inoculation. Intraperitoneal

tumor formation was monitored by the accumulation of ascitic fluid. Approximately two weeks after the development of visible ascites (detected by abdominal swelling) the animals were sacrificed. Ascitic fluid was collected at the time of sacrifice and the tumor sizes were noted. As a control, mice were injected with DMEM medium free cells to ensure that the observed tumors are due to the inoculated tumor cells. Animal experiment was performed according to protocols approved by the Austrian Federal Ministry for Education, Science and Art

H&E staining and Immunohistochemistry

H&E staining and Immunohistochemistry were performed as described before in sections 3.1 and 3.2. The following primary antibodies were used: monoclonal anti-mouse TRAIL-R2 (DR5) antibody (dilution 1:100, R&D systems), goat anti-mouse TRAIL antibody (dilution 1:1200, R&D systems), and monoclonal rat anti-mouse Ki-67 (dilution 1:25, Dako).

Tunel assay

Apoptosis was assessed by TUNEL (Roche) according to the manufacturer's instructions. As described before in sections 3.1 and 3.2, cells were analyzed on a fluorescence microscope (Nikon Eclipse 800) equipped with a Nikon DS-R1 camera, using the NIS-Elements software. Positive and negative controls were performed by treating samples with DNase I or excluding incubation with primary antibody, and yielded positive and negative results, respectively.

Statistical analysis

Data were analyzed using the Student's t-tests. *P* values below 0.05 were considered as statistically significant, and *P* values below 0.005 were considered highly significant.

Results

Tumorigenic MOSE cell lines regulate differentially mDR5 and c-FLIP, and are resistant to TRAIL-induced apoptosis

Tumorigenic clonal MOSE cell lines (kindly provided by a collaboration partner) were derived from the ovarian surface epithelium of C57BL/6 mice (30). MOSE cell lines were isolated and cultured *in vitro* and underwent spontaneous transformation after multiple passages. The parental cell line was cloned and ten lines were established [(30) and Fig. 3.3.1 in Materials and Methods].

First, I aimed to characterize the ten tumorigenic MOSE cell lines and to examine the status of the TRAIL-dependent apoptosis signaling pathway in each of them. I isolated MOSE cells from C57BL/6 mice as outlined in (30) and used as normal (non-tumorigenic) MOSE cell control for the endogenous expression of the target genes. The expression of the target molecules mDR5, c-FLIP and caspase-8 were determined on the mRNA and protein level by qRT-PCR and Western blot respectively, and compared to normal MOSE cell levels. Unexpectedly, all ten tumorigenic MOSE cell lines displayed a downregulation of mDR5 as compared with the non-tumorigenic MOSE cell at mRNA and protein level (Fig. 3.3.3*A*, *B* and *C*). By contrast, c-FLIP showed an upregulation in four out of ten tumorigenic MOSE cell lines (IC5, ID3, 2C12 and 3E3) compared with the non-tumorigenic MOSE cells at protein level (Fig. 3.3.3*B* and *C* upper panel). Expression of caspase-8 was unaltered in all ten tumorigenic MOSE cell lines as compared with the non-tumorigenic MOSE cell control at protein level (Fig. 3.3.3*B* and *C* lower panel).

Furthermore, the sensitivity of the established MOSE cell lines to TRAIL were measured by stimulating with soluble mouse recombinant TRAIL, and the degree of apoptosis, in a concentration-dependent manner, was determined (Fig. 3.3.3*D*). I incubated the ten cell lines with recombinant mouse soluble TRAIL at final concentrations of 100, 500 and 1000 ng/ml for 24 hours. Apoptosis was then detected by Annexin-V and PI staining and compared with untreated controls. Three out of ten tumorigenic MOSE cell lines (IC5, ID9, and 3B11) showed response to TRAIL-induced apoptosis only at very high concentrations (1 µg/ml, Fig. 3.3.3*D*). As mentioned above, all ten tumorigenic MOSE cell lines downregulated mDR5 but at different levels. The expression of mDR5 in all ten tumorigenic MOSE cell lines was positively correlated with apoptosis rate. For example, IC5 and 3B11 tumorigenic MOSE cell lines showed high apoptosis upon stimulation with TRAIL and expressed high mDR5 in comparison with other tumorigenic MOSE cell lines.

Taken together, these data show that all ten tumorigenic MOSE cell lines showed differential expression of the most relevant players in the TRAIL pathway (mDR5 and c-FLIP) when compared with normal (non-tumorigenic) MOSE cells. I further showed that 70% of tumorigenic MOSE cell lines were resistant to TRAIL-induced apoptosis. In conclusion, these results indicate that mDR5 and c-FLIP in the context of TRAIL pathway were highly modified in mouse OC cells.

A)

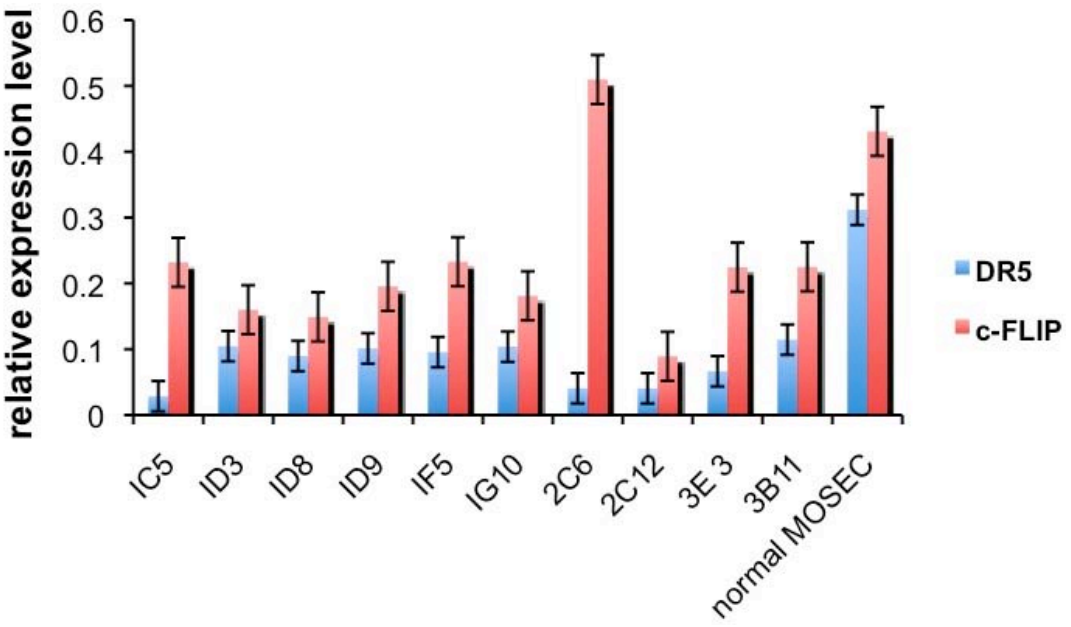
relative expression level
0.6
0.5
0.4
0.3
0.2
0.1
0
IC5
ID3
ID8
ID9
IF5
IG10
2C6
2C12
3E 3
3B11
normal MOSEC
DR5
c-FLIP

B)

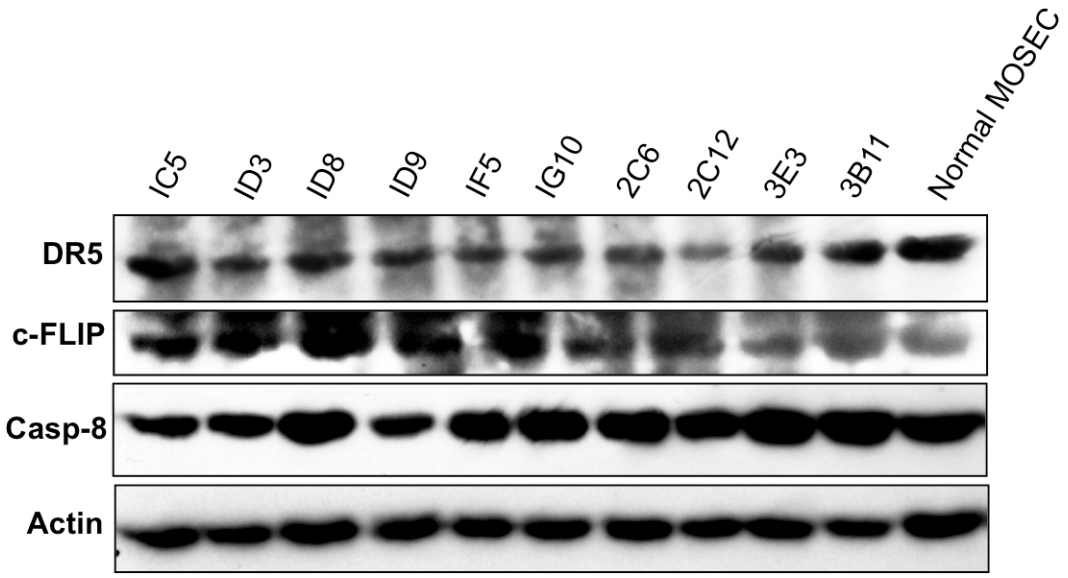
IC5
ID3
ID8
ID9
IF5
IG10
2C6
2C12
3E3
3B11
Normal MOSEC
DR5
c-FLIP
Casp-8
Actin

C)

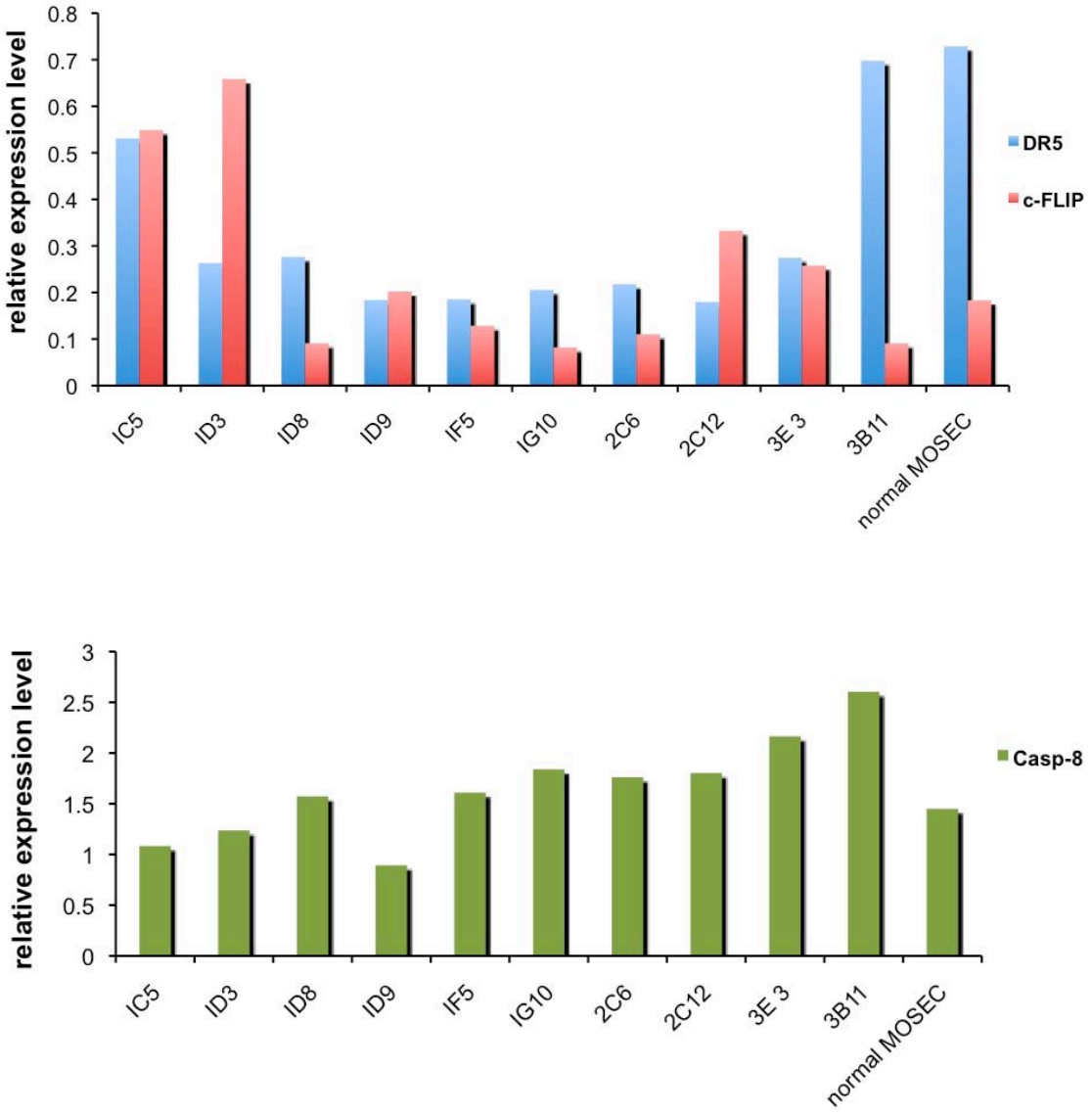
relative expression level
0.8
0.7
0.6
0.5
0.4
0.3
0.2
0.1
0
DR5
c-FLIP
IC5
ID3
ID8
ID9
IF5
IG10
2C6
2C12
3E 3
3B11
normal MOSEC
relative expression level
3
2.5
2
1.5
1
0.5
0
Casp-8
IC5
ID3
ID8
ID9
IF5
IG10
2C6
2C12
3E 3
3B11
normal MOSEC

D)

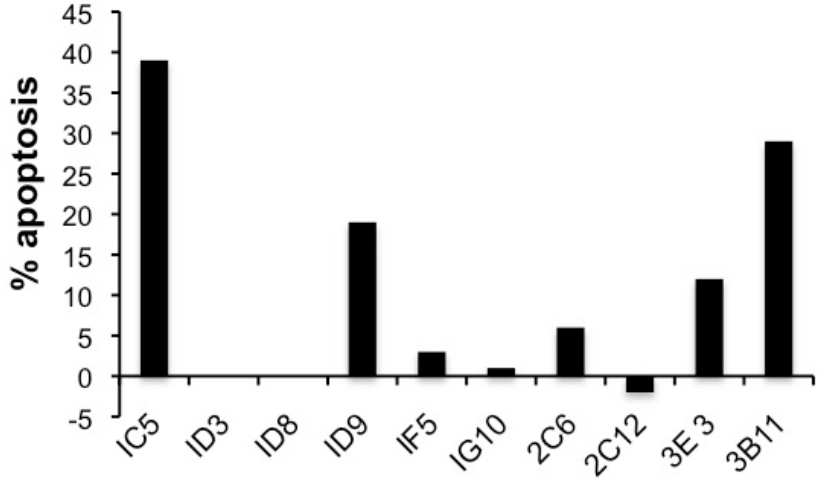
% apoptosis
45
40
35
30
25
20
15
10
5
0
-5
IC5
ID3
ID8
ID9
IF5
IG10
2C6
2C12
3E 3
3B11

Figure 3.3.3. Tumorigenic MOSE cell lines regulate differentially mDR5 and c-FLIP, and are resistant to TRAIL-induced apoptosis. A) mRNA expression levels of mDR5 and c-FLIP in tumorigenic MOSE cell lines were determined by qRT-PCR. **B)** Western blot analysis of mDR5, c-FLIP and caspase-8 expression in ten tumorigenic MOSE cell lines. Western blots were performed with the total cellular proteins of the given cell lines. **C)** Quantitative evaluation of Western blot for mDR5, c-FLIP (upper panel) and caspase-8 (lower panel). Protein bands were quantified and standardized with actin. **D)** Measured TRAIL sensitivity on tumorigenic MOSE cell lines. MOSE cell lines were treated with recombinant mouse soluble TRAIL at final concentrations of 100, 500 and 1000 ng/ml and incubated for 24 hours. Cells were then assessed for apoptosis by Annexin-V and PI staining and compared with untreated controls. No effects were observed with 100 and 500 ng/ml soluble TRAIL (data not shown).

Knockdown of mDR5 leads to an increase in transformation and a shorter life span

To analyze the influence of differentially expressed mDR5 on the development of OC in immunocompetent mice, the loss of function approach was applied using RNAi technology. The well-characterized tumorigenic mouse OC cell line ID8 (of which the chromosomes were analyzed and structural abnormalities were described (30)), which displays an abnormal regulation of mDR5 and c-FLIP (Fig. 3.3.3*A*, *B* and *C*), was selected and considered for further work. To shutdown (or at least reduce) mDR5 expression by RNAi approach, five synthetic shRNA oligonucleotides (A, B, C, D, and E; sequence shown in Table 3.3.1 in Material and Methods) spanning various regions of the mDR5 open-reading frame were designed and cloned into pSilencer 4.1-CMV neo vector.

The effects of shRNA constructs were controlled by comparing mRNA and protein levels from pSilencer mDR5 vector-transfected ID8 cells with non-transfected ID8 cells or with cells transfected with control shRNA. Control shRNA sequence was designed not to target any gene in the whole genome. One out of five generated shRNAs showed highly efficient downregulation of

mDR5 on mRNA and protein level as shown in qRT-PCR and Western blot respectively (Fig. 3.3.4*A* and *B*).

Consequently, 5×10^6 of the manipulated and parental tumorigenic MOSE cell lines were transplanted intraperitoneally with a single cell suspension into female immunocompetent C57BL/6 mice individually, and tumor development was determined. Three mice were analyzed per group. Mice were weighed every second day, and intraperitoneal tumor formation was monitored by the accumulation of ascitic fluid. Approximately 9-18 days after the development of visible ascites (detected by abdominal swelling) the animals were sacrificed. Interestingly, I observed that suppression of mDR5 led to an increase in transformation and, consequently, a shortened life span (Fig. 3.3.4*C*). This might be explained by the inhibition of mDR5 expression thereby increasing the resistance of ID8 cell lines to TRAIL-induced apoptosis expressed by immune cells. I could not observe any tumors outside the peritoneal cavity. Notably, these *in vivo* data were obtained from single experiment and, therefore, should be considered preliminary results. My preliminary *in vivo* results indicate that mDR5 is a key player in OC progression.

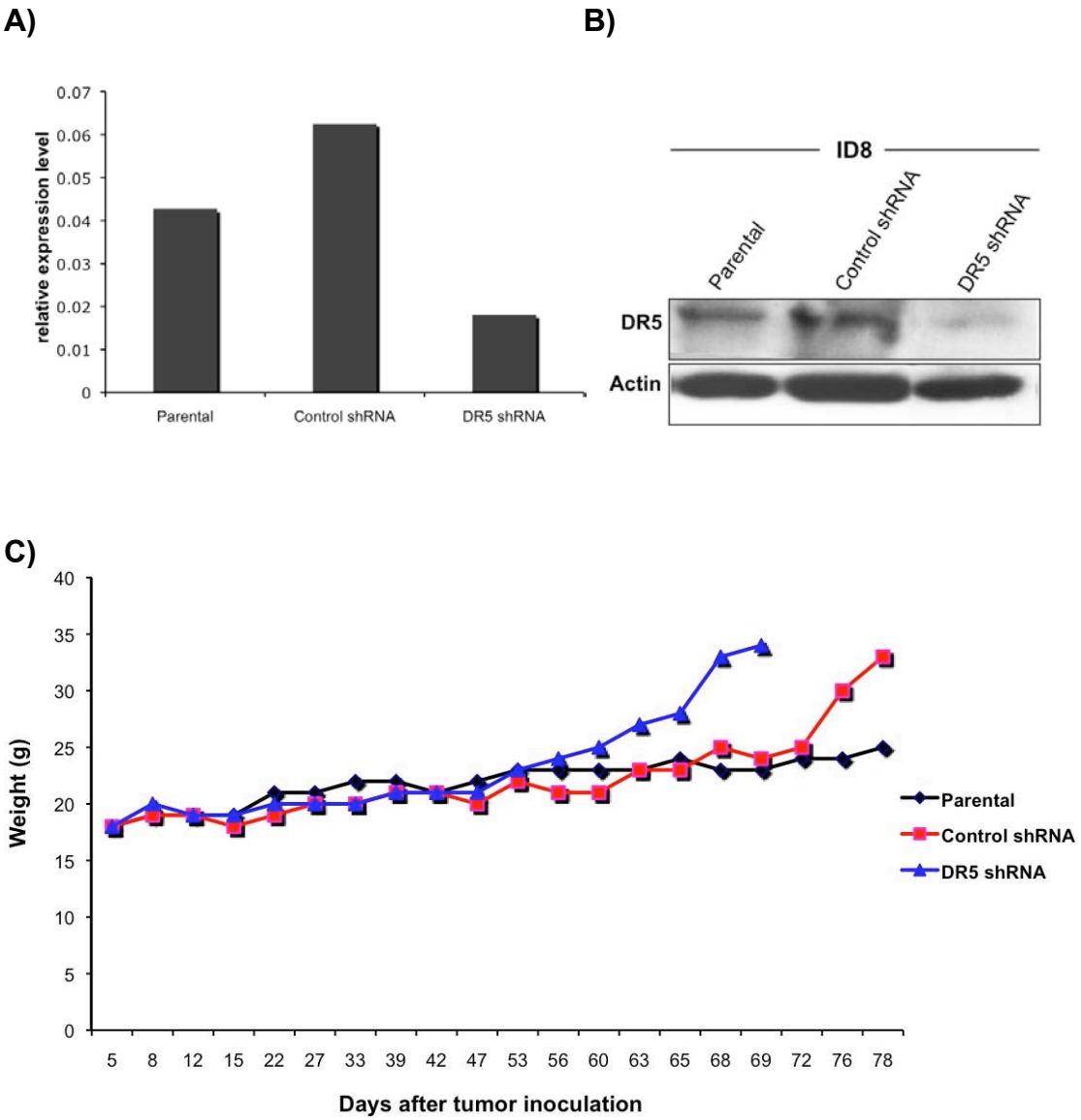

Figure 3.3.4. Knockdown of mDR5 leads to an increase in transformation and shorter life span. A and B) Knockdown of mDR5 in the established OC mouse model. ID8 tumorigenic MOSE cells were either left untransfected or transfected with control shRNA or mDR5 shRNA. RNA and protein were isolated and the efficiency of mDR5 shRNA was determined by qRT-PCR (left panel) and Western blot (right panel). **C)** The phenotypic effect of mDR5 suppression on OC progression in a syngeneic OC mouse model. Groups of female immunocompetent C57BL/6 mice (three mice each), eight weeks of age were either left or transplanted intraperitoneally with 5×10^6 ID8 cells of the individual parental or control shRNA or mDR5 shRNA MOSE cells. Mice were weighed twice per week after inoculation and tumor formation was monitored by the accumulation of ascitic fluid (detected by abdominal swelling).

Knockdown of mDR5 increases the resistance to TRAIL-induced apoptosis *in vivo*

To correlate the observed tumor growth with the rate of apoptosis *in vivo*, isolated tumors were subsequently sectioned for pathological analysis. Tumors stained with mDR5 confirmed that mDR5 is silenced *in vivo* compared with the control shRNA or parental cells (Fig. 3.3.5*A*). Immunohistochemical analysis for TRAIL indicated that it is highly expressed in the tumor microenvironment (Fig. 3.3.5*A*), which is in line with my previous data from a xenograft mouse model (section 3.1). Tumor tissues stained with proliferating cell nuclear antigen (Ki-67) showed no significant increase in the proliferation in mDR5 downregulated tumors compared with controls (Fig. 3.3.5*A* and *B*). In contrast, tumor tissues stained via TUNEL assay, which detects 3' DNA strand breaks, showed marked decrease in the frequency of apoptosis occurring in mDR5 shRNA expressing tumor tissues compared with the control shRNA or parental cells (Fig. 3.3.5*A* and *C*). Soluble TRAIL induces apoptosis in tumor cells and membrane-bound TRAIL is known to be more active than soluble TRAIL. Moreover, specific microenvironment plays a role *in vivo.* These facts might explain the reason of reduced apoptosis (only 4%) in parental cells *in vivo* and not *in vitro* (Fig. 3.3.3*D* and 3.3.5*C*). These data obtained from preliminary *in vivo* results suggest that the increase in tumor development and shorter life span occurring in mDR5 shRNA expressing cells is because of a decrease in apoptosis rate *in vivo*. Taken together, these preliminary *in vivo* results next to my previous data (section 3.1) highlight DR5 as a potential target for OC therapy.

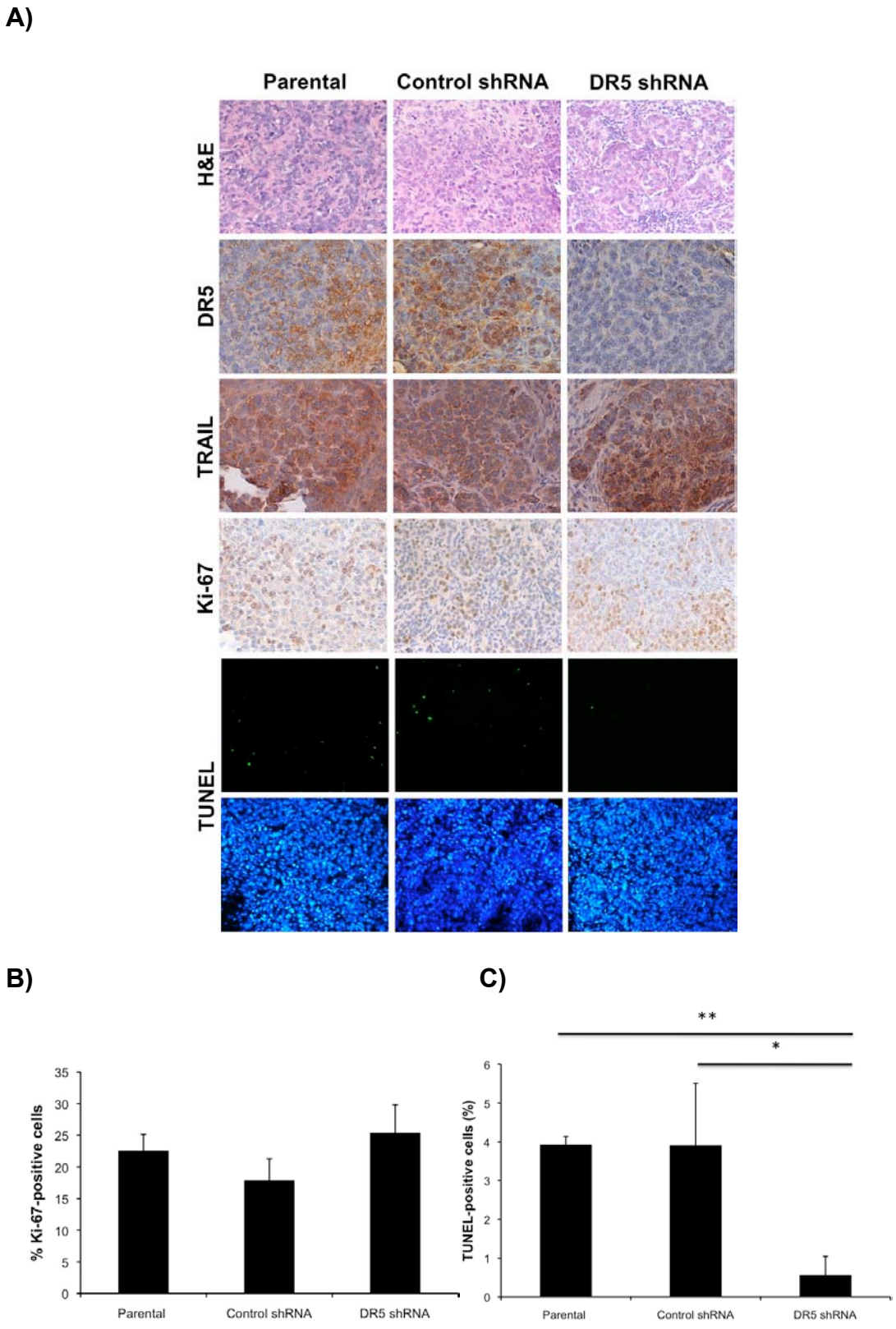

Figure 3.3.5. Knockdown of mDR5 increases the resistance to TRAIL-induced apoptosis *in vivo.* A) Immunohistochemical analysis of tumor sections isolated from the given groups and stained with mDR5, TRAIL or Ki-67. In addition, apoptosis was determined by TUNEL assay. **B)** The percentage of Ki-67 positive cells in each group is shown. Columns represent the mean of proportional cell numbers of Ki-67 positive staining of three different tumor sections per group; bars, ±SE. No statically

significant (P<0.05) difference was obtained by comparing the mDR5 shRNA group with parental or control shRNA groups. **C)** Percentage of TUNEL positive cells is shown. Columns represent the mean of the proportional cell numbers of TUNEL positive staining of three different tumor sections per group; bars, ±SE; *statically significant (P<0.05) or **highly significant (P<0.005) differences comparing the mDR5 shRNA group with parental or control shRNA groups.

Discussion

TRAIL is a natural immune system associated molecule that has been shown to play an important role in tumor immunosurveillance, and is in the meantime also being developed for clinical trials in cancer patients (15, 16, 35, 36). In this study, I applied an immunocompetent C57BL/6 OC mouse model (30) to address the molecular and cellular events of the TRAIL/TRAIL-R system in host protection from ovarian tumor development. This immunocompetent OC mouse model, reflecting both the early and late stages of the disease, is ideal for the investigation of the molecular and immune interaction of the TRAIL pathway in OC progression. The model has the following benefits. First, the ability of tumorigenic MOSE cells to grow in mice with an intact immune system, which makes it possible to study the interaction of the immune system during the development, progression and treatment of ovarian carcinogenesis in contrast to xenograft mouse models, which lack a functional immune system. Second, the development of the tumor requires a long time (about 2-3 months), which allows for the detection and manipulation of cellular and molecular processes during development of the disease. Third, the ability to maintain the tumorigenic MOSE cell lines in culture aids genetic manipulation. Fourth, the ability of tumorigenic MOSE cells (manipulated and parental) to grow in gene deficient mice i.e. TRAIL knock-out C57BL/6 mice, makes this model a potential tool for further TRAIL-based studies.

MOSE cells were isolated and cultured *in vitro* and underwent spontaneous transformation after multiple passages (30). The parental cell line was cloned and ten lines were established [(30) and Fig. 3.3.1 in Materials and Methods]. Upon intraperitoneal application in a syngeneic

C57BL/6 mice, all ten cell lines were capable of inducing intraperitoneal tumors, with ascitic fluids accumulating at a late stage of OC, like in women (30). In fact, epithelial cells isolated from the surface of mouse ovaries grew very slowly. Therefore, to establish these tumorigenic MOSE cells, EGF was added to the culture medium to accelerate its growth. In another experiment, in the absence of EGF, transformed phenotype was also observed *in vitro* (30). This observation suggested that the transformation of these cells is related to the degree of proliferation (30). Remarkably, incessant ovulation is a risk factor in OC because it increases the proliferation of the surface epithelium (34). Early MOSE cell passages exhibit classical morphology of epithelial cells; proliferation was stopped when cells became confluent. However, with multiple passages the morphology of cells changed, with the contact inhibition of growth mainly lost and cell proliferation continuing. In this study, I identified that the TRAIL pathway is altered in malignant cells, which might be one of the factors responsible for that transformation.

Established tumorigenic MOSE cell lines were kindly provided by collaboration partner (30). I isolated MOSE cells from C57BL/6 mice and used a normal (non-tumorigenic) MOSE cell control for the endogenous expression of the target genes. I characterized ten tumorigenic MOSE cell lines in terms of their expression of mDR5, c-FLIP and caspase-8, and furthermore measured their sensitivity to TRAIL-mediated apoptosis. I observed that mDR5 is downregulated in all ten tumorigenic MOSE cell lines when compared with normal (non-tumorigenic MOSE cells) (Fig. 3.3.3*A, B,* and *C*). Moreover, I documented that 70% of tumorigenic MOSE cell lines are resistant to TRAIL-induced apoptosis, and 30% showed apoptosis upon

treatment with mouse soluble TRAIL. These cells showing a response to TRAIL-induced apoptosis expressed higher levels of mDR5 compared with those resistant to TRAIL-induced apoptosis (Fig. 3.3.3). These data suggest that the sensitivity of tumorigenic MOSE cell lines to TRAIL-induced apoptosis is directly correlated with mDR5 expression. My observation in mice is in line with my previous finding in humans that resistance to TRAIL in OC can be overcome by an agonistic anti-human DR5 monoclonal antibody, such as AD5-10, together with an application of TRAIL (section 3.1). c-FLIP expression was altered in 40% of the tumorigenic MOSE cell lines at protein level when compared with non-tumorigenic MOSE cell control (Fig. 3.3.3*B* and *C*). This finding reflects our lab's observation in humans that about 40% of OC patients overexpressed c-$FLIP_L$, and that c-$FLIP_L$ suppression enhanced OC to TRAIL-induced apoptosis (22, 37). Taken together, these data indicate that the immunocompetent OC mouse model I applied in this study closely mimics human disease, proving valuable in current investigations.

The immunocompetent OC mouse model develops widespread intraperitoneal disease with morphological characteristics of epithelial OC within two to three months after injection. No metastatic disease could be observed in these mice, and this fact is verified in my study. Notably, human OC metastasizes into the free peritoneal cavity and is restricted to the peritoneal cavity. Metastases at other sites are a rare event. The well-characterized tumorigenic mouse OC cell line ID8 was genetically manipulated by inhibiting mDR5 expression using shRNA (Fig. 3.3.4*A* and *B*). Interestingly, the preliminary data of a syngeneic OC model showed that

silencing mDR5 expression decreased the life span of OC mice. Moreover, ascite development was accelerated and apoptosis was decreased in tumor tissues downregulated mDR5 compared with control shRNA or parental cells (Fig. 3.3.4*C*, 3.3.5*A* and *B*). These results indicate that mDR5 contributes significantly to TRAIL-induced apoptosis in OC cells and support my previous findings in humans that AD5-10 sensitized OC cells to TRAIL mediate apoptosis *in vitro* and decreased dramatically tumor size *in vivo* (section 3.1).

In conclusion, my data show that the TRAIL/TRAIL-R system in addition to the caspase-8 inhibitor protein c-FLIP is modified in mouse OC, and that the alterations are very similar to that observed in human OC. This fact indicates the value of my study, and adds additional weight for applying syngeneic OC models to the study of the TRAIL pathway in an immunocompetent setting. Moreover, immunotherapeutic strategies designed to treat OC will be evaluated using this model in future experiments.

Future Directions

In the future experiments, we will explore the role of TRAIL in natural antimetastatic function of immunosurveillance against ovarian transformed cells *in vivo*, using TRAIL knock-out mice (will be kindly provided by collaboration partner). We will analyze the inhibitory effect of TRAIL on the outgrowth of OC by reconstituting TRAIL deficient C57BL/6 mice with parental or manipulated tumorigenic MOSE cell lines and detect the metastatic spread of the tumor cells.

Next, in order to demonstrate the contribution of TRAIL in NK cell surveillance of OC; **first,** we will assess the primary growth of tumorigenic MOSE cells transplanted into pathogen-free C57BL/6 and TRAIL knock-out mice (having the same genetic background). **Second**, pathogen-free C57BL/6 mice reconstituted with tumorigenic MOSE cells will be treated with IL-12 and either depleted from NK cells or treated with anti-TRAIL mAb. Notably, IL-12 has been shown to induce proliferation, IFN-production and cytotoxicity of NK cells *in vivo,* which is associated with their antitumor effects (38-40). Subsequently, the antitumor effect will be detected and compared to TRAIL knock-out mice reconstituted with the same tumorigenic MOSE cells. This experiment will illustrate the critical role of TRAIL expressed on NK cell in mediating antitumor activity against OC.

References

1. Smyth MJ, Dunn GP, Schreiber RD. Cancer immunosurveillance and immunoediting: the roles of immunity in suppressing tumor development and shaping tumor immunogenicity. Adv Immunol 2006;90:1-50.

2. Swann JB, Smyth MJ. Immune surveillance of tumors. J Clin Invest 2007 May;117(5):1137-46.

3. Zitvogel L, Tesniere A, Kroemer G. Cancer despite immunosurveillance: immunoselection and immunosubversion. Nat Rev Immunol 2006 Oct;6(10):715-27.

4. Fanger NA, Maliszewski CR, Schooley K, Griffith TS. Human dendritic cells mediate cellular apoptosis via tumor necrosis factor-related apoptosis-inducing ligand (TRAIL). J Exp Med 1999 Oct 18;190(8):1155-64.

5. Griffith TS, Wiley SR, Kubin MZ, Sedger LM, Maliszewski CR, Fanger NA. Monocyte-mediated tumoricidal activity via the tumor necrosis factor-related cytokine, TRAIL. J Exp Med 1999 Apr 19;189(8):1343-54.

6. Kayagaki N, Yamaguchi N, Nakayama M, Eto H, Okumura K, Yagita H. Type I interferons (IFNs) regulate tumor necrosis factor-related apoptosis-inducing ligand (TRAIL) expression on human T cells: A novel mechanism for the antitumor effects of type I IFNs. J Exp Med 1999 May 3;189(9):1451-60.

7. Kayagaki N, Yamaguchi N, Nakayama M, et al. Involvement of TNF-related apoptosis-inducing ligand in human CD4+ T cell-mediated cytotoxicity. J Immunol 1999 Mar 1;162(5):2639-47.

8. Kayagaki N, Yamaguchi N, Nakayama M, et al. Expression and function of TNF-related apoptosis-inducing ligand on murine activated NK cells. J Immunol 1999 Aug 15;163(4):1906-13.

9. Koga Y, Matsuzaki A, Suminoe A, Hattori H, Hara T. Neutrophil-derived TNF-related apoptosis-inducing ligand (TRAIL): a novel mechanism of antitumor effect by neutrophils. Cancer Res 2004 Feb 1;64(3):1037-43.

10. Nakayama M, Kayagaki N, Yamaguchi N, Okumura K, Yagita H. Involvement of TWEAK in interferon gamma-stimulated monocyte cytotoxicity. J Exp Med 2000 Nov 6;192(9):1373-80.

11. Ehrlich S, Infante-Duarte C, Seeger B, Zipp F. Regulation of soluble and surface-bound TRAIL in human T cells, B cells, and monocytes. Cytokine 2003 Dec 21;24(6):244-53.

12. Halaas O, Vik R, Ashkenazi A, Espevik T. Lipopolysaccharide induces expression of APO2 ligand/TRAIL in human monocytes and macrophages. Scand J Immunol 2000 Mar;51(3):244-50.

13. Sedger LM, Shows DM, Blanton RA, et al. IFN-gamma mediates a novel antiviral activity through dynamic modulation of TRAIL and TRAIL receptor expression. J Immunol 1999 Jul 15;163(2):920-6.

14. Seki N, Hayakawa Y, Brooks AD, et al. Tumor necrosis factor-related apoptosis-inducing ligand-mediated apoptosis is an important endogenous mechanism for resistance to liver metastases in murine renal cancer. Cancer Res 2003 Jan 1;63(1):207-13.

15. Smyth MJ, Cretney E, Takeda K, et al. Tumor necrosis factor-related apoptosis-inducing ligand (TRAIL) contributes to interferon gamma-dependent

natural killer cell protection from tumor metastasis. J Exp Med 2001 Mar 19;193(6):661-70.

16. Takeda K, Hayakawa Y, Smyth MJ, et al. Involvement of tumor necrosis factor-related apoptosis-inducing ligand in surveillance of tumor metastasis by liver natural killer cells. Nat Med 2001 Jan;7(1):94-100.

17. Ashkenazi A. Targeting death and decoy receptors of the tumour-necrosis factor superfamily. Nat Rev Cancer 2002 Jun;2(6):420-30.

18. Falschlehner C, Schaefer U, Walczak H. Following TRAIL's path in the immune system. Immunology 2009 Jun;127(2):145-54.

19. Schneider P, Olson D, Tardivel A, et al. Identification of a new murine tumor necrosis factor receptor locus that contains two novel murine receptors for tumor necrosis factor-related apoptosis-inducing ligand (TRAIL). J Biol Chem 2003 Feb 14;278(7):5444-54.

20. Wiley SR, Schooley K, Smolak PJ, et al. Identification and characterization of a new member of the TNF family that induces apoptosis. Immunity 1995 Dec;3(6):673-82.

21. Yagita H, Takeda K, Hayakawa Y, Smyth MJ, Okumura K. TRAIL and its receptors as targets for cancer therapy. Cancer Sci 2004 Oct;95(10):777-83.

22. Ahmed El-Gazzar, Michael Wittinger, Paul Perco, Mariam Annes, Reinhard Horvat, Wolfgang Mikulits, Thomas Grunt, Bernd Mayer, Michael Krainer. c-FLIPL contributes to ovarian cancer (OC) development in a dual way: by escaping OC cells from immunosurveillance and increasing their invasive potential. Submitted 2009.

23. Ahmed El-Gazzar, Paul Perco, Eva Eckelhart, Mariam Anees, Veronika Sexl, Bernd Mayer, Yanxin Liu, Wolfgang Mikulits, Reinhard Horvat, Thomas Pangerl, Dexian Zheng, Michael Krainer. Natural immunity enhances the activity of a DR5 agonistic antibody and carboplatin in the treatment of ovarian cancer. Submitted 2009.

24. Chen X, Pine P, Knapp AM, Tuse D, Laderoute KR. Oncocidin A1: a novel tubulin-binding drug with antitumor activity against human breast and ovarian carcinoma xenografts in nude mice. Biochem Pharmacol 1998 Sep 1;56(5):623-33.

25. Mesiano S, Ferrara N, Jaffe RB. Role of vascular endothelial growth factor in ovarian cancer: inhibition of ascites formation by immunoneutralization. Am J Pathol 1998 Oct;153(4):1249-56.

26. Plumb JA, Strathdee G, Sludden J, Kaye SB, Brown R. Reversal of drug resistance in human tumor xenografts by 2'-deoxy-5-azacytidine-induced demethylation of the hMLH1 gene promoter. Cancer Res 2000 Nov 1;60(21):6039-44.

27. Rancourt C, Rogers BE, Sosnowski BA, et al. Basic fibroblast growth factor enhancement of adenovirus-mediated delivery of the herpes simplex virus thymidine kinase gene results in augmented therapeutic benefit in a murine model of ovarian cancer. Clin Cancer Res 1998 Oct;4(10):2455-61.

28. Rosenfeld ME, Wang M, Siegal GP, et al. Adenoviral-mediated delivery of herpes simplex virus thymidine kinase results in tumor reduction and prolonged survival in a SCID mouse model of human ovarian carcinoma. J Mol Med 1996 Aug;74(8):455-62.

29. Stackhouse MA, Buchsbaum DJ, Grizzle WE, et al. Radiosensitization mediated by a transfected anti-erbB-2 single-chain antibody in vitro and in vivo. Int J Radiat Oncol Biol Phys 1998 Nov 1;42(4):817-22.

30. Roby KF, Taylor CC, Sweetwood JP, et al. Development of a syngeneic mouse model for events related to ovarian cancer. Carcinogenesis 2000 Apr;21(4):585-91.

31. Dyck HG, Hamilton TC, Godwin AK, Lynch HT, Maines-Bandiera S, Auersperg N. Autonomy of the epithelial phenotype in human ovarian surface epithelium: changes with neoplastic progression and with a family history of ovarian cancer. Int J Cancer 1996 Dec 20;69(6):429-36.

32. Godwin AK, Testa JR, Handel LM, et al. Spontaneous transformation of rat ovarian surface epithelial cells: association with cytogenetic changes and implications of repeated ovulation in the etiology of ovarian cancer. J Natl Cancer Inst 1992 Apr 15;84(8):592-601.

33. Testa JR, Getts LA, Salazar H, et al. Spontaneous transformation of rat ovarian surface epithelial cells results in well to poorly differentiated tumors with a parallel range of cytogenetic complexity. Cancer Res 1994 May 15;54(10):2778-84.

34. Fathalla MF. Factors in the causation and incidence of ovarian cancer. Obstet Gynecol Surv 1972 Nov;27(11):751-68.

35. Cretney E, Takeda K, Yagita H, Glaccum M, Peschon JJ, Smyth MJ. Increased susceptibility to tumor initiation and metastasis in TNF-related apoptosis-inducing ligand-deficient mice. J Immunol 2002 Feb 1;168(3):1356-61.

36. Takeda K, Smyth MJ, Cretney E, et al. Critical role for tumor necrosis factor-related apoptosis-inducing ligand in immune surveillance against tumor development. J Exp Med 2002 Jan 21;195(2):161-9.

37. Horak P, Pils D, Kaider A, et al. Perturbation of the tumor necrosis factor--related apoptosis-inducing ligand cascade in ovarian cancer: overexpression of FLIPL and deregulation of the functional receptors DR4 and DR5. Clin Cancer Res 2005 Dec 15;11(24 Pt 1):8585-91.

38. Gately MK, Warrier RR, Honasoge S, et al. Administration of recombinant IL-12 to normal mice enhances cytolytic lymphocyte activity and induces production of IFN-gamma in vivo. Int Immunol 1994 Jan;6(1):157-67.

39. Kawamura T, Takeda K, Mendiratta SK, et al. Critical role of NK1+ T cells in IL-12-induced immune responses in vivo. J Immunol 1998 Jan 1;160(1):16-9.

40. Trinchieri G. Proinflammatory and immunoregulatory functions of interleukin-12. Int Rev Immunol 1998;16(3-4):365-96.

4. Conclusions

The main focus of my PhD work was to demonstrate the key role of the most relevant player in TRAIL signaling pathway, namely the TRAIL functional receptor 2 (DR5) and c-FLIP$_L$, in suppressing tumor initiation of OC. TRAIL has been shown to be one of the most promising agents in selectively inducing apoptosis in tumor cells. However, many cancer cells including OC are inherently resistant to TRAIL-induced apoptosis, presumably as a result of multiple genetic alterations in the TRAIL signaling pathway. Several mechanisms underlying TRAIL resistance have been suggested, including mutation in DR5 and/or anti-apoptotic protein c-FLIP$_L$.

During the course of my PhD thesis, I identified the role of DR5 as well as c-FLIP$_L$ in OC development. In a study using primary tumor material, I selected three different human OC cell lines, namely MDAH-2774, A2780 and ES-2. Selected OC cell lines harbored different mutations, ranging from silent DR4 expression, upregulation of the inhibitor protein c-FLIP$_L$, and further to mutated p53, representing the majority of OC patients. Moreover, these cell lines are resistant to carboplatin and recombinant soluble human TRAIL. I succeeded to show that stimulation of OC cells with an agonistic antibody (AD5-10) against human DR5 in presence of carboplatin restored sensitivity of platin-resistance OC cells to apoptosis *in vitro* and *in vivo*. Moreover, I could show that carboplatin forced expression of DR5 on OC cells independent of the p53 status, which might explain the high apoptosis rate observed after treating OC cells with a combination of AD5-10 and carboplatin. Furthermore, I described that NK cells play a critical role in immunosurveillance and in the

function of the agonistic antibody AD5-10 in OC. I reported that depletion of mice from NK cells led to increased tumor development and abolished the cytotoxic effect of AD5-10 in xenograft mouse model.

As second part in my PhD thesis, I aimed to clarify the antagonistic role of c-FLIP$_L$ in OC progression. I found that c-FLIP$_L$ downregulation enhanced significantly OC cells to TRAIL-induced apoptosis in both *in vitro* and decreased tumor growth rate *in vivo*. Moreover, c-FLIP$_L$ underexpression inhibited migration of OC cells in presence of soluble TRAIL *in vitro*, and hindered invasion of ovarian tumors in a preclinical OC mouse model. Interestingly, c-FLIP$_L$ suppression inhibits proliferation of OC cells *in vivo*, which might be in line with previous findings that c-FLIP$_L$ activates ERK and NF-κB -mediated cell proliferation. This finding adds additional weight in the role of c-FLIP$_L$ in mediating OC development. The summary of this study was that c-FLIP$_L$ is a fundamental player in controlling the balance between proliferation and apoptosis in human OC cells.

The results provided in this study, and also complemented by other studies showed that TRAIL and DR5 play an essential role in immunosurveillance, it was important to further investigate this finding in an appropriate animal model. Therefore, in the last part of my PhD thesis, I applied an immunocompetent OC mouse model to study TRAIL and DR5 in the interplay between cancer cells, microenvironment, and immune system. An established immunocompetent OC mouse model showed close resemblance to human OC in context of the TRAIL pathway. Accordingly, I found that mouse DR5 is an important player in OC progression, since silencing mouse DR5 increased ascites development and decreased life span

of a syngenic OC mouse in a preliminary animal experiment. Indeed, this observation is in line with my previous finding on the key role of DR5 in OC development.

Collectively, my PhD study provided a unique strategy to illustrate the basic framework for the natural TRAIL effector molecule in host protection against ovarian tumorigenesis. These results might add new insight into several additional aspects of this disease, furthermore supporting novel therapy options.

5. Acknowledgments

I would like to thank Prof. Michael Krainer for the opportunity to work in his lab and to complete my PhD thesis.

My special thanks goes to Dr. Bernd Mayer not only for his knowledge and guidance but also for his help in words and deeds during my PhD work at any time. I am extremely thankful for his encouragement and precious advice throughout.

I would especially like to thank all my collaborators, specifically Dr. Paul Perco, Prof. Reinhard Horvat, Prof. Dexian Zheng, Prof. Wolfgang Mikulits, Dr. Kathy Roby, Prof. Veronika Sexl, Prof. Udo Losert, and Prof. Thomas Grunt, whose scientific expertise and support added important insights for my PhD.

With warm thanks to all my colleagues, particularly Mag. Mariam Annes, Dr. Michael Wittinger, Dr. Dietmar Pils, Thomas Pangerl, Alfred Gugerell, Dr. Ronald Rapberger, Mag. Andreas Bernthaler, Dr. Johannes Söllner, Dr. Arno Lukas, and Mag. Martin Haiduk,

I also wish to acknowledge and thank my PhD committee members: Prof. Pavel Kovarik, Wolfgang Mikulits, Dr. Bernd Mayer and Prof. Michael Krainer for guiding me in my studies and for their valuable suggestions and feedback that was very helpful during the course of my PhD.

Many thanks to Sabine Strommer, Dr. Katrina Vanura, Dr. Mario Mairhofer, and Anita Brandstetter for coffee breaks, moral support and scientific help during my PhD thesis.

I would also like to thank all my friends who are always beside me, especially Dr. Tibor Altenberger and his family, Dr. Branko Ott, Alex Mikayel, Louisa Ertl, and Dr. Martin Melcher.

I am very grateful to the University of Vienna for the permission to study.

Last but not least, I would like to acknowledge all my family members especially my parents, my wife Sabine, uncle Ali, and my grandparents. Without them, my research work would not be possible. I am sorry that my grandfather cannot see my completing my PhD thesis as he always wished to.

6. Curriculum Vitae

Personal Details

Name:	**Ahmed El-Gazzar**
Date of Birth:	**May 25, 1980 in Tanta, Egypt**
Nationality:	**Egyptian**
Martial Status:	**Married**
Address:	**Heiligenstaedter Strasse 189-191/1/2, 1190 Vienna, Austria**
Telephone:	**+43-676 6490604**
E-mail:	**ahmed.el-gazzar@meduniwien.ac.at**

Education

Sep. 1997 – Jun. 2001	Studies at Tanta University of Science in Microbiology (BSc Degree in Microbiology), Egypt
Jun. 2002 – Dec. 2002	Study of the German language
Dec. 2002	Diploma in German from Wiener Internationale Hochschule, Vienna, Austria
Mar. 2003 – Nov. 2005	Registered student at the University of Vienna, Austria, in Biology/Microbiology and Genetics
Aug. 2004 – Oct. 2005	**Masters's thesis** at the Medical Universitiy of Vienna, Institute of Immunology, in the laboratory of Prof. Wilfried Ellmeier. Supervisor: Dr. Martin Melcher Title: ***Identification and characterization of genes involved in T-cell development***
Nov. 2005	**Master of Science** (MSc) in Biology/Microbiology and Genetics at the University of Vienna with final grade **"Passed with Honours"**
since Oct. 2005	PhD studies in Science, Biology/Microbiology and Genetics at the University of Vienna, Austria
since Oct. 2006	**PhD thesis** at the Medical University of Vienna, Division of Oncology of the Department of Medicine I, in the laboratory of Prof. Michael Krainer Title: ***Deciphering the role of the TRAIL pathway as a potential tumor escape mechanism in ovarian cancer***

Honours, Scholarships, and Awards

"One World" Scholarship from the Afro-Asian Institute (AAI), Vienna, Austria, from November 2003 to March 2006.

Master's thesis with a final grade "Passed with Honours", May 2005

Membership of International Scientific Associations

AACR – American Association for Cancer Research, Philadelphia, Pennsylvania, USA

Grants

The Austrian Science Fund (FWF) funding project number P20715 **"**Deciphering the role of the TRAIL pathway as a potential tumor escape mechanism in ovarian cancer" from May 1, 2008, to May 1, 2011**.**

Animal application within the project **"**Deciphering the role of the TRAIL pathway as a potential tumor escape mechanism in ovarian cancer". Authorized by the Austrian Federal Ministry of Science and Research for three years (until June 30, 2010).

Scientific Publications

Natural immunity enhances the activity of a DR5 agonistic antibody and carboplatin in the treatment of ovarian cancer
Ahmed El-Gazzar, Paul Perco, Eva Eckelhart, Mariam Anees, Veronika Sexl, Bernd Mayer, Yanxin Liu, Wolfgang Mikulits, Reinhard Horvat, Thomas Pangerl, Dexian Zheng, and Michael Krainer (submitted)

The role of c-FLIP$_L$ in ovarian cancer: chaperoning tumor cells from immunosurveillance and increasing their invasive potential
Ahmed El-Gazzar, Michael Wittinger, Paul Perco, Mariam Annes, Reinhard Horvat, Wolfgang Mikulits, Thomas W. Grunt, Bernd Mayer, and Michael Krainer (submitted)

Recurrence free survival in prostate cancer is related to increased stromal TRAIL expression
Mariam Anees, Peter Horak, **Ahmed El-Gazzar**, Martin Susani, Georg Heinze, Paul Perco, Thomas Pangerl, Michael Krainer, and William K. Oh (submitted)

hVps37A is a novel tumor suppressor gene for EGFR-driven tumors
Michael Wittinger, **Ahmed El-Gazzar**, Dietmar Pils, Thomas W. Grunt, Maria Sibilia, Martin Holcmann, Reinhard Horvat, Michael Schemper, Robert Zeillinger, Christian Schöfer, Helmut Dolznig, and Michael Krainer (in progress)

Oral presentation

Deciphering the role of the TRAIL pathway as a potential tumor escape mechanism in ovarian cancer
Joint Annual Meeting of the Austrian, German, and Swiss Society of Haematology and Oncology (DGHO, ÖGHO, SGH, & SGMO), Vienna, Austria, October 10–14, 2008

Poster presentations

Characterization and modulation of TRAIL-mediated proliferation in tumor cells
Ahmed El-Gazzar, Guido Maa Bared, and Irmela Jeremias
Joint Annual Meeting of Helmholtz Centre for Infection Research and GSF – National Research Center for Envirnoment and Health and the EU PhD Program MIDITRAIN. Hotel Dchlossmühle, Quedlinburg, Germany, May 28 – June 2, 2006

Deciphering the role of the TRAIL pathway as a potential tumor escape mechanism in ovarian cancer

Ahmed EL-Gazzar, Peter Horak, Bernd Mayer, Michael Wittinger, Dexian Zheng, and Michael Krainer
Poster presentation at the AACR, San Diego, USA, April 12–16, 2008, abstract # 824

HCRP1 contributes to degradation of activated EGFR, a mechanism highly relevant for ovarian cancer
Michael Wittinger, Dietmar Pils, **Ahmed El-Gazzar**, Robert Zeillinger, Thomas Grunt, and Michael Krainer
Poster presentation at the AACR 99th Annual Meeting, San Diego, USA, April 12–16, 2008, abstract # 3427

Deciphering the role of the TRAIL pathway as a potential tumor escape mechanism in ovarian cancer
Ahmed El-Gazzar, Michael Wittinger, Bernd Mayer, and Michael Krainer
Poster presentation at the 4th PhD Symposium 2008, Vienna, Austria, May 28–29, 2008, abstract # P12

FLIP shows a dual impact on ovarian cancer (OC) development: chaperoning OC cells from immunosurveillance and increasing their invasive potential
Ahmed El-Gazzar, Paul Perco, Michael Wittinger, Reinhard Horvat, Wolfgang Mikulits, Bernd Mayer, and Michael Krainer
Poster presentation at the AACR 100th Annual Meeting, Colorado Convention Center, Denver, Colorado, USA, April 18–22, 2009, abstract # 5127

Characterization of the TRAIL pathway in a syngeneic mouse model of ovarian cancer
Ahmed El-Gazzar, Mariam Anees, Reinhard Horvat, Bernd Mayer, and Michael Krainer
Poster presentation at the AACR 100th Annual Meeting, Colorado Convention Center, Denver, Colorado, USA, April 18–22, 2009, abstract # 5128

Combination of DR5 agonistic antibody and chemotherapy eliminates ovarian cancer in mice
Ahmed El-Gazzar, Paul Perco, Eva Eckelhart, Mariam Anees, Veronika Sexl, Bernd Mayer, Yanxin Liu, Wolfgang Mikulits, Reinhard Horvat, Dexian Zheng, and Michael Krainer
Poster presentation at the 5th PhD Symposium 2009, Vienna, Austria, June 17–19, 2009, abstract # P20

TRAIL in tumor microenvironment influences prostate cancer survival
Mariam Anees, Peter Horak, **Ahmed El-Gazzar**, Thomas Pangerl, Martin Susani, William Kyu Oh, and Michael Krainer
Poster presentation at the 5th PhD Symposium 2009, Vienna, Austria, June 17–19, 2009, abstract # P20

Skills

I. Scientific skills

Generation of RNA interference (RNAi) constructs. Generation of full length cDNAs and cloning into episomal overexpression vectors. Knockdown and overexpression of target genes in stable transfections. Cloning full length cDNAs into retroviral vectors and establishing stable retrovirus producing cell lines. Measurement of gene expression level by qRT-PCR, Western blotting, and flow cytometry staining. Establishment of inducible Tet-Off and Tet-On shRNA silencing system. Cell culturing of different primary cells and tumor cell lines, flow cytometry analysis, immunohistochemistry, and fluorescence microscopy as well as confocal microscopy. Apoptosis and proliferation assays, as well as migration and invasion assays. Establishment of immunocompetent and immunodeficient ovarian cancer

mouse models. Application of murine fetal thymic organ culture (FTOC) and bone marrow transplantation.

II. Computer skills

Competent on both Microsoft PC and Apple Mac for word-processing, spreadsheet construction, SPSS software for statistical analysis, CELLQuest Pro software for flow cytometry analysis, and use of common Molecular Biology databases for sequence analysis and design of oligoDNA/RNA.

III. Languages

Arabic: mother language
English: competent in everyday communication, both spoken and written
German: competent in everyday communication, both spoken and written
French: basic spoken